Doctoral Thesis

Shibaura Institute of Technology

Research on the Unified Threshold Criteria of Installed Filter Leak Test in Cleanrooms

2020 March

Muhammad Aiman bin Mohd Nor

Research on the Unified Threshold Criteria of Installed Filter Leak Test in Cleanrooms

by

Muhammad Aiman bin Mohd Nor

Department of Regional Environment System

Shibaura Institute of Technology

under the supervision of

Prof. Yoshihide Suwa

Abstract

Currently, ISO 14644 Part 3: 2005 (equivalent to JIS B 9917-3: 2009) have been used as a standard leakage test method of a high-performance air filter installed in a cleanroom. For the leak test, two methods of leakage detection using Aerosol photometer and discrete particle counter (DPC) are presented. Both of test methods are performed by introducing an evenly distributed challenge aerosol at upstream of the filter unit and scanning immediately at the downstream side of the filter gasket, filter frame and filter media but different leakage threshold criteria are used. In the aerosol photometer method, a leak is detected when the downstream concentration measurement is larger than 0.01% of the upstream concentration measurement. Meanwhile, in the DPC method, the leak threshold uses the value obtained by multiplying the MPPS of the test filter with a factor K (usually K=10) as the threshold value. When the scanning probe scanning at the immediate filter downstream, a leak could be detected when particles exceeded the 95% upper confidence limit of the Poisson distribution. When a possible leak is detected, the stationary re-measurement should be performed. In order to set the leakage threshold, users need to know the performance of the installed filters. However, in various cases users will not be known of this information. Therefore, an additional test needs to be done to determine the filter's performance which further creates complexity and adding unnecessary procedure in the process.

This dissertation is a work based on an effort to unify the threshold criteria of installed filter leak test in cleanrooms for both aerosol photometer method and DPC method presented in ISO 14644-3: 2005. The idea is to use the same leakage threshold criterion of aerosol photometer method in the DPC method. First, a comparison based on the difference in measuring unit and leakage evaluation method are done. It was clearly shown that the measuring unit for both instruments provide different platform in the instrument's measurement and DPC always has a more severe leak evaluation. However, we found that this matter could be countered if a different leak evaluation method is being used. Instead of discrete leakage evaluation method that is currently stated in ISO 14644-3: 2005, a cumulative leak evaluation method provides more reliable leak rate for the DPC method. The obtained values are comparable with the aerosol photometer method. Therefore, throughout this dissertation, the cumulative leakage evaluation was tested for its validity towards the possibility of a unified threshold criterion.

This evaluation method was tested further in the leak rate calculation with the instrument responses considered. There was only slight change observed for DPC as compared to the number of concentration values. However, the leak rate evaluated by aerosol photometer has a relatively big change in comparison to the mass concentration measurement. This is all due to the natural behaviour of the aerosol photometer response in which a different weight is applied for each particle size. As a result, it was found that for a filter having H14 or higher performance in European standard EN 1822-1: 2009, the same leakage evaluation standardized at 0.01% as the photometer method can be applied in the DPC method. On the other hand, similar to results obtained in measuring unit comparison, it was found that it would not be possible to apply the uniform criterion for filters with H13 or lower performance, therefore, it was necessary to establish criteria for each of the filter grade instead. Next, different DPC responses by changing the counting efficiencies in accordance with the limitations provided by the ISO 21501-4: 2018, were modelled to test the reliability of DPC to produce leak rate value below 0.01%. All filter grades were tested, and the result showed that only the filter grade of H13 which some

DPCs failed to produce leak rate value below 0.01%. The same threshold as for aerosol photometer can only be used for filter grade equal to H14 or higher, but for filter grade equal to H13 or a looser threshold should be used instead.

The results presented in this dissertation were presented in the working group 3(WG3) consists of Technical Committee (TC) whose representing their respective standard organisations to discuss the revision of the ISO 14644-3: 2005 organised by International Standard Organization (ISO) named ISO/TC209. The Final Draft International Standard (FDIS) consisting the results and findings of this dissertation were proposed and through voting process by the principal members (P-members) carried out in July 2019, with 19 out of 20 votes with 95% acceptance rate (requirement: $\geq$66.66%) and 1 negative vote out of 23 votes in the member bodies meeting (requirement: $\leq$25%). Then, the FDIS was approved and ISO 14644-3: 2005 was also withdrawn and a new ISO 14644-3: 2019 was established. As a result, a leak detection threshold of 0.01% (same as used in aerosol photometer method) of the upstream challenge aerosol concentration for the H14 filter grade and higher, and a 0.1% threshold of the upstream challenge aerosol concentration for the H13 and lower were established in the new ISO 14644-3: 2019.

Acknowledgements

This thesis was submitted to the Graduate School of Engineering and Science, Department of Regional Environment System, Shibaura Institute of Technology, as a partial fulfilment of the requirements to obtain the Doctoral degree. The work presented was carried out in the years of 2017-2019 in the laboratory of Prof. Yoshihide Suwa at the Department of Mechanical Engineering of Shibaura Institute of Technology. I would like to acknowledge and express my gratitude to Prof. Yoshihide Suwa for his guidance and supervision. During those years, he has been a father figure to me. He always provides me with fruitful discussion and ideas throughout this study. I would also like to thank Dr Yuji Yahagi and Dr Kazumi Tsunoda, Professor of Department of Mechanical Engineering, Faculty of Science and Engineering, Shibaura Institute of Technology; Dr Naoya Nishimura, Professor of Department of Architecture, Faculty of Science and Engineering, Shibaura Institute of Technology; and Dr Naoki Kagi, Associate Professor of Department of Architecture and Building Science, Faculty of Environment and Society, Tokyo Institute of Technology for their valuable guidance and advice in the dissertation screening.

I am very thankful to the Shibaura Institute of Technology and Yayasan Pelajaran MARA, for providing a conducive condition for my Doctoral degree journey. I want to thank my PhD batch mates, fellows, and all the laboratory mates I encountered during these whole three years. They have all made my stay at the Shibaura Institute of Technology very special. I wish to thank those who were the source of joy and pleasure outside the research arena. I am thankful to my friend Mr Sabri, Teh, and Adilin with whom I shared my sorrow and happiness. I also wish to thank all my friends in the

Malaysian Student Associate for the enjoyable occasions we spent together. I am forever indebted to those that have shared their wisdom with me throughout the entire journey.

Lastly, I am most grateful to my parent and brother (Mr Mohd Nor; Mrs Radiah and Mr Muhd. Naiem) for their wholehearted encouragement and companionship throughout the years I spent in Tokyo, Japan. Thanks to mentors who have instilled in me the importance of learning and the value of knowledge. Thanks to all who have brought great joy to my life and have managed to live through the demands of my career. If it would not have been without these people, I do not think I can manage to finish my doctoral degree within three years, thank you so much.

Contents

Nomenclature

Roman symbols

C_{DPC}	Discrete particle counter concentration	[cm^{-3}]
CF	Conversion factor	[mV/mgm^3]
C_M	Mass of particle per unit volume	[mg/m^3]
C_N	Number of particles per unit volume	[cm^{-3}]
C_{PHO}	Aerosol photometer aerosol concentration	[mg/m^3]
D_{bin}	Diameter of respective channel upper or lower channel bin	[µm]
D_p	Diameter of aerosol particle	[µm]
f	Particle size distribution function	[-]
F_M	Particle size mass distribution	[-]
F_N	Particle size number distribution	[-]
I	Intensity of scattering light	[W/m^2]
I_0	Intensity of incident natural light	[W/m^2]
i_1,i_2	Intensity functions of scattered light perpendicularly and parallelly polarised	[-]
I_M	Cumulative mass concentration	[mg/m^3]
I_N	Cumulative number concentration	[-]
K	Constant used to determine leak threshold criteria in the DPC method	[-]

k	Calibration constant	[mV]
k/CF	Calibration factor	[$mg^{-1}\,m^3$]
L_{DPC}	Leakage rate evaluated by discrete particle counter	[-]
L_M	Leakage rate evaluated by mass concentration	[-]
L_N	Leakage rate evaluated by number concentration	[-]
L_{PHO}	Leakage rate evaluated by aerosol photometer	[-]
m	Refractive index	[-]
N_T	Total number of particles per unit volume	[cm^{-3}]
P	Standard penetration rate of a filter	[-]
R	Distance from centre of spherical particle	[µm]
S_1, S_2	Amplitude function	[-]
V_s	Volume of optical sensing zone of aerosol photometer	[cm^3]
W	Measure of the distribution width	[-]

Greek symbols

α	Particle size parameter	[-]
β	Semi-angle of light collection	[°]
γ	Semi-angle of projecting aperture	[°]
η	Semi-angle of dark-stop aperture	[°]
η_{eff}	Counting efficiency of discrete particle counter	[-]
θ	Scattering angle measured from direction of propagation of incident light	[°]
λ	Wavelength of incident light	[nm]
π_n, τ_n	Angular functions	[-]

ρ_p	Density of aerosol particle	[g/cm^3]
ϕ	Angle	[°]
ψ	Angle of light scattering	[°]
ω	Fraction of scattering light at angle θ collected by collecting aperture	[-]

Abbreviations

BCR	Biological Cleanroom
CMD	Count Median Diameter
DOP	Dioctyl (2-ethyl hexyl) phthalate
DPC	Discrete-Particle Counter
GSD	Geometric Standard Deviation
HEPA	High-Efficiency Particulate Air
ICR	Industrial Cleanroom
IEST	Institute of Environmental Sciences and Technology
ISO	International Organization for Standardization
JIS	Japanese Industrial Standards
MCA	Multichannel Analyser
MMD	Median Mass Diameter
MPPS	Most Penetrating Particle Size
PAO	Poly-alpha olefin
PHA	Pulse Height Analyser
RP	Recommended Practice
TC	Technical Committee

ULPA Ultra Low Penetration Air

WG Working Group

Terms and Definitions

Aerodynamic (equivalent) diameter

Diameter of a unit-density sphere having the same gravitational settling velocity as the particle in question.

Aerosol photometer

Light-scattering airborne particle mass concentration measuring instrument, which measures the amount of light scattered from a particle cloud.

Coincidence

Simultaneous presence of two or more particles in the sensing volume of a particle counter.

Dynamic shape factor

Ratio of the drag force on a particle to that on a sphere of equivalent.

Gaussian curve

Profile of distribution or curve similar that observed for the normal distribution.

Geometric standard deviation (GSD)

Measure of dispersion in a lognormal distribution (always>1).

High-Efficiency Particulate Air (HEPA)

A filter is defined as having a minimum efficiency in removing small particles (approximately equal to 0.3 µm) from air of 99.97% (i.e. only three out of 10000 particles, 0.3 µm in size, can penetrate through the filter) and an initial pressure loss of 245 Pa or less at a rated airflow.

Lognormal size distribution

Particle size distribution characterized by a bell-shaped of Gaussian distribution shape when plotted on a logarithmic size scale.

Mass (equivalent) diameter

Diameter of a sphere composed of the particle bulk material with no voids that has the same mass as the particle in question.

Mass concentration

Mass of particle in a unit volume of aerosol.

Mass median diameter (MMD)

Median particle diameter based on the particle mass.

Monodisperse

Composed of particles with a single size or a small range of sizes.

Most Penetrating Particle Size (MPPS)

Particle diameter at which the minimum efficiency occurs.

Normal size distribution

Particle size distribution characterized by a bell-shaped or Gaussian.

Number concentration

Number of particles in a unit volume of aerosol.

Optical (equivalent) diameter

Diameter of a calibration particle that scatters as much light in a specific instrument as the particle being measured.

Particle size

Diameter of a sphere that produces responses, by a given particle-sizing instrument, that is equivalent to the response produced by the particle being measured.

Particle size distribution

Cumulative distribution of particle concentration as a function of particle size.

Penetration

Ratio of the particle concentration downstream of the filter to the concentration upstream.

Polydisperse

Composed of particles with a range of sizes.

Shape factor

Factor that relates the drag force on a particle to that on an equivalent sphere.

Standard penetration

Leak penetration detected by a discrete-particle counter or aerosol photometer with a standard sample flow rate when the sampling probe is stationary in front of the leak.

Ultra-Low Penetration Air (ULPA)

A filter having an efficiency greater than 99.999% against 0.1-0.2 µm particles.

List of Figures

List of Tables

Chapter 1

Introduction

Contents

1.1 High-Efficiency Air Filtration

A High-Efficiency Particulate Air (HEPA) filters are installed at the final stage of the air filtration system in the air cleaners and cleanrooms. Until the early 1980s, HEPA filters are the most efficient air filters available. Till this day, HEPA filters are still being used in many types of cleanrooms, but as technology progresses, a cleanroom with higher cleanliness is necessary; thus, Ultra Low Penetration Air (ULPA) filters were introduced. A HEPA and ULPA filter is characterized by its particle collection (also can be defined in the inversed way called penetration) efficiency and its pressure drop at a rated airflow. According to the JIS Z 8122 [24], a HEPA filter is defined as having a minimum efficiency in removing small particles (approximately equal to 0.3 µm) from air of 99.97% (i.e. only three out of 10000 particles, 0.3 µm in size, can penetrate through the filter) and an initial pressure loss of 245 Pa or less at a rated airflow. A ULPA filter will have an efficiency higher than 99.999% against 0.1-0.2 µm particles. These filters are constructed in the same purpose to capture particles. They differ in that the filter medium used has a higher proportion of smaller fibres changing what is called packing density. Packing density will determine the resistance filter media gives towards airflow. A filter with a higher packing density will have higher collection efficiency but will result in a higher pressure drop across the filter medium.

1.1.1 Filtration Mechanisms

Most of a high-efficiency air filter is designed to remove particles of about 2 µm and smaller. These filters are mainly made of glass fibres ranging in diameter from as small as 0.1 µm up to 10 µm. These fibres are distributed randomly and crisscrossing each other throughout the depth of the filter medium, resulting in heterogeneous pore sizes. As airborne particles move through the filter medium, they will bump into the fibres, or onto particles already accumulated on the surface of the fibres. Many theoretical and experimental studies [7, 8] have been carried out on the filtration mechanisms of these fibres. The physical filtration mechanism that results in particle removal is discussed

briefly here. The three main mechanisms are impaction, diffusion and interception. The other relatively lesser importance mechanisms are sieving or straining, gravity settling and electrostatic. In a typical air filter, electrostatic effects are relatively small and usually ignored in high-efficiency air filters. The mechanism of particle capture effects particle differently depending on the particle size. Large particles are mainly being captured due to the impaction and interception while small particles are due to diffusion. These are shown diagrammatically in Figure 1.1.

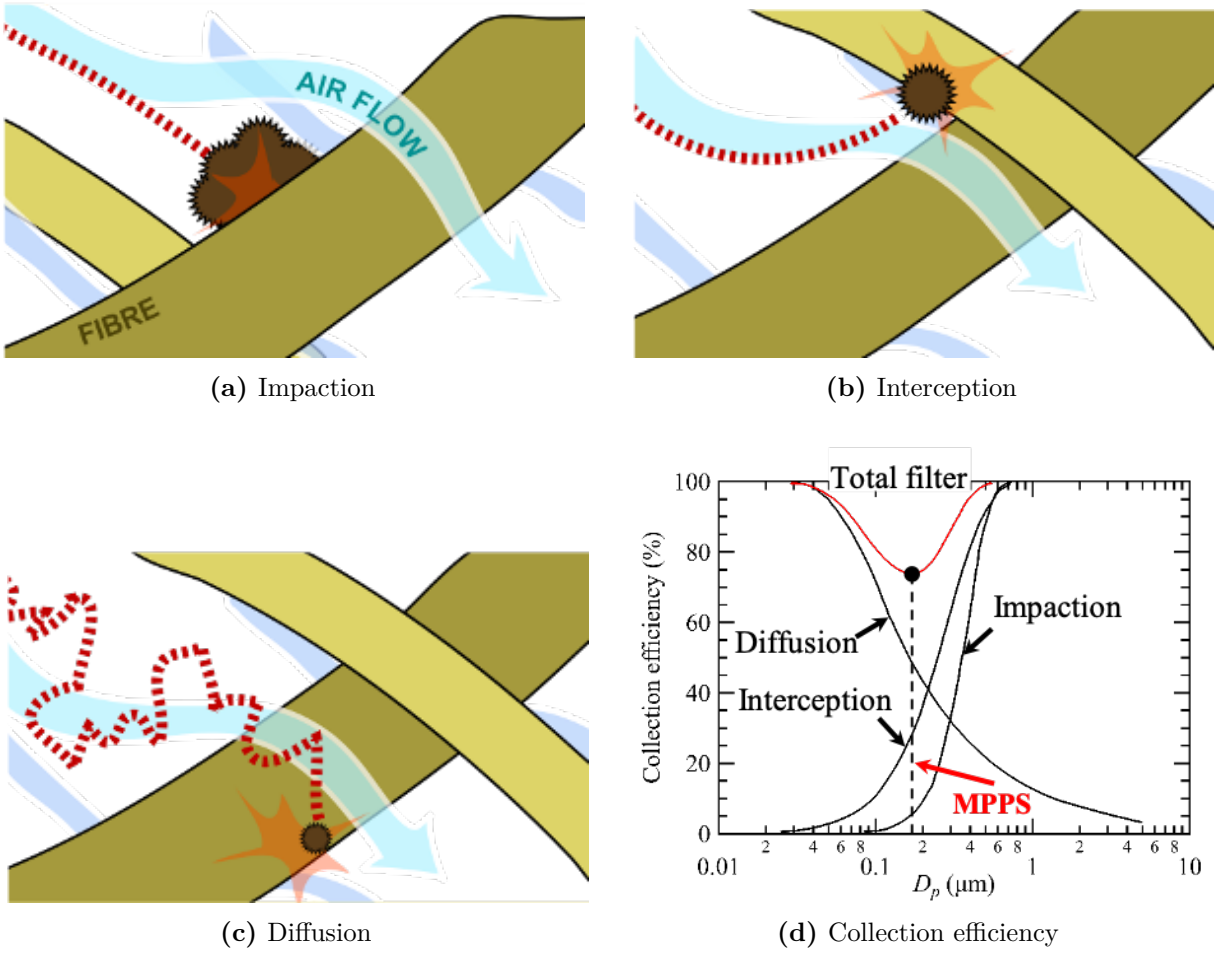

(a) Impaction

(b) Interception

(c) Diffusion

(d) Collection efficiency

Figure 1.1: Type of capture mechanism in fibrous filter with it respective value and importance. **(a)**, **(b)** and **(c)**: impaction, interception and diffusion capture mechanism of a fibrous filter media, repectively. Adapted and modified from https://upload.wikimedia.org/wikipedia/commons/b/b1/HEPA_Filter_diagram_en.svg. **(d)**: collection efficiency of each capture mechanism and total collection efficiency of a filter media.

As the particle size increases, the particles cannot follow the movement of air due to inertia. Therefore, when the gas passes around the fibre, the particles collide with

the fibre surface. This capture mechanism is called impaction and often becomes a dominant capture mechanism for particles having a particle size of several µm or more. In interception mechanism, particles that do not have enough inertia but with a large enough size will flow along with the airflow and hit fibre at around 90 degrees at where the streamline is closest to the fibre surface. As the particles become smaller, they will follow the motion of the gas, but the Brownian motion becomes more active because there are continually colliding with other particles and smaller gas molecules. Brownian motion cause small particles to hit fibre surface or particles that already captured by fibres. The collection efficiency of these capture mechanisms is shown in Figure 1.1. The total collection efficiency of these mechanisms produces distribution with the smallest value at a specific particle size and particles that are smaller or larger than this particle size exhibit lower collection efficiency value. Inversion of the collection efficiency is the penetration curve of an air filter. A particle size that having the lowest collection efficiency and the highest penetration value is called Most Penetrating Particle Size (MPPS). At this particle size, the filtration performance of an air filter is usually defined.

1.1.2 Structure of A High-Efficiency Air Filter

High-efficiency air filters are usually constructed in two ways, either deep-pleated or mini-pleated. In both methods, the filter paper is folded into a pleated form in order to increase the surface area of filtration and then fixed into a compact frame. The difference between deep and mini-pleated filter is mainly based on the number of pleat per unit length. Deep-pleated filter has a lower number of pleats compared to mini pleated filter. Due to its lower number of pleats, corrugated aluminium separators typically is fixed between filter paper pleats for support to keep its shape. Then assembled filter media is then glued into a frame which gives it final structure to be used. The structure and cross-section of deep-pleated filter media are depicted in Figure 1.2a. A deep-pleated filter is usually used in facilities with higher velocity and temperature, due to its strength and temperature resistance advantage. However, the deep-pleated filter is relatively heavy and

not flexible to any change in ventilation system design. This lead to the development of a deep-pleated filter without separators. This is done by corrugating the filter paper and fold the media directly into a pleated pack. The structure and cross-section of deep-pleated filter media without separator is depicted in Figure 1.2b.

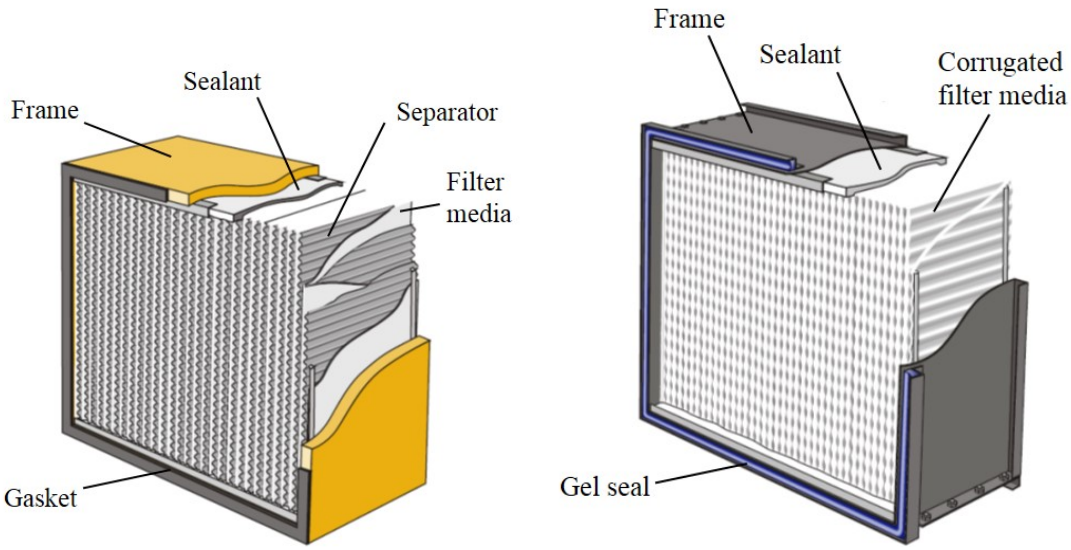

(a) with separators **(b)** without separators

Figure 1.2: Deep-pleated high-efficiency air filter. Adapted with permission from [41].

Recently, high-efficiency air filters for the cleanroom application is mainly in the mini-pleated form. Aluminium separators are not used between filter media; instead, lines of ribbon, glued strings or raised dimples run through the length of the paper medium acting as separators to maintain an air gap between each pleat. In mini-pleated filters, six to eight pleats per 2.5 cm are packed into a frame compared with approximately only two to three pleats per 2.5 cm for the deep-pleated filters. The mini-pleated filter contains much more filter medium for the same surface area so that these filters can be made more compact and significantly lighter. Mini-pleated construction is the most widely used method of construction for a unidirectional flow cleanroom because the larger media area yields a lower pressure drop than deep-pleated construction for common unidirectional flow velocities of 0.35-0.5 m/s. Such methods of construction are shown in Figure 1.3. Constructed Filters need to be passed through factory test at the manufacturer's premises

where filters are classified accordingly to their performance and later another test usually performed in field test after the installation of the filters at the user's facilities.

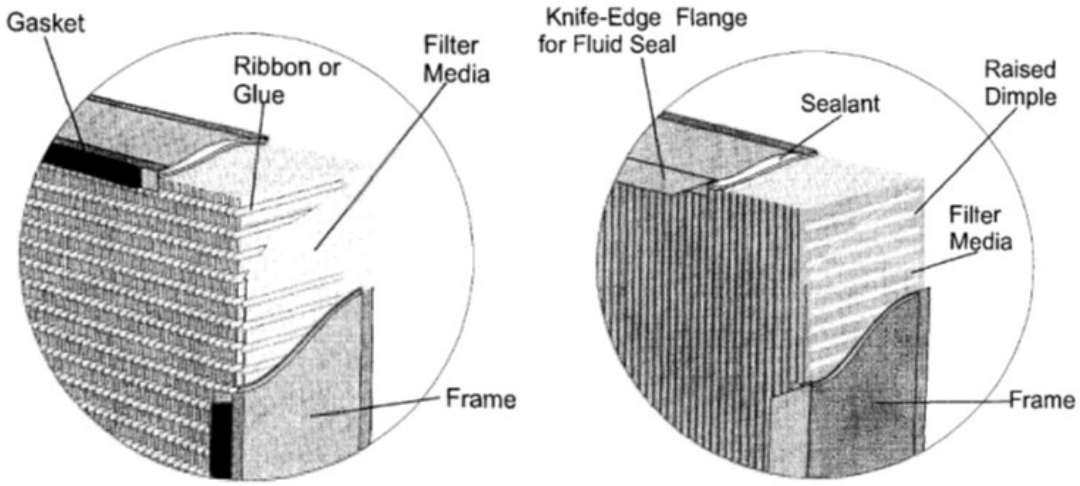

(a) with separators **(b)** without separators

Figure 1.3: Mini-pleated high-efficiency air filter. Adapted with permission from [41].

1.2 Filter Factory Test and Filter Classification

There are two different kinds of HEPA and ULPA filter integrity tests throughout the filter lifetime using for a clean space environment. Figure 1.4 illustrates the filter integrity tests done to HEPA and ULPA filters before and after the installation at the users' facilities. Filter factory test is to be made at manufacturer site uses and uses test rigs; complicated and expensive equipment. Manufacture can and must provide comprehensive testing of his products. Then after being installed at a facility, installed leak test is to be made at the point of use in cleanrooms. The latter test used simpler procedures and equipment than the factory test. Table 1.1 summarises a list of some of air filter standards practised at the manufacture's premises with different application such as nuclear air cleaning systems, cleanroom, ventilation and electric air cleaners.

In this study, we are going to be focusing on air filters used in cleanrooms that are built for the electronics industry, hospital surgery rooms and medicine or food production which require very high level of cleanliness. The commonly used and generally known

standards for filter factory testing and classification are EN 1822-1: 2009 [9] (Europe), the RPs of the IEST (USA). Bin Zhou et al. [42] provided detailed discussions on these standards and comparison between them. Table 1.2 lists filter class and type for both EN 1822-1: 2009 [9] and IEST RPs with their respective filter performance classification. A brief description of these two standards will be given in the next subsection.

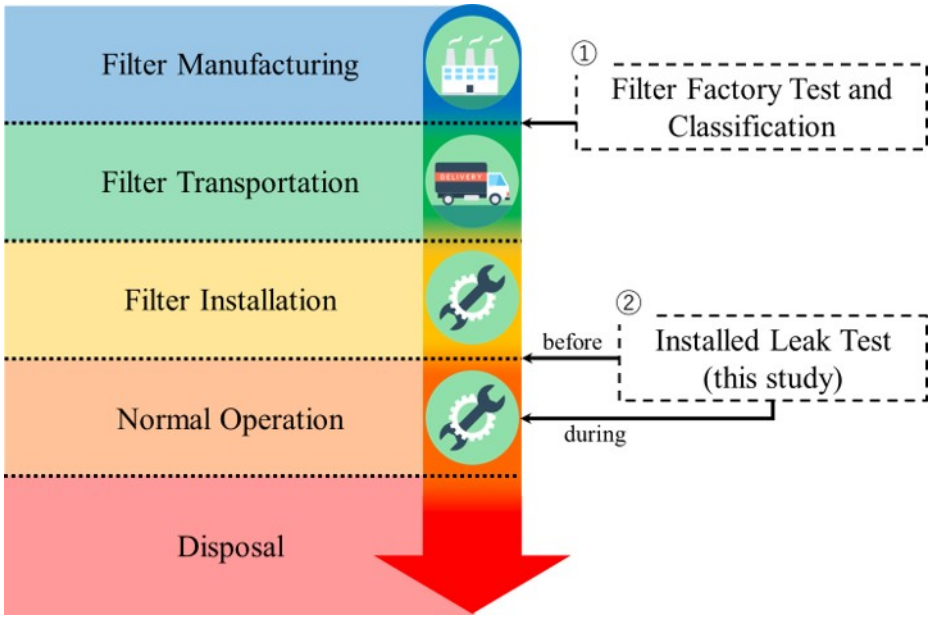

Figure 1.4: A typical flow of Filter integrity test went through by HEPA and ULPA filters before and after installed in a facility.

Table 1.1: International standard concerning HEPA and ULPA filters factory test.

Country/region	Standard	Title
Japan	JIS Z 4812 JIS B 9927	HEPA Filters for radioactive aerosols Cleanroom- Air filters- Test methods
USA	IEST-RP-CC001 MIL STD-282	HEPA and ULPA Filters Filter units: Performance Test Methods
Europe	EN 1822	High-efficiency air filters (HEPA and ULPA)

1.2.1 EN 1822: 2009

The latest version of EN 1822: 2009 has five parts:

Table 1.2: EN 1822-1: 2009 [9] and IEST-RP-CC001 filter classifications.

EN 1822						IEST RP-CC001						
Class	Reference Particle Size µm	Overall value (%)		Local value (%)		Type	Test Method	Reference Particle Size	Overall value (%)		Local value (%)	
		Collection	Penetration	Collection	Penetration				Collection	Penetration	Collection	Penetration
E10	-	≥85	≤15	N/A	N/A	-	-	-	-	-	-	-
E11	-	≥95	≤5	N/A	N/A	-	-	-	-	-	-	-
E12	-	≥99.5	≤0.5	N/A	N/A	-	-	-	-	-	-	-
H13	MPPS[a]	≥99.95	≤0.05	≥99.75	≤0.25	A	MIL-STD-282	0.3[b]	≥99.97	≤0.03	N/A	N/A
						B						
						E						
						H	IEST RP-CC021	0.1-0.2 or 0.2-0.3[c]				
						I	IEST RP-CC007					
						C	MIL-STD-282	0.3[b]	≥99.99	≤0.01	≥99.99	≤0.01
						J	IEST-RP-CC007	0.1-0.2 or 0.2-0.3[c]				
H14		≥99.995	≤0.005	≥99.975	≤0.025	K			≥99.995	≤0.005	≥99.992	≤0.008
						D	MIL-STD-282	0.3	≥99.999	≤0.001	≥99.99	≤0.005
U15		≥99.9995	≤0.0005	≥99.9975	≤0.0025	F	IEST RP-CC007	0.1-0.2 or 0.2-0.3[c]	≥99.9995	≤0.0005	≥99.995	≤0.0025
U16		≥99.99995	≤0.00005	≥99.99975	≤0.00025	G		0.1-0.2	≥99.9999	≤0.0001	≥99.999	≤0.001
U17		≥99.999995	≤0.000005	≥99.9999	≤0.0001							

[a] MPPS = Most Penetrating Particle Size.
[b] Mass median diameter particles (or with a count median diameter typically smaller that 0.2 µm).
[c] Use the particle size range that yields the lowest efficiency.

1. EN 1822-1: Classification, Performance Testing and Labelling
2. EN 1822-2: Aerosol Production, Measuring Equipment and Particle Count Statistics
3. EN 1822-3: Testing Flat Sheet Filter Media[1].
4. EN 1822-4: Determining Leakage of Filter Elements
5. EN 1822-5: Determining the Efficiency of Filter Elements

EN 1822-1: 2009 [9] is based on an MPPS. MPPS has been previously discussed in section 1.1. It applies to ULPA filters as well as HEPA filters. The efficiency is determined by particle number counting. If the aerosol is quasi-monodispersed, the aerosol generated has to have a particle size near MPPS. If the aerosol is polydisperse its fractional efficiency counting is done to determine MPPS. MPPS is determined from flat sheet testing of the filter medium in accordance with EN 1822-3. The filter is tested at this predetermined particle size. The E classes (E10, E11 and E12) were designated as efficiencies (>85%), but are in the sub-HEPA in their ratings (<99.95%). EN 1822-1: 2009 [9] continued to rate H13 and H14 as HEPA class filters and U15, U16 and U17 as ULPA class filters.

1.2.2 IEST Recommended Practice (RP)

The IEST issues RPs for testing HEPA and ULPA filters. Below are related RPs:

1. IEST RP-CC-001.5: "HEPA and ULPA Filters": provides a glossary, definitions and classifications of HEPA and ULPA filters, test instruments and requirements for other RPs. This RP describes 11 levels of filter performance and six grades of filter construction.
2. IEST RP-CC-007.2: "Testing ULPA Filters": provides the test methodology for the overall efficiency of ULPA filters using particle counter(s). The penetration range of this procedure is 0.001-0.0001%.
3. IEST RP-CC-021.3: discusses test methods for physical and filtration properties of HEPA and ULPA filtration media.

[1]EN 1822-3 is used for flat sheet testing to determine most penetrating particle size (MPPS)

The testing of HEPA filters is different that ULPA filters. The RPs recommended that the less efficient HEPA filters be tested with an aerosol photometer and the efficiency based on 0.3 µm particles. The assumption is that the particles are more or less the same diameter. The RPs recommendation for ULPA filters is that they are being tested for a fractional efficiency test using a particle counter. The size range for the particles is 0.1-0.2 µm. There is also a filter medium identified as a Super ULPA which efficiency is rated at 99.9999%. MPPS is recommended as the rating method for this type of filter.

1.3 Installation of High-Efficiency Air Filters in Cleanroom

As mentioned briefly by name at the previous section, cleanrooms can be classified by airflow type into unidirectional and non-unidirectional flow type cleanroom. Both of these cleanrooms use different configuration of high-efficiency air filter at the upstream of the air ventilation system. Filters are being installed at the ceiling of cleanrooms with various installation type. Figure 1.5 type shows two examples of a conventional filters installation type in cleanrooms. The first type is called gel-seal type. This type commonly used in a central system type cleanroom which has been widely adopted since the early days of the cleanroom. High-efficiency air filters are installed by covering a lot of surface area of the ceiling at the plenum chamber. The indoor air pressure at the downstream side of the filter on the ceiling has a higher pressure compared to the upstream side of the filter, so it is necessary to pay close attention to unfiltered air leakage from the filter frame. As a result, method of ensuring the airtightness which is highly important for leak countermeasure by inserting a packing between a filter housing and an installation ceiling surface and a method of improving airtightness by pouring gel into the channel on the filter, or mounting frame or ceiling grid has been put into practical use.

The second system is called the Fan Filter Unit (FFU) which is a pair of high-efficiency air filter, and a small blower unit is simply set on the ceiling. This creates lower pressure at the upstream side of FFU compared to the downstream side, thus, significantly reduced

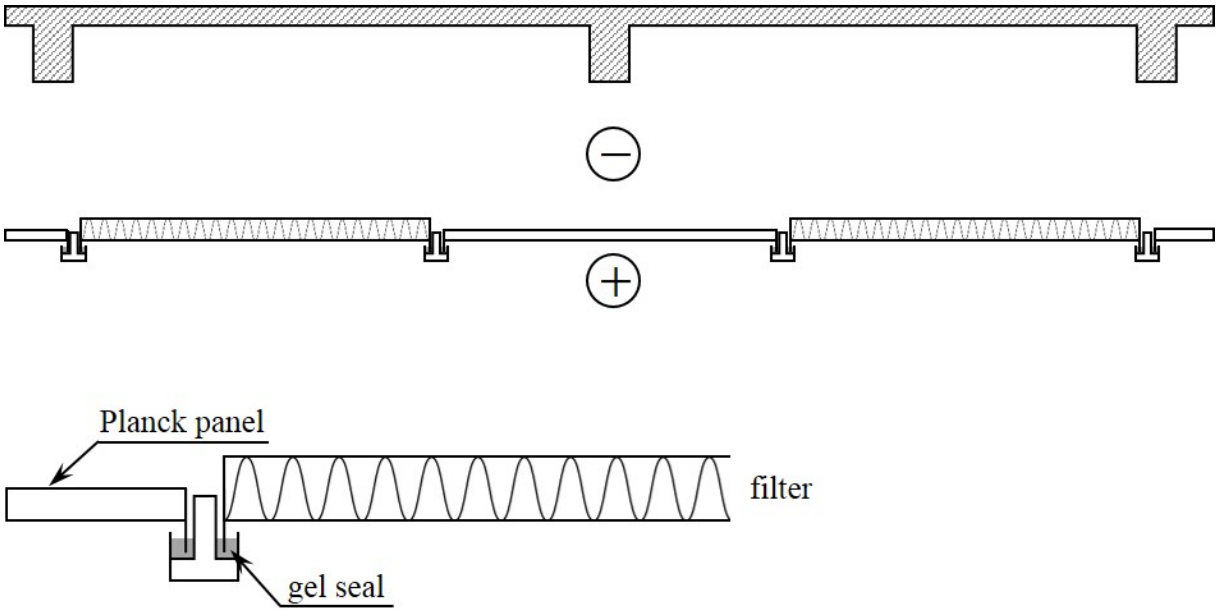

(a) Gel-seal type

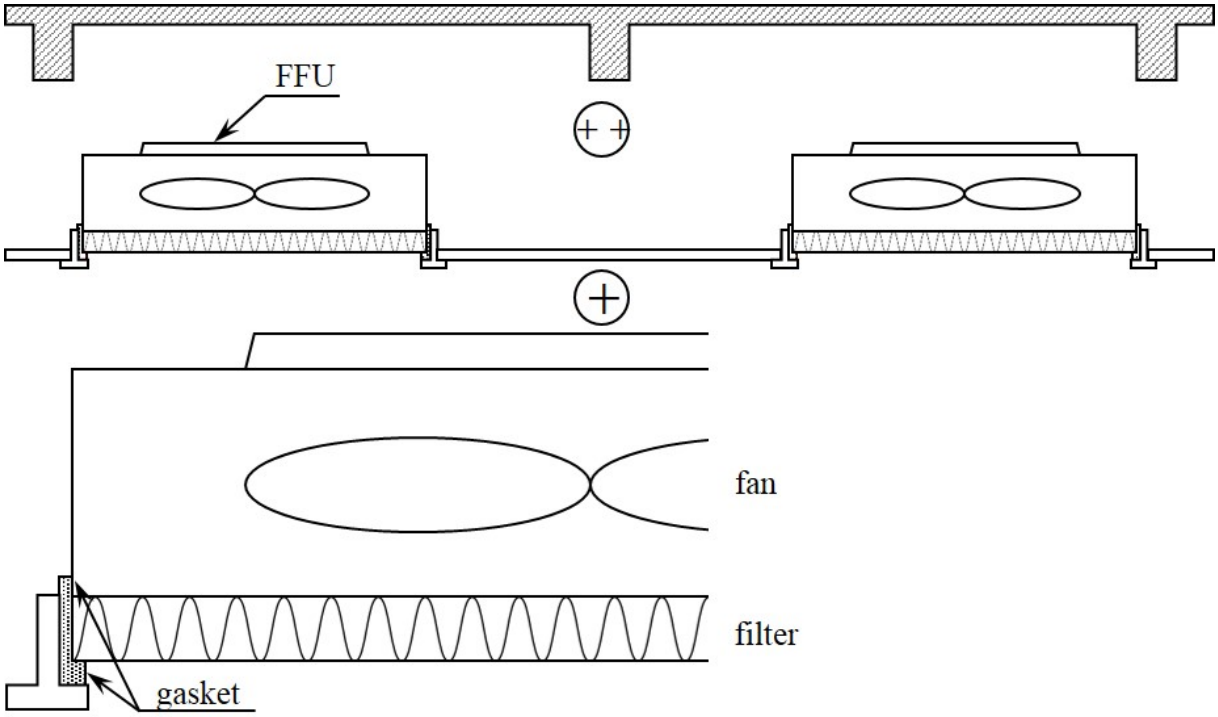

(b) FFU type

Figure 1.5: Filter installation type in cleanrooms.

the importance of leakage countermeasures. Besides, this also will give more freedom for the layout change in the cleanroom. The FFU type installation type emerged in the cleanroom world in the latter half of 1980 and until now most of the current cleanrooms adopted FFU unit for the air ventilation system.

1.3.1 Causes of Filter Leaks in Cleanrooms

At the time before the shipment from filter manufacturer factory, all filters were inspected and guaranteed to have specified performance, but any improper treatment during transportation, filter installation and cleanroom operation, filter surface or frame may be damaged and causing leaks. In addition, even for filters that have been used for a long period of time may produce leaks due to ageing and deterioration. These possible leak factors and actual damage cases are shown in Figure 1.6.

Table 1.3: Failure mode

Failure Mode	Number	% of Total
Failure mode unknown	702	64
Handling or installation damage	213	19
Frame failure	65	6
Gasket or seal failure	62	6
Media rupture	54	5
Filter construction	6	<1
Media to frame sealant failure	3	<1

Furthermore, reports concerning the reliability and performance characteristics of HEPA filters have been reported in several studies supporting all type of leak factors stated in the previous paragraph. For example, Carbough [5] reported the results of a survey of HEPA filter applications and experience at the Department of Energy (DOE). Table 1.3 summarises the findings of this study with reference to the filter failure modes reported in this study. Filter failures occurred with approximately 12% of all installed filters. Of these failures, most occurred for unknown or unreported reasons with 64%. Handling or installation damage accounted for an additional 19% of reported failures. Media ruptures,

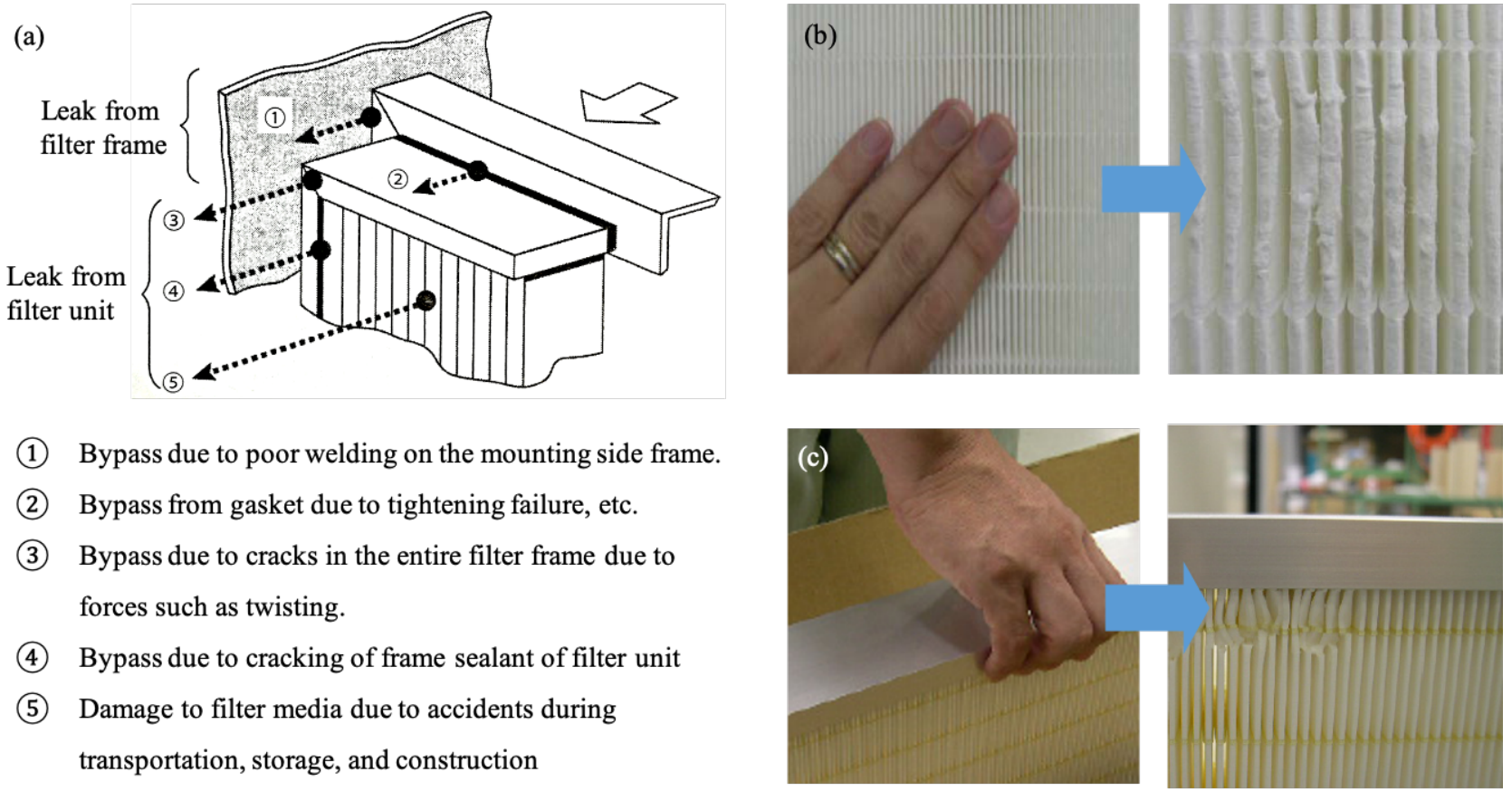

① Bypass due to poor welding on the mounting side frame.

② Bypass from gasket due to tightening failure, etc.

③ Bypass due to cracks in the entire filter frame due to forces such as twisting.

④ Bypass due to cracking of frame sealant of filter unit

⑤ Damage to filter media due to accidents during transportation, storage, and construction

Figure 1.6: The possible leak factors and places with the right side shows the actual example of damages during installation.**(a)**: place of a possible leak. **(b)** and **(c)**: example of damage occurred during installation of a filter media.

filter frame failures and seal failures each accounted for approximately 5 to 6% of the reported failures. Except for the 19% resulting from handling or installation damage, the other modes are likely due to deterioration and ageing effects which accumulates up to 81%. Most of the filter leaks associated with damage from handling and installation or ageing and deterioration are considerably larger than the normal undamaged filter. To put into perspective, when a filter surface is scanned by a particle counter, there is almost no count at the undamaged part of a filter, while a count in the order of several hundred to thousands is detected at the damaged part of a filter.

1.4 Installed Filter Leak Testing at Cleanrooms

A filter leak test is performed after filters were installed in a cleanroom. This is to ensure that HEPA or ULPA filters are free of damages and small leaks described in the previous section. ISO 14644-3: 2005 [21] (International) and IEST RP-CC0034 (USA) are two very commonly known and generally practised standards. In particular, ISO 14644-3: 2005 [21] is the first International standard established for the installed filter leak test which gives cleanroom community a common standard to work to. Before ISO 14644-3: 2005 [21], there was no international standard on the installed filter leak test, but due to progress in technology, there is a need for international standard as a base for contamination control and monitoring. This is really important for a country that does not have any related standard locally available at that time, especially japan which experiencing fast-growing and mass-production in electronic devices industry. Without any locally or internationally available standard, cleanroom users did not have any reliable method for an installed filter leak test. In the industry such as the production of semiconductor devices, a huge cleanroom with a floor area over 1000 m^2 has been built. Furthermore, it is near impossible to do a leak test manually. Therefore, autonomous robots have been actively developed.

In ISO 14644-3: 2005 [21], two conditions of Installed filter leak test are presented: a final filter installed at a predetermined location in a cleanroom and a system of air supply

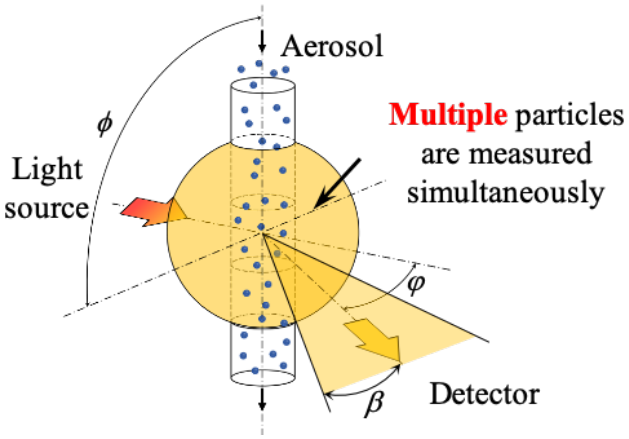

Figure 1.7: An illustration of the internal components and measurement principle of an aerosol photometer.

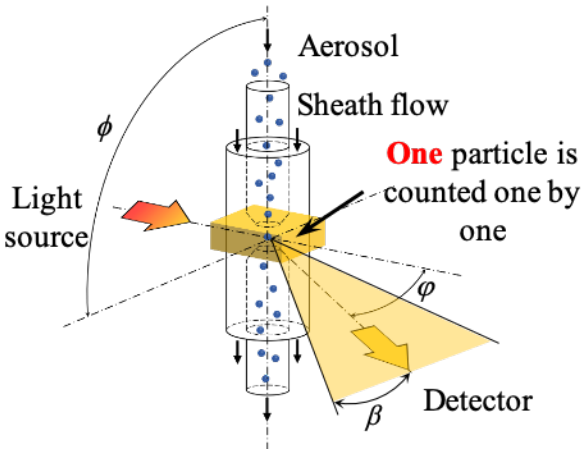

Figure 1.8: An illustration of the internal components and measurement principle of a discrete particle counter.

or duct used for testing. In this study, we will be focusing on the former condition. Two different leak detection methods are given in annexe B.6 of the standard. The procedure B.6.2 for installed filter system leak scan test with an aerosol photometer and the procedure B.6.3 for installed filter system leak scan test with a Discrete Particle Counter (DPC). Both test methods are performed by introducing an evenly distributed challenge aerosol at upstream of the filter unit and scanning immediately at the downstream side of the filter gasket, filter frame and filter media. The Figure 1.9 shows the measurement method diagrammatically using an aerosol photometer and DPC, respectively.

The first in situ test method is the traditional aerosol photometer test. Figure 1.7 shows a simple illustration describing the general internal components of an aerosol photometer.

This is commonly known as the DOP integrity test and utilizes the aerosol photometer as the primary measuring instrument and an aerosol generator to produce a uniformly distributed aerosol challenge at the upstream of filter media. Historically, this method has been used since the 1950s and appears in many different standards throughout the world such as IEST RPs. The aerosol photometer uses light scattering techniques and scattered an ensemble of particles and a photomultiplier tube as its detection method. The scattered light is directly proportional to the aerosol mass concentration. The instrument is a continuous real-time detector and usually allows a pre-set alarm point to be set for easy detection leaks. An upstream concentration is taken, and the aerosol generator is adjusted to achieve a challenge level approximately 10 mg/m^3 to 100 mg/m^3 with a mass median particle diameter (MMD) typically between 0.5 µm to 0.7 µm and a geometric standard deviation (GSD) of up to 1.7. The aerosol photometer method requires the upstream challenge aerosol to be set into 100% as a reference for the downstream concentration measurement. The downstream concentration measurement of the filter is then directly scanned using a probe and turns into percentage penetration. A leak is detected when the downstream measurement is larger than 0.01% of the upstream concentration.

The second method offered in the standard is the particle counting method. Figure 1.8 shows a simple illustration describing the general internal components of a DPC.This method also requires is evenly challenged with a known recorded concentration of aerosol, an aerosol diluter (optional if aerosol generator could not produce concentration low enough) and a discrete particle counter (DPC). This method is relatively new and uses DPC. The DPC uses the light scattering technique to count particles by measuring the peak light scattered height of the individual particle passing through the beam sensing area. It cannot count two particles in the sensing area at the same time (known as coincidence counting), and therefore a diluter has to be used to measure the upstream aerosol challenge if aerosol generator could not produce concentration low enough. Due to its reliance on a low concentration, the upstream challenge aerosol concentration is determined based on relatively complex sets of mathematical relation with a count median

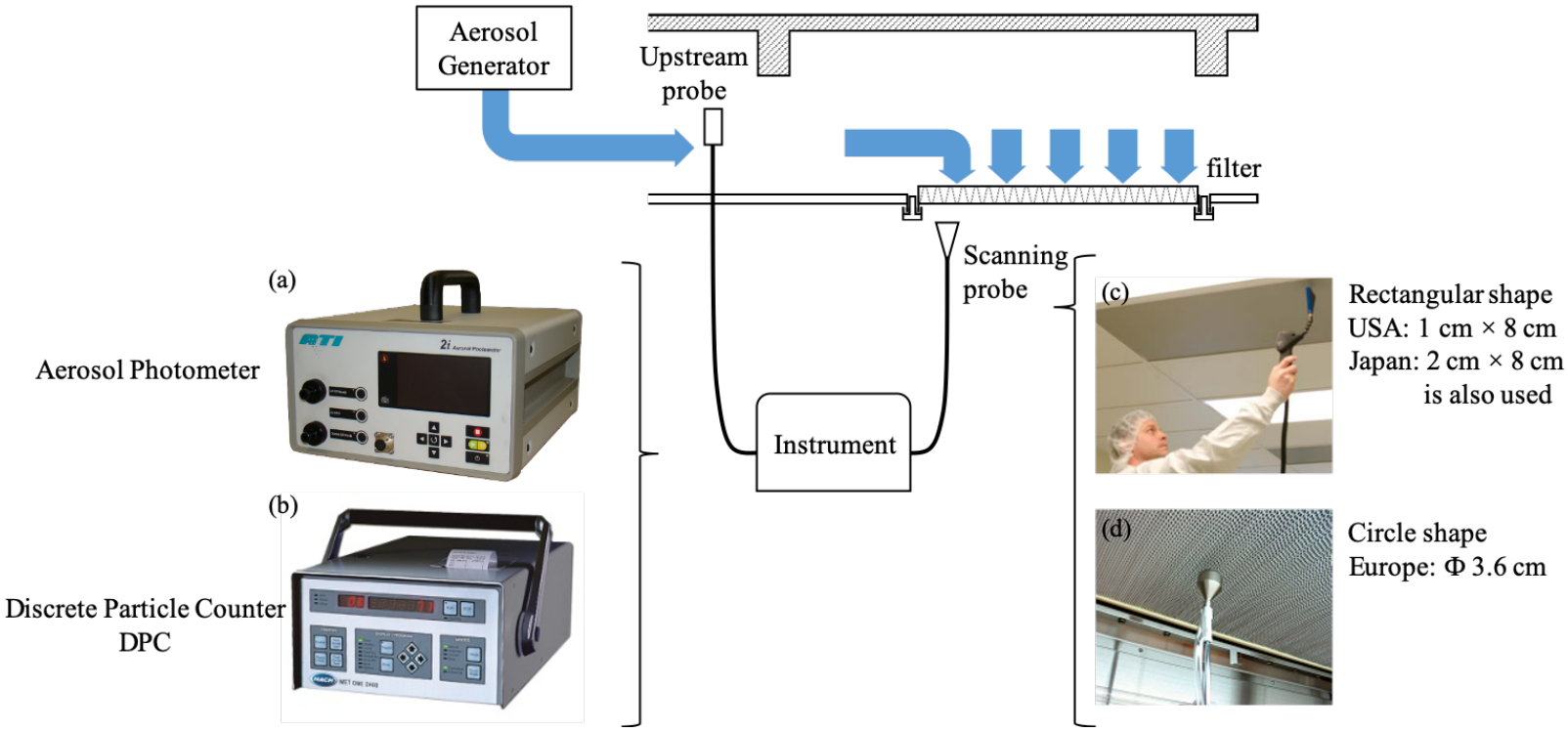

Figure 1.9: Illustration of currently available leak test arrangement in aerosol photometer method and DPC method. **(a)**: example of an aerosol photometer model adapted from http://www.nextech.com.my/product/ati-aerosol-photometer-2i-photometer/. **(b)** : example of an DPC model adapted from https://ca.hach.com/asset-get.download.jsa?id=7672738047. **(c)**: rectangular scanning prob used in USA and Japan adapted from https://www.mtstesting.com/hepa-leak-testing.php. **(d)**: rectangular scanning prob used in Europe adapted from https://www.kanyaku.co.jp/business/clean_area.html.

particle diameter (CMD) typically between 0.1 µm to 0.5 µm and a GSD of up to 1.7. In the DPC method, the leak threshold uses the value obtained by multiplying the MPPS of the test filter with a factor K (usually K=10) as the threshold value. When the scanning probe scanning at the immediate filter downstream, a leak is detected when particles exceed the 95% upper confidence limit of the Poisson distribution. When a possible leak is detected the stationary re-measurement should be performed.

1.5 Problems in ISO 14644-3: 2005 [21]

The aerosol photometer has a long history while DPC method is relatively new and far from perfect. For example, at the time of this standard establishment, many of the members who created this standard did not truly understand the characteristics of leaks occurred in the field test of an installed filter as previously mentioned in section 1.2. Because of this matter, a very strict and unpractical test similar to the filter factory test (section 1.2) at the time before the shipment was established. Since the establishment of this standard, below are problems encountered by the users presented in the DPC method:

Problem 1: MPPS as the test particle size

In the DPC method, the test particle size is MPPS but most of the penetration rate for filter specification are available at a particle size of 0.3 µm. Besides, the penetration rate at MPPS is often one order larger than at 0.3 µm and due to this, there is a possibility that a small leak will not be able to be determined.

Problem 2: Short sampling time interval

The sample acquisition time stated in ISO 14644-3: 2005 [21] is about 0.4 second. A normal commercially available DPCs have the minimum sampling about 1 second, which makes this standard inapplicable.

Problem 3: Impractical ULPA filter leak test

In a cleanroom where ULPA filters are installed, applying the threshold value determined from the penetration rate of the filter, it is necessary to set the upstream

concentration to a considerably high concentration making an initial condition difficult to set. In addition, from the viewpoint of contamination control, it is not desirable to produce a very high upstream concentration more than necessary. Subsequently, lower concentration means longer sampling time to produce a statistically valid result.

Problem 4: Difficulty in parameter determination

All parameters are described so that they can be freely selected to some extent by the user. Conversely, this further complicates the selection of test parameters. In addition, there are parameters such as upstream concentration which it is more reasonable to perform reverse calculation after pre-determine first the allowable count. This also creates confusion for users in knowing the order of determining the parameters if the whole calculation is not well understood.

Problem 5: Different leak threshold criteria depending on filter grade

In order to set the threshold, users need to know the performance of the installed filters. However, in many cases, users will not know this information. Therefore, an additional test needs to be done to determine the filter's performance which further creates complexity and adding unnecessary procedure.

Suzuki et. al. [36] addressed problems 1 to 4 and but did not cover problem 5 in their work. They gave a new proposal from a practical viewpoint to problems 1,2 and 3. Meanwhile, for problem 4, they only gave countermeasure suggestion without proposing any new method unlike in the previously mentioned problems. The summary of the proposal respectively to each problem is written below:

Problem 1 :

They experimentally proved that leaks could not be detected even when K=10 when applying MPPS as the test particle size. A designated pinhole leak was artificially produced and they found that test particle size at 0.3 µm or larger are observed to clearly differentiate between normal filter and damage filter even when K=10 is used.

As a result, they proposed 0.3 µm or larger shall be used as the test particle size instead of MPPS.

Problem 2 :

Based on the Poisson distribution, they proposed a series of test conditions that can detect the possibility of a leak according to the number of acceptable counts occurred during the scanning process, and the existence of leaks is being alarmed by a sound of a buzzer of the measuring instrument.

Problem 3 :

In the case of ULPA, they proposed a new evaluation method based on the specification of the cleanroom cleanliness class monitoring concept. For example, in an Industrial Cleanroom (ICR) used in the semiconductor processing process, it is only necessary to ensure the cleanliness of the cleanroom in the entire ventilation system. If the cleanliness inside the ventilation system is maintained and satisfied, it can be considered that there will not be any failure happened at the filter downstream and passed the filter leak test.

Problem 4 :

They proposed to simplify the selection of test conditions by fixing some parameter values.

Since 2010, ISO organized a working group (WG) consists of Technical Committee (TC) who represented their respective standard organisations to discuss the revision of the ISO 14644-3: 2005 [21] named ISO/TC209. Since then, with regards to problems 1 to 4, in order to solve the problems related to the installed filter leak test, they decided to incorporate the results presented in Suzuki et al. [36] Some adjustments were made to fit the requirement of general cleanroom community. However, for problem 5, Suzuki et al. [36], did not address this problem thus no solution was provided. Revision for each problem are summarized as below:

Problems 1 and 2 :

The test particle size is set to 0.3 µm, and the possibility of a leak is determined

when the measuring instrument counts one or more counts during the scanning process and the presence or absence of a leak is alarms by a buzzer sound.

Problem 3 :

Prior to the paper by Suzuki et al. [36], ULPA filters were mainly used in cleanrooms for manufacturing semiconductor devices (ICR). However, since then, the number of cleanrooms in the biological (BCR) field started using ULPA in their air filtration system. In BCR the contamination control is very strict and the method proposed by Suzuki et al. [36] is not suitable to be applied. Therefore, it was cancelled and not incorporate into ISO 14644-3: 2005 [21].

Problem 4 :

Selection of test conditions is greatly simplified by fixing the probe size and scan speed.

Problem 5 :

This problem was based on the result produced by this study. As a result, the Technical Committee decided to use leak detection threshold of 0.01% (same as used in aerosol photometer method) of the upstream challenge aerosol concentration for the H14 filter grade and higher and a 0.1% threshold of the upstream challenge aerosol concentration for the H13 and lower.

1.6 Research Motivation and Problem Statement

This dissertation is the product on tackling problem 5 found in the current ISO 14644-3: 2005 [21]. This problem is have been circling around for a long time in the cleanroom community. This is because complexity in the DPC method presented in current ISO 14644-3: 2005 [21] always been critiqued by the non-DPC country users. The DPC method for the installed leak test is relatively new compared to the traditional aerosol photometer method. It is far from perfect and needs to be evaluated time by time to make it more user-friendly and practical.

The other thing regarding the difference in the leak threshold criterion between aerosol photometer and DPC method, currently available threshold for both of these threshold mentioned in ISO 14644-3: 2005 [21] are inconsistent with some of the locally available standards that came before ISO 14644-3: 2005 [21]. For example, the same 0.01% threshold criterion has been long used for both aerosol photometer and DPC as in IEST-RP-CC034.4 in the United States of America. However, to our knowledge, the basis of this implementation is not mentioned in any of the filter leak test-related Recommended Practice series by the IEST organisation which remain suspicious and need to be studied and explored. This suspicion is natural since the leak evaluation methods provided are different between these two methods. Aerosol photometer evaluates leak rate in term of a ratio of the total mass concentration of the existing challenge aerosol at the downstream and upstream side of a filter media, while DPC evaluates leak rate discretely in term of a ratio between the number concentration of a particular particle size or range at the downstream and upstream of a filter media. In logic, difference in the leak evaluation method between these two instruments will not produce similar a degree of value.

Although many studies have been conducted on the differences in measurement sensitivity of aerosol photometer and DPC, however, so far relatively only a few studies have been conducted on the comparison between these two instruments in the context of a leak test of an air filter and those studies produced inconsistent results with each other. Some researchers [10, 14, 40] observed a good correlation between DPC, while others [12, 26] found a significant difference between these two instruments. This contradiction probably caused by the difference in the limitation of the experimental conditions. Most of these studies where done before the establishment of the ISO 14644-3: 2005 [21]. Which means the experiments were not done based on the range of the allowable condition stated in the ISO 14644-3: 2005 [21]. This remains the case for current ISO 14644-3: 2005 [21] which is very few literature dedicated to test and challenge the validity of ISO 14644-3: 2005 [21].

1.7 Research Aim and Objective

The main aim of this dissertation herein is to unify the leak threshold criteria for the installed filter leak test in cleanrooms for aerosol photometer and DPC method. The idea is to use the same leak threshold criterion of aerosol photometer in the DPC method. The focus of this dissertation circulating around the fundamental differences between aerosol photometer and DPC method and extended to the use for various DPC specifications. In order to achieve the main aim, three key objectives are being set as below,

Objective 1 :

To study the difference between aerosol photometer and DPC on the measurement unit and leak evaluation method.

Objective 2 :

To study the difference between aerosol photometer and DPC on the instrument response.

Objective 3 :

To determine the Leak rate for various DPC specifications.

As a final remark, this dissertation intends to build the underlying platform on a uniform leak threshold criterion to improve the complexity present in the current ISO 14644-3: 2005 [21] standard. As such, we have tried to communicate the work as plainly and clearly as possible through the use of diagrams, charts and simple mathematical modelling. We have also included additional detail to show where the work could be extended, in the hope that this dissertation will form a point of reference for future work.

1.8 Dissertation Outline

This dissertation consists of five chapters.

Chapter 1: Introduction

This chapter sets the tone and direction of this dissertation. In this chapter, we present the background, motivation, problem statement and objectives.

Chapter 2: Measurement unit and Leak Evaluation Method

In this chapter, we investigate the comparison between aerosol photometer and DPC method on the measurement unit and leak evaluation methods (**Objective 1**). The comparison is done solely based on the measurement unit. Aerosol photometer and DPC are represented by mass and number concentration, respectively. We also study two leak evaluation method used in DPC method, which is discrete and cumulative leak evaluation method. The sensitivity of leak rate values for different filter grade (H13 to U16 according to EN 1822-1: 2009 [9]) by aerosol photometer and DPC based on the difference in measurement unit and leak evaluation method according to the installed filter leak test requirements stated in ISO 14644-3: 2005 [21] are discussed..

Chapter 3: Instrument Responses

In this chapter, we extend the comparison made in Chapter 2 by considering the instrument responses (**Objective 2**). We model the instrument response of aerosol photometer and DPC to reproduce the real measurement value. A theoretical model of the response of aerosol photometer and DPC is described, and then, as in Chapter 2, the sensitivity of leak rate values by aerosol photometer and DPC for different filter grade are discussed.

Chapter 4: Evaluation by Differen DPCs

In this chapter, we revisit the model of DPC response (i.e counting efficiency function) proposed in Chapter 3 and explore the leak evaluation by different DPCs (**Objective 3**). Extending the calculation made in Chapter 3, we calculate the leak rate values within the allowable range of the counting efficiency for a DPC stated in ISO 21501-4: 2018 [22].

Chapter 5: Conclusion and Future Work

This chapter summarizes and concludes the dissertation, stating the benefits, limitations and difficulties. Finally, the research direction for possible future works is suggested.

Chapter 2

Measurement Unit and leakage evaluation Method[1]

Contents

[1]Content of this chapter is submitted for publication by Mohd Nor, M. A. B. and Suwa Y. in an article entitled "Study on the Possibility of a Unified Criterion for a Leakage Test of an Installed Filter System [31]"

2.1 Introduction

Aerosol instrument does not only differ in term of different measuring technique (which will be further discussed in Chapter 3 that is utilised to quantify aerosol, but also differ on how they "weigh" the particle size. In the case of aerosol photometer and DPC, a different measurement unit is being used for these two instruments. The aerosol photometer measures particles in term of mass concentration, whereas DPC measures particles in term of number concentration. The way mass and number concentration measure sample of particles are very different. Furthermore, in ISO 14644-3: 2005 [21], the leak evaluation method is also different. The aerosol photometer measures aerosol by the total mass concentration of a sample, in a way, evaluated the leak cumulatively.

In contrast, DPC sizing aerosol into discrete groups and evaluates leak discretely which we called as discrete leak evaluation method. With a different measurement unit and leak evaluation method between aerosol photometer and DPC, different leak rate value is expected as reported by many studies. The difference between these two instruments needs to be critically studied in order to find a possible common ground on the evaluation of leak between these two instruments.

As mentioned in Chapter 1, the downstream concentration equal to 0.01% of the upstream concentration has been used as the threshold criterion for the leak detection in aerosol photometer method. Therefore, in this chapter, based on the comparison between measurement unit and leak evaluation method, we explore the possibility of unified threshold criteria for DPC method using the same threshold criterion as in the aerosol photometer method. The comparison is just based on the measurement unit, and the instrument response is not considered and will further address in Chapter 3. In this chapter, aerosol photometer and DPC are being represented by mass concentration and number concentration, respectively. Furthermore, we will test the difference in leak evaluation methods for the DPC method using discrete and cumulative leak evaluation method to find which one produces comparable values to the aerosol photometer method.

2.2 General Knowledge and Terms in Aerosol Research

Before moving forward, it is appropriate to highlight some of the important general knowledge and terms used throughout this dissertation.

2.2.1 Definition of Particle Size

In the studies of aerosol, particle size is often expressed in terms of equivalent diameter to represent the specific property or behaviour of interest in a given system. For a spherical particle, the geometric diameter is simply used to define the size whereas, for an aspherical particle, the equivalent diameter is used. The most common one is the aerodynamic diameter which is defined as the diameter of a spherical particle of a unit density having the same terminal settling velocity as that of the particle in question. The aerodynamic diameter is useful to describe particles in a system where the inertial behaviour dominates such as inertial impactor and cyclones.

For devices that use light scattering technique as the principle of the measurement such as aerosol photometer and DPC, an optical diameter is commonly used. The optical diameter is defined as the diameter of a calibration particle scattering the same amount of light in a specific instrument as the particle being measured. An extensive calibration is needed before any measurement because the scattering properties of the particles are very dependent on the physical size, chemical composition of the particles, and the optical configuration. According to ISO 21501-4 [22], polystyrene latex (PSL) is normally used by manufacturers to calibrate the DPC. Therefore, particle diameter reported by the DPC in many cases is the PSL equivalent diameter. There are also equivalent diameters based on a particle property such as mass, volume, or surface area. These equivalent diameters often used in the chemical reaction and multiphase flow-related field. It is important to know the details of the data represented by a particular instrument when comparing measurements between different instruments.

2.2.2 Particle Concentration and Size Distribution

Particle concentration is used to quantify particles in a particular aerosol property of particle suspension per unit volume of gas. Mass and number concentration are two of the most commonly used types of particle concentration. Particle concentration is defined as the number of particles per unit volume of gas with a unit often denoted as particles/cm^3. In contrast, mass concentration is defined as the mass of particles per unit of volume of gas with unit such as mg/cm^3.

For a monodisperse aerosol, conversion between different measurement units is rather simple. For example, assuming a spherical particle with a diameter of D_p, the mass concentration can be obtained from

$$M = \frac{\rho_p \pi}{6} D_p^3 \quad . \tag{2.1}$$

Then, for a sample consists of N number of monodisperse aerosol having the same diameter of D_p, the mass concentration for the sample is

$$M = N \times \frac{\rho_p \pi}{6} D_p^3 \quad , \tag{2.2}$$

where, ρ_p is the particle density. In a very controlled experimental setup, a particle population with a relatively high monodispersity can be artificially generated. However, this is not the case for most of the natural and artificial particle systems. They have a certain degree of dispersity and exhibits a range of particle sizes that we called as polydisperse aerosol. It is more complicated to do conversion between different measurement units. This is because a different measurement unit might exhibit different particle size distribution. Different measurement units weigh the particle size differently when they construct a size distribution.

When sampling a population of particles, particles are "sized" and "counted" into different discrete groups, we called bins. These bins then plotted into a histogram with the particle "number" on the y-axis versus particle size on the x-axis to represent a particle size distribution. The total area of all block is the total number of particles in the sample.

However, in this way, the particle "number" is very dependent on the size of the bin width. Larger bin width will cover a broader range of particle size, thus, increases the number of particle for the respective bin. Therefore, in order to remove this dependency, it is necessary to normalise the particle "number" in each bin by their respective bin width. Furthermore, by dividing each block with the total number of particles, describes each block as the fraction of the total number of particles. In this way, connecting the midpoint of at the top of each block of particle "number" with a continuous smooth curve, we can represent the particle size distribution in term of any probability density function (PDF) since the total area of all block is equal to unity.

Following the above explanation, if $\mathrm{d}N$ is the number of particles in size intervals (bins) of $D_p + \mathrm{d}D_p$, the number distribution function as

$$\mathrm{d}N = F_N \, \mathrm{d}D_p \quad . \tag{2.3}$$

The number distribution can be expressed in term of any PDFs $f(D_p)$ and the total number of particles N_T in a sample as below

$$F_N = \frac{\mathrm{d}N}{\mathrm{d}D_p} = N_T f(D_p) \quad . \tag{2.4}$$

2.2.3 Lognormal Distribution

As explained in section 2.2.2, particle size distribution can be represented in term of PDF. However, even with a known PDF, it is not very easy for direct conversion between different measurement unit for a polydisperse aerosol. This is not the case for a lognormal distribution. A lognormal distribution can be described as a positively skewed (asymmetrical) unimodal distribution, as shown in Figure 2.1a. When the abscissa is plotted in a logarithmic scale, it produces a normal (Gaussian) distribution (see Figure 2.1b). Due to its non-negative value and broad range values coverage properties, it is very useful to describe particle size distribution which often covers a broad magnitude of particle

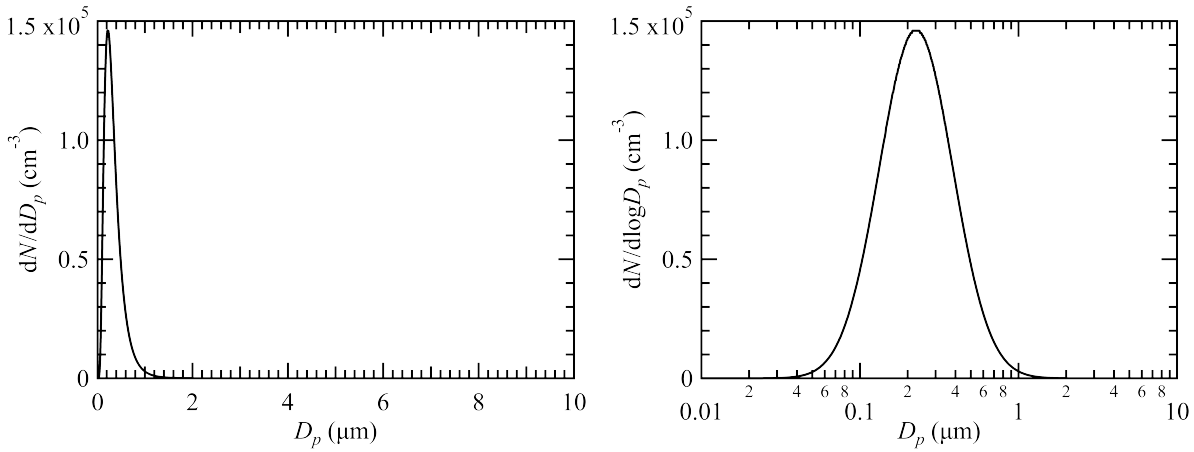

(a) Linear abscissa **(b)** Logarithmic abscissa (semi-logarithmic)

Figure 2.1: Particle number concentration distribution at the upstream side of the filter media.

sizes with different orders. A lognormal distribution is given by

$$f\left(D_p\right) = \frac{1}{\sqrt{2\pi}\log\sigma_g}\exp\left[-\frac{\left(\log D_p - \log D_{pg}\right)^2}{2\left(\log\sigma_g\right)^2}\right] \quad , \tag{2.5}$$

where, D_{pg} is the geometric mean diameter and σ_g is the geometric standard deviation (GSD). The lognormal distribution is a very robust and many studies have found that it fits well with most of particle size distribution[2]. Statistically, lognormal distribution gives a distribution of the same GSD throughout all of its moments. The median diameter of the distribution of any moment is equal to the corresponding geometric mean diameter and is related to the integral by a simple factor (due to a Gaussian-like distribution). This also means that the median diameter of any moment is connected to the median diameter of any other moment by an analytical relationship. This was shown by Hatch and Choate [15] in their paper which derivation of the relation between the median diameter of different moments with GSD was done.

For a particle size distribution describing particle count (number concentration), D_{pg} is replaced by count median diameter (CMD). To avoid any symbols complexity σ_g is replaced with an abbreviation GSD throughout this dissertation. Thus, for lognormal

[2]There is no fundamental theoretical reason why particle size data should approximate the lognormal distribution, but it has been found to apply to most single-source aerosols. Hinds addresses the theoretical basis for aerosol particle size distribution in his book [16].

number distribution, the PDF can be expressed as

$$f\left(D_p\right) = \frac{1}{\sqrt{2\pi}\log \mathrm{GSD}} \exp\left[-\frac{\left(\log D_p - \log \mathrm{CMD}\right)^2}{2\left(\log \mathrm{GSD}\right)^2}\right] \quad . \tag{2.6}$$

Substituting Equation (2.6) into Equation (2.4), the particle number distribution is

$$F_N\left(D_p\right) = \frac{\mathrm{d}N}{\mathrm{d}\log D_p} = \frac{N_T}{\sqrt{2\pi}\log \mathrm{GSD}} \exp\left[-\frac{\left(\log D_p - \log \mathrm{CMD}\right)^2}{2\left(\log \mathrm{GSD}\right)^2}\right] \quad . \tag{2.7}$$

One can obtain the lognormal mass distribution can by converting the CMD to MMD using the relation by Hatch and Choate as below

$$\mathrm{MMD} = \mathrm{CMD} \exp\left(3 \times \ln^2 \mathrm{GSD}\right) \quad . \tag{2.8}$$

2.3 Difference in leak detection sensitivity by photometer method and DPC method

Using an example of apple and grape, Hinds [16] explains the relationship between the number concentration and mass concentration of particles with different particle sizes in the book *Aerosol Technology: Properties, Behavior, and Measurement of Airborne Particles*. By assuming a case where one apple and ten grapes are in a basket as in Figure 2.2a, comparing only based on the sheer number, the ratio is 10:1. The number of grapes is larger in number, but in term of mass, apple has a relatively larger mass. Applying the same analogy, we try to explain the difference in sensitivity of filter leak detection with different particle sizes between number concentration and mass concentration as follows.

Given the principle of particle capture on or inside a filter medium, the smaller particles (grapes) have a higher possibility to pass through the filter medium as compared to larger particles (apples). In the current filter leak test, leak is evaluated by the penetration of the filter defined as the ratio between the concentration of challenge aerosol particles at the downstream side of filter media and the concentration of challenge aerosol particles at the upstream side of filter media. In term of logic and possibility, at the upstream side, larger number of large particles (apples) will be present, while possibly only small

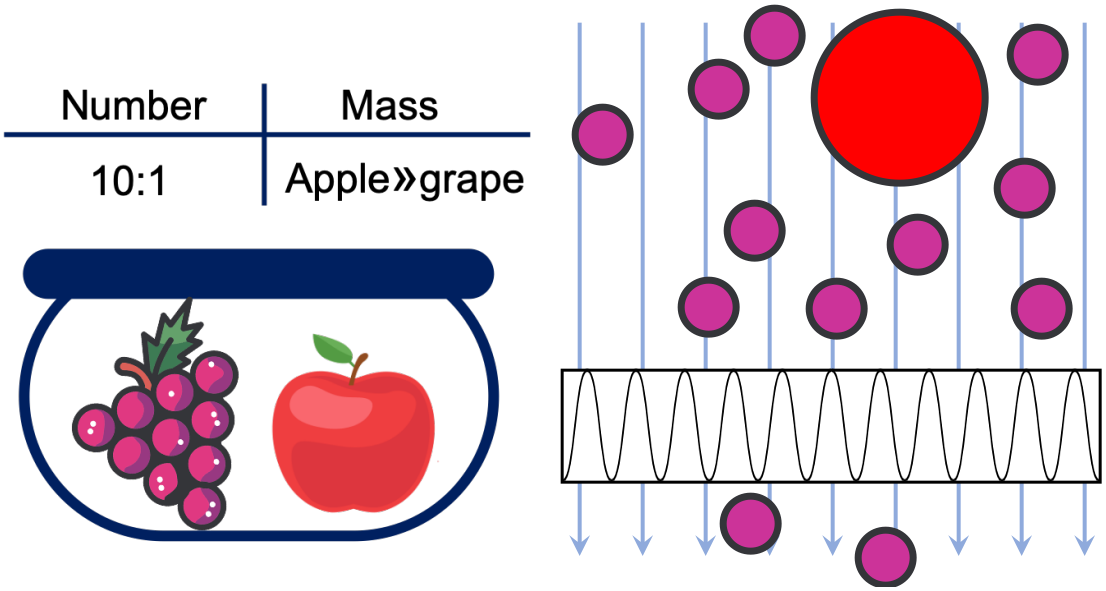

(a) Apple and grape in a basket **(b)** Particle passing through a filter media

Figure 2.2: Difference in leak detection sensitivity between mass and number concentration.

particles without any large particles will be present at the downstream side of the filter media as illustrated in Figure 2.2b.

Based on the explanation above, since a mass concentration measurement is applied in the aerosol photometer method and a number concentration for DPC method, the particle concentration at the upstream side which acts as the denominator in the evaluation of the penetration rate (leak rate) is significantly larger in the aerosol photometer method. Therefore, even if a cumulative number exceeding a specified particle size is used in the filter leak test, the leak evaluation by the DPC method applying the number concentration measurement can be expected to be more severe than the aerosol photometer applying mass concentration measurement. The word severe here is because of a higher leak evaluation (penetration rate) will be produced by the DPC method as compared to the aerosol photometer method. We will confirm and investigate this effect through different leak evaluation methods presented in the ISO 14644-3: 2005 [21] which are the cumulative evaluation method and discrete evaluation method representing aerosol photometer method and DPC method, respectively. Furthermore, we also explore the possibility of cumulative leak evaluation method in the DPC method.

2.4 The Nature of Data Acquisitions and Assumptions

2.4.1 Particle Diameter Range and Upstream Concentration of Challenge Aerosol

In ISO 14644 Part 3: 2005 [21], the requirement of the upstream aerosol of photometer is presented as "the Mass Median Particle Diameter (MMD) for this production method will be between 0.5 µm to 0.7 µm with a Geometric Standard Deviation (GSD) of up to 1.7", while for DPC, "the Count Median Diameter (CMD) for this production will typically be between 0.1 µm to 0.5 µm with a GSD of up to 1.7". In order to satisfy the requirements mentioned, the particle number distribution of poly-alpha olefin (PAO) particles generated from the Laskin nozzle type polydisperse particle generator plotted against the logarithmic particle diameter as shown in the Figure 2.1 is used. The physical properties of PAO is tabulated in Table 2.1. The particle number distribution in Figure 2.1 shows a curve having the form of log-normal probability density distribution with a GSD of 1.7, MMD of 0.53 µm and CMD of 0.23 µm as expressed in Equation (2.7). In addition to this, a parametric study is also done by varying the value of MMD and CMD within the value accepted by the ISO 14644-3: 2005 [21] standard to produce different particle size distribution.

Table 2.1: The physical properties of PAO[a]

Relative Density[c]	Viscosity at 293 K [20 °C] (Pa · s)	Refractive Index
0.819[b]	0.027[b]	1.456[b]

[a] Poly-alpha olefin, with a Chemical Abstracts Service Registry Number of CAS No. 68649-12-7 issued by American Chemical Society.
[b] Data for Emery 3004 as a specific example of a PAO [16].
[c] Density relative to water. Multiply by 1000 for density in kg/m^3 or by 1.0 for density in g/cm^3.

2.4.2 Standard Penetration of a filter and its Particle Size Distribution

For the whole calculation conducted in this dissertation, filters equivalent to H13, H14, U15 and U16 of the European standard EN 1822-1: 2009 [9] standard[3] are chosen as the test filters. These filter grades are frequently used in the cleanroom as the final filter in the air ventilation system. The penetration as a function of particle diameter for various filter standards, including the filter mentioned above, is shown in Figures 2.3a and 2.3b. Figures 2.3a and 2.3b show the penetration for each particle diameter plotted for filter grade H13 and H14 in a linear and log-log plot, respectively. The penetration curve of these filters is denoted as the standard penetration curve to avoid any confusion. The standard penetration curve represented by a linear plot shows a steep curvature change, and it is difficult to use a simple function for a data fitting. However, by converting it to a log-log plot, the data fitting process can be easily done using a quadratic function expressed in the summation notation as follows

$$P_{std}(D_p) = \exp\left\{ B \sum_{n=0}^{2} b_n \left(\frac{\ln D_p}{B} \right)^n \right\} \quad , \tag{2.9}$$

where, B is the constant and b_n is the coefficient of the quadratic equation at n^{th} degree.

Data retrieved from [39] are in the range of 0.05 µm to 0.4 µm in particle diameter. In order to compare the characteristics between the aerosol photometer method and the DPC method aimed in this study, data on the large particle diameter side is insufficient. Therefore, the standard penetration data is plotted in a log-log plot and then a quadratic function is used as a fitting line as described by Equation (2.9) to approximately extend the particle size range from 0.01 µm to 10 µm considered in the numerical integration. The penetration curve from the original data is not a symmetrical curve. Two quadratic curves are used to extrapolate the original data at the small particle size (0.01 µm to 0.05 µm) and large particle side (0.4 µm to 10 µm). The coefficients used for the extrapolation lines are tabulated in Table 2.2.

[3] These correspond to ISO 35, ISO 45, ISO 55 and ISO 65 by the classification of ISO 29463-112 [23], respectively.

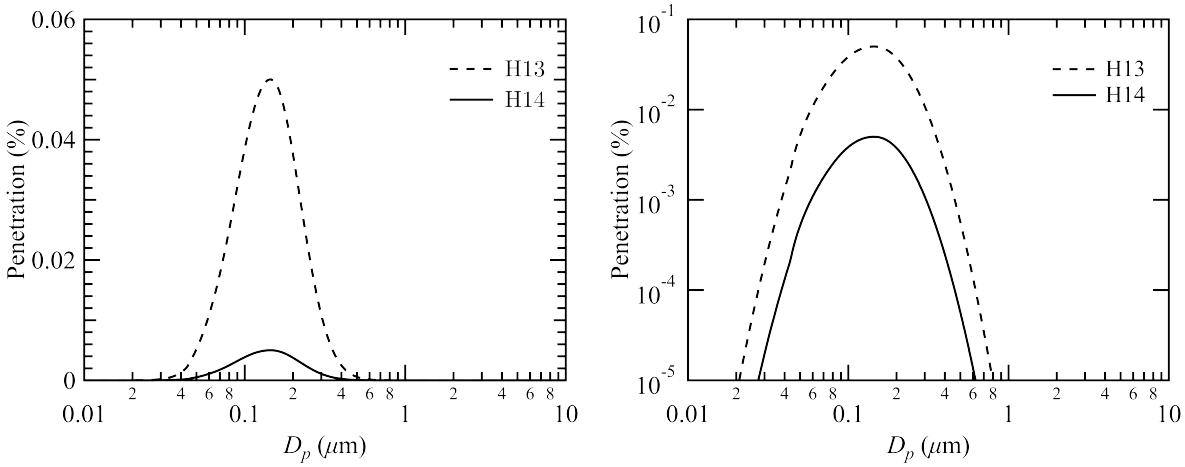

(a) Semi-logarithmic scale **(b)** log-log scale

Figure 2.3: Standard penetration as a function of particle size distribution of a H13 and H14 filters with two different scale plots.

As can be seen from Figures 2.3a and 2.3b, the standard penetration of particles with a particle diameter of 0.05 µm or less and particle sizes of 2 µm or more have significantly decreased. When comparing the area under the penetration curve between the extrapolated particle range and the whole integration range (0.01 µm to 10 µm), the effect of small particle size is less than 1%, and large particle size is less than 2%. These values indicate that even in the most extreme case of 100% margin of error when absolutely no data representing small particles and large particles considered in the penetration curve function relatively small margin of error can be achieved. However, since the original data is smoothly extrapolated at both ends, a much smaller margin of error can be expected.

Table 2.2: The coefficient of the fitting line used in the extrapolation of the standard penetration curve.

Coefficient	H13		H14	
	0.01-0.05 µm	0.4-10 µm	0.01-0.05 µm	0.4-10 µm
B	2.509	2.632	2.775	2.502
b_0	-9.540	-7.049	-9.456	-8.337
b_1	-13.098	-11.408	-14.157	-11.408
b_2	-7.805	-7.819	-8.769	-7.431

2.5 Downstream Concentration of Challenge Aerosol

Using the data in Figures 2.1 and 2.3, the challenge aerosol concentration at the downstream side of a filter media was calculated as follows

$$F_{N,d}\left(D_p\right) = F_{N,u}\left(D_p\right) \times P_{std}\left(D_p\right) \quad , \tag{2.10}$$

where, F_N is the number of particles per unit volume with size parameter between D_p and $D_p + \mathrm{d}D_p$ (as in Equation (2.7)), with u and d as subscripts to indicate upstream and downstream and $P_{std}(D_p)$ standard penetration rate for different filter grades. Leak rate evaluates by both methods are defined by L with subscripts of M and N denoting mass (aerosol photometer) and number (DPC) concentration, respectively.

2.6 Leak Evaluation Method

Filter leak test evaluation by the aerosol photometer and DPC method were calculated by the following procedure. It is important to note that, here, the comparison between both methods is only done in the context of the difference between evaluation by mass concentration and number concentration representing aerosol photometer and DPC method, respectively.

2.6.1 Reproduction of an Evaluation by the Aerosol Photometer Method (Mass Concentration)

For aerosol photometer method, measurement unit of mass concentration is used. In the calculation of the penetration rate (leak rate), particle shape factor is cancelled out since the downstream side concentration is divided by the upstream side concentration. For this reason, in the present calculation, a particle with a perfectly spherical shape is assumed. Following Equations (2.1) and (2.2), the particle mass distribution of the

challenge aerosol at the upstream and downstream side of the filter media can be expressed as particle number distribution as follows

$$\begin{aligned} F_{M,u}(D_p) &= F_{N,u}(D_p) \times \frac{\rho_p \pi}{6} {D_p}^3 \quad , \\ F_{M,d}(D_p) &= F_{N,d}(D_p) \times \frac{\rho_p \pi}{6} {D_p}^3 \quad , \end{aligned} \tag{2.11}$$

where, $F_M(D_p)$ is the mass of particles per unit volume with size parameter between D_p and $D_p + \mathrm{d}D_p$. Aerosol photometer produces a single value measurement of mass concentration which is in the integral form of Equation (2.11) of an effective particle range. The integral form of Equation (2.11) is given by

$$\begin{aligned} I_{M,u} &= \int_{D_{p,\min}}^{D_{p,\max}} F_{M,u}(D_p)\, \mathrm{d}D_p \quad , \\ I_{M,d} &= \int_{D_{p,\min}}^{D_{p,\max}} F_{M,d}(D_p)\, \mathrm{d}D_p \quad , \end{aligned} \tag{2.12}$$

where, I_M is the cumulative mass concentration. Finally, the leak evaluation L_M by the aerosol photometer is defined as the ratio between cumulative mass concentration at the downstream side and upstream side which can be expressed by

$$L_M = \frac{I_{M,d}}{I_{M,u}} \quad . \tag{2.13}$$

2.6.2 Reproduction of an Evaluation by the Discrete Particle Counter (DPC) Method (Number Concentration)

In current ISO 14644-3: 2005 [21], DPC method leak evaluation is presented as the ratio between number concentration of the challenge aerosol at the downstream and upstream side of filter media discretely at certain particle size. In this study, we called this evaluation method as the discrete leak evaluation method. This method calculates leak rate using the following relations

$$L_{N,discrete}(D_p) = \frac{F_{N,d}(D_p)}{F_{N,u}(D_p)} \quad . \tag{2.14}$$

In this study, aside from the discrete leak evaluation method, we will also consider the cumulative leak evaluation method similar to the concept in aerosol photometer but

with number concentration. The cumulative form of number concentration is

$$\begin{aligned} I_{N,u} &= \int_{D_{p,\min}}^{D_{p,\max}} F_{N,u}\left(D_p\right)\,\mathrm{d}D_p \quad , \\ I_{N,d} &= \int_{D_{p,\min}}^{D_{p,\max}} F_{N,d}\left(D_p\right)\,\mathrm{d}D_p \quad . \end{aligned} \tag{2.15}$$

Thus, the leak rate $L_N, cumulative$ is given by

$$L_{N,cumulative} = \frac{I_{N,d}}{I_{N,u}} \quad . \tag{2.16}$$

2.7 The Process of Numerical Experiments Calculations

Given the data for the filter penetration (Figure 2.3) and aerosol distribution functions at upstream and downstream (Figures 2.4 and 2.5), leak rate evaluated by both aerosol photometer and DPC method can be calculated. Numerical integration is done by writing a FORTRAN programming on a computer, and for this, we calculated the integrals over particle size distributions for both methods. First, the discrete leak evaluation method by the DPC method is done by comparing the downstream and upstream number concentration at a particle size of 0.1 µm, MPPS, 0.2 µm, 0.3 µm, 0.4 µm and 0.5 µm. Next, as for the cumulative leak evaluation method by the DPC method, we did an integration for several particle size ranges of ≥0.1 µm, ≥MPPS, ≥0.2 µm, ≥0.3 µm, ≥0.4 µm and ≥0.5 µm. As for aerosol photometer, we did the integration between 0.01 µm to 10 µm. In a preliminary study, we found that the ratio between DPC and aerosol photometer method converged at a particle size equal to 5.8 µm. Integration at where the maximum particle size limit more than of this particle size will give the same value, regardless of any particle size. Therefore, we set the maximum particle size limit for all integration calculations to 10 µm.

2.8 Results and Discussion

Table 2.3 shows the leak rate for filter grade H13 to U16 which was evaluated by the cumulative leak evaluation method for aerosol photometer method and the discrete leak

evaluation method for DPC method (at particle size of 0.1 µm, MPPS, 0.2 µm, 0.3 µm, 0.4 µm and 0.5 µm) calculated using data presented in Figures 2.4 and 2.5. The aerosol photometer method produced leak rate lower than currently presented in the ISO 14644-3: 2005 [21] for aerosol photometer method (0.01% or 1×10^{-4}). Meanwhile, for the DPC method, discrete leak rate for filter grade H13 at particle sizes 0.1 µm, MPPS, 0.2 µm and 0.3 µm exceeded the threshold value of 0.01%. If the same threshold criterion of 0.01% shall be used for the DPC method with a discrete leak evaluation method filter grade H13 will be mistakenly concluded to have leaks. It is important to remember that currently used standard penetration rate function described in section 2.4.2 are barely positioned at the boundary of each filter grade classification presented in EN 1822-1: 2009 [9]. Therefore, the leak evaluation in this dissertation will be very severe.

Table 2.3: Leakage rate value for aerosol photometer method and DPC method (discrete leakage evaluation method). Green and red coloured cells represent leak rate value smaller and greater than 0.01% (1×10^{-4}), respectively.

Filter Grade	Aerosol Photometer	DPC					
		0.1 µm	MPPS	0.2 µm	0.3 µm	0.4 µm	0.5 µm
H13	2.06×10^{-5}	3.85×10^{-4}	5.00×10^{-4}	3.75×10^{-4}	1.09×10^{-4}	2.50×10^{-5}	5.69×10^{-6}
H14	2.06×10^{-6}	3.85×10^{-5}	5.00×10^{-5}	3.75×10^{-5}	1.09×10^{-5}	2.50×10^{-6}	5.69×10^{-7}
U15	2.06×10^{-7}	3.85×10^{-6}	5.00×10^{-6}	3.75×10^{-6}	1.09×10^{-6}	2.50×10^{-7}	5.69×10^{-8}
U16	2.06×10^{-8}	3.85×10^{-7}	5.00×10^{-7}	3.75×10^{-7}	1.09×10^{-7}	2.50×10^{-8}	5.69×10^{-9}

Interestingly, the filter grade of H14 for the DPC method has a value a 1.09×10^{-5} which indicates that, if 0.01% is being used, this value corresponds to the threshold of 0.001%, currently used in the DPC method for discrete leak evaluation method. This is in a good agreement with the suggestion made by Suzuki et al. [36] as discussed in Chapter 1. Suzuki et al. [36] showed that a pinhole leak could not be determined clearly unless a leak evaluation criterion about ten times of the standard penetration rate is being used. Therefore, the leak evaluation criterion of 0.01% perfectly matches with the filter grade of H14. The advantage of the discrete leak evaluation in the DPC method is the value of leak rate will not be affected by the changes of upstream challenge aerosol. This is because a pointwise (discrete) measurement is used to compare the upstream and downstream

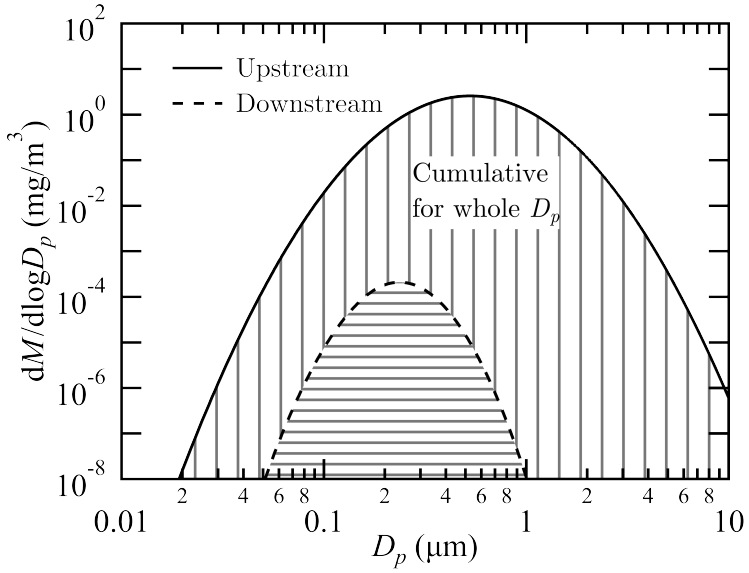

(a) H13 filter

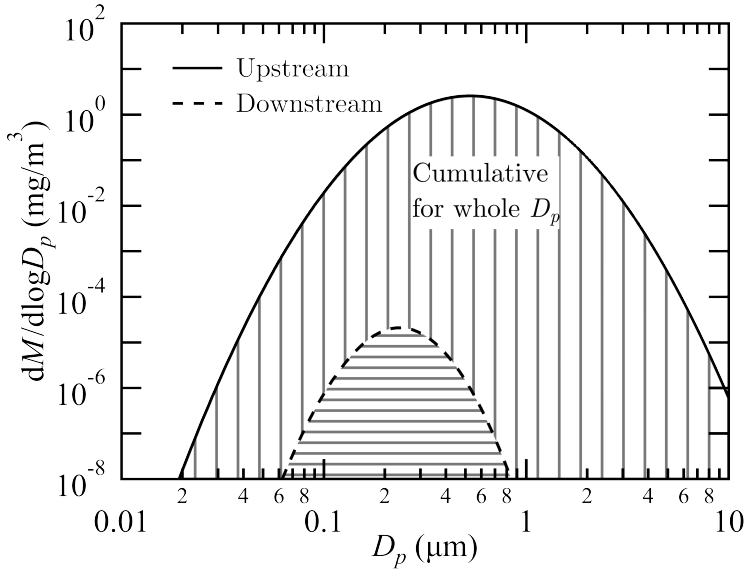

(b) H14 filter

Figure 2.4: Particle mass concentration distribution at the upstream and downstream of a H13 and H14 filters. The shaded regions are the area considered in the integration calculation for the leak rate evaluation.

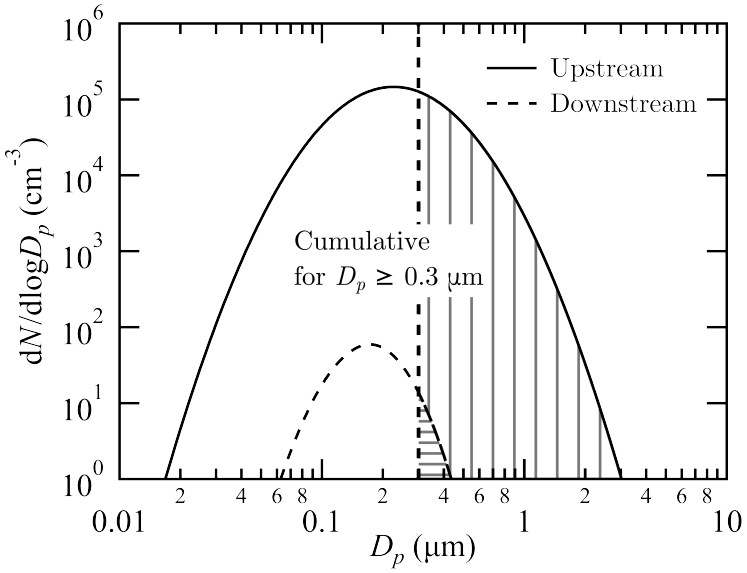

(a) H13 filter

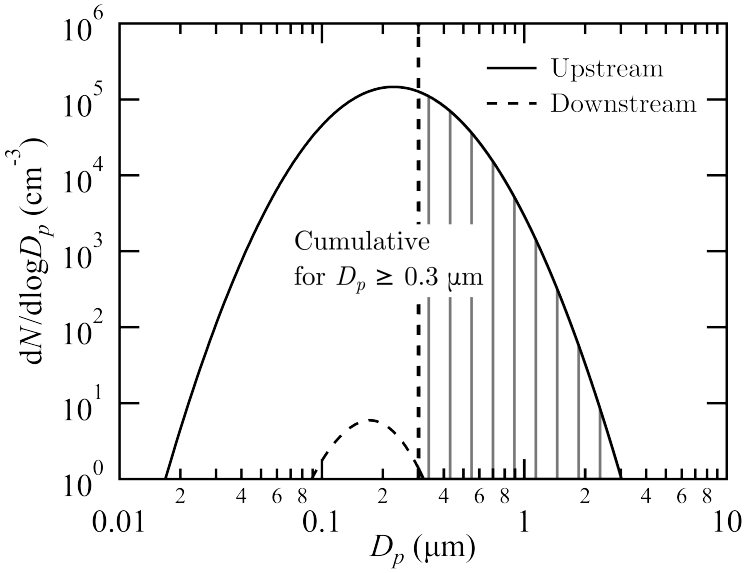

(b) H14 filter

Figure 2.5: Particle mass concentration distribution at the upstream and downstream of H13 and H14 filters for discrete leak evaluation method at 0.3 μm and cumulative leak evaluation method of ≥0.3 μm. The discrete leak evaluation method represented by the points at the intersections between the dashed line and the upstream and downstream distribution value. The shaded regions are the area considered in the integration calculation for the leak rate by cumulative leak evaluation method.

concentration. However, if the same leak threshold as in aerosol photometer shall be used for DPC method, a different leak evaluation method need to be applied since the discrete leak rate produced by the DPC method does not have the same order and any correlation with the leak evaluation by the aerosol photometer. As explained in the leak evaluation method in section 2.1, we will investigate the possibility of unifying the threshold leak criteria by adapting the cumulative leak evaluation method to the DPC method.

Table 2.4 shows the leak rate for filter grade H13 to U16 which was evaluated by the cumulative leak evaluation method for both the aerosol photometer method and the DPC method (at particle size ranges of ≥0.1 µm, ≥MPPS, ≥0.2 µm, ≥0.3 µm, ≥0.4 µm and ≥0.5 µm). A similar trend as in the discrete leak evaluation method for the DPC method were observed but the values seems to have a correlation to the leak rate of the aerosol photometer. First of all, leak rate evaluated cumulatively produced values that is near or below that of 0.01%. All leak rates except for ≥0.1 µm, ≥MPPS and ≥0.2 µm for filter grade H13 by the DPC method were below than 0.01%. Based on these results, at ≥0.3 µm, ≥0.4 µm and ≥0.5 µm, the DPC method consistently produced leak rate values. These create a question needs to be answered, which particle range are the most suitable for cumulative leak evaluation method by the DPC method.

Table 2.4: Leakage rate value for aerosol photometer method and DPC method (cumulative leakage evaluation method). Green and red coloured cells represent leak rate value smaller and greater than 0.01% (1×10^{-4}), respectively.

Filter Grade	Aerosol Photometer	DPC					
		≥0.1 µm	≥MPPS	≥0.2 µm	≥0.3 µm	≥0.4 µm	≥0.5 µm
H13	2.06×10^{-5}	1.73×10^{-4}	1.85×10^{-4}	9.86×10^{-5}	2.86×10^{-5}	6.79×10^{-6}	1.59×10^{-6}
H14	2.06×10^{-6}	1.73×10^{-5}	1.85×10^{-5}	9.86×10^{-6}	2.86×10^{-6}	6.79×10^{-7}	1.59×10^{-7}
U15	2.06×10^{-7}	1.73×10^{-6}	1.85×10^{-6}	9.86×10^{-7}	2.86×10^{-7}	6.79×10^{-8}	1.59×10^{-8}
U16	2.06×10^{-8}	1.73×10^{-7}	1.85×10^{-7}	9.86×10^{-8}	2.86×10^{-8}	6.79×10^{-9}	1.59×10^{-9}

Cumulative leak evaluation method differs from the discrete leak evaluation method in the sense of dependency on the particle size distribution. When the filter performance does not change with time, the discrete method will produce the same value regardless of a change occurred in the upstream challenge aerosol particle distribution. This is

unlikely the case for the cumulative evaluation method. Thus, we did a parametric study by varying the MMDs (CMDs also directly changes) to observe the characteristic of the cumulative evaluation method when adapting it to the filter leak test. First, Figure 2.6 illustrates the leak rate for filter grades H13 and H14 at different polydisperse aerosols distribution with a GSD=1.7 and plotted against variation of MMDs from 0.01 µm to 1.5 µm. The green and yellow coloured shaded region shows the allowable range of MMD (0.5 µm to 0.7 µm) and CMD (0.1 µm to 0.5 µm), respectively. The DPC method observed to have a relatively flatter curve as compared to the aerosol photometer method. Once again, ≥0.1 µm and ≥MPPS constantly produced leak rate larger than the aerosol photometer method by 0.01%. The other particle ranges were observed to have a region where the higher and lower leak rate values than aerosol but seems to have comparable values within the allowable MMD and CMD.

Within the allowable MMD and CMD region, only ≥0.3 µm, ≥0.4 µm and ≥0.5 µm produced values that are smaller than 0.01% with ≥0.3 µm is found to be the nearest to the aerosol photometer method. In a practical point of view, both ≥0.3 µm and ≥0.5 µm are frequently used as the reference particle for many tests in contamination control monitoring such as in ISO 14644-1: 2015 [20] to determine the class of a cleanroom. Therefore, unlike ≥0.4 µm, most of the commercially existed DPCs usually have the channel specification being set to these sets of particle range. However, comparing between ≥0.3 µm and ≥0.5 µm, 0.5 µm is too large and there will be a lot of loss in information regarding the smaller particle. Smaller particles will not have any effect on the leak rate value, resulting in a very unreliable leak test. Therefore, based on this reason, we deduced that ≥0.3 µm is the most suitable particle range for the cumulative leak evaluation by the DPC method. Cumulative leak evaluation method for particles ≥0.3 µm will be used throughout this dissertation for the DPC method.

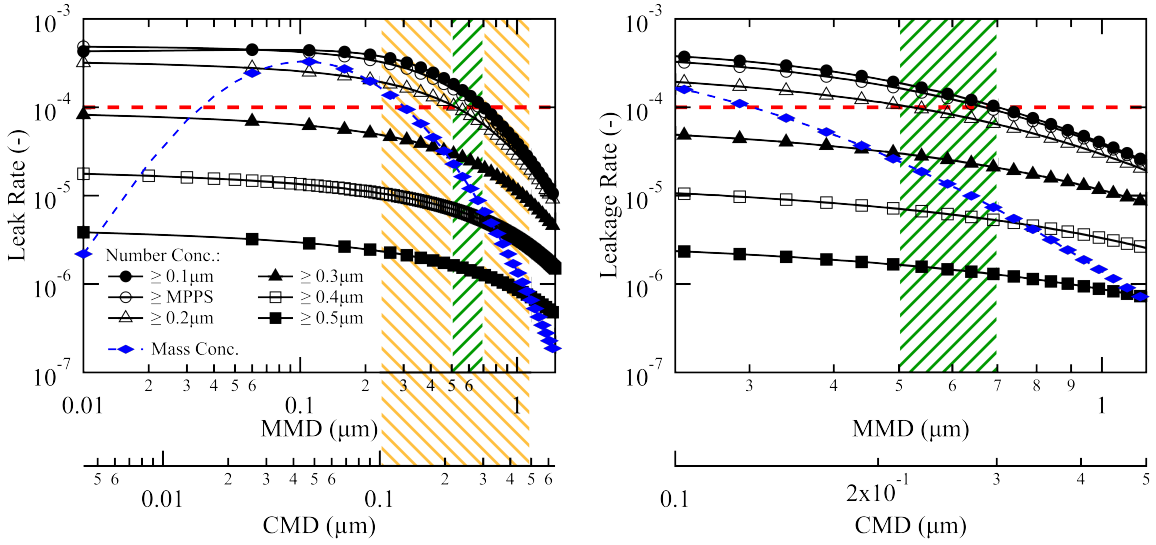

(a) H13 filter

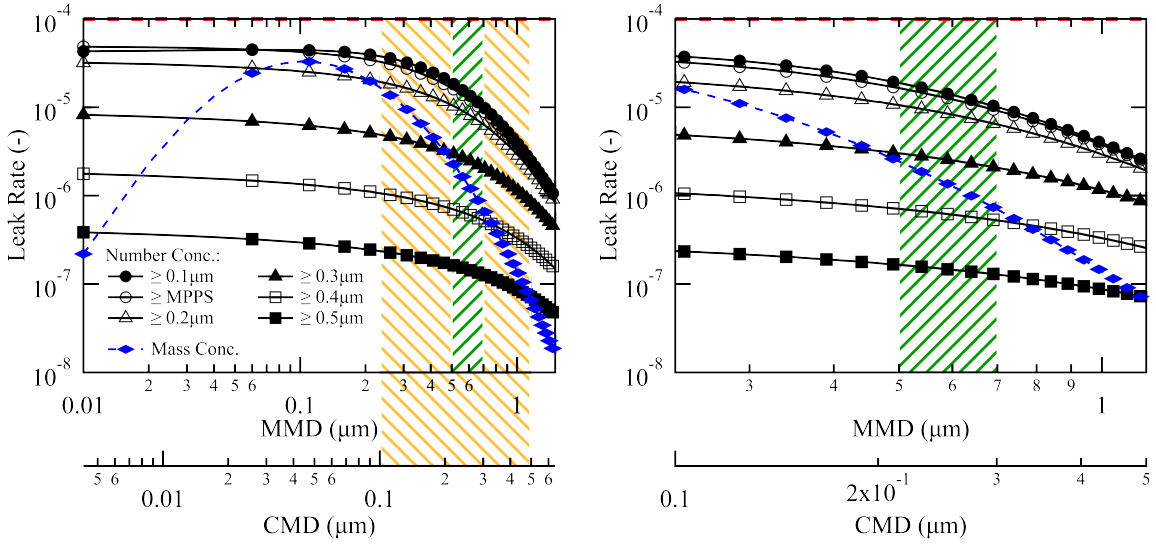

(b) H14 filter

Figure 2.6: Leak rate calculated by the cumulative leak evaluation method for DPC method and aerosol photometer at GSD=1.7. The shaded areas represent the allowable MMD (0.5 to 0.7 µm) and CMD (0.1 to 0.5 µm) range for aerosol photometer and DPC in ISO 14644-3: 2005 [21], respectively. The left figure shows the result for MMD range (0.01 to 1.5 µm) used in the calculation. The right figure shows the zoomed-in result within the allowable CMD range. The red dashed line indicates the threshold criteria of 0.01% (1×10^{-4}).

2.9 Conclusion

A comparison between the aerosol photometer method and DPC method presented in ISO 14644-3: 2005 [21] were done in term of difference in the measurement unit and the leak evaluation method. Aerosol photometer and DPC were represented by mass concentration and number concentration by their respective measurement unit. Furthermore, two types of leak evaluation method were considered in the calculation of the leak rate by the DPC method which are the discrete leak evaluation method and the cumulative leak evaluation method. The discrete leak evaluation method by DPC produced values that is higher than 0.01% leak threshold criteria and about one order difference with the leak rate of the aerosol photometer method were observed at particle size 0.1 µm, MPPS, 0.2 µm and 0.3 µm. On the other side, when cumulative leak evaluation method is used, the values of leak rate for DPC method showed a good agreement with the aerosol photometer method and fulfil the requirement of below the value of 0.01%. We found that $\geq$0.3 µm is the best particle range for the cumulative leak evaluation method. As a result, for a filter having a filter grade of H14 or higher in EN 1822-1: 2009 [9], the same leak threshold criterion of 0.01% as the aerosol photometer method can also be applied in the DPC method. On the other hand, considering the risk of misevaluation and misjudgement, it was found that it is not possible to apply the threshold criterion of 0.01% for filters with a grade of H13 or lower. Therefore, it is impossible to apply the same threshold criterion through all the filter grades but based on the results, it is possible to use unified threshold criterion at certain range of filter grades.

Chapter 3

Instruments Responses[1]

Contents

[1]Content of this chapter is submitted for publication by Mohd Nor, M. A. B. and Suwa Y. in an article entitled "Study on The Installed Filter Leakage Evaluation Criterion for Particle Counter and Aerosol Photometer".

3.1 Introduction

In Chapter 2, a theoretical comparison on the filter leak test result based on the direct comparison between the mass concentration and number concentration which is the yield measurement of aerosol photometer and DPC respectively was done. It was found that a significant difference obtained between leak evaluation by these two concentration measurements. In particular, DPC produced more severe result as compared to aerosol photometer and if the same leak criterion of 0.01% is used for filter grade lower than H14 as in EN 1822-1: 2009 [9], this can easily be misevaluated as leak by the inspector during a leak test even though there is no leak on the filter. On the other hand, since filter H14 or higher grade have relatively higher performance, it is possible to use the same criteria of 0.01% for aerosol photometer and DPC. In this chapter, we extend our investigations by considering instrument responses to describe more accurately on the different leak test evaluation by aerosol photometer and DPC method.

3.2 Light Scattering by a Sphere

Figure 3.1 shows an incident light pass along Z-axis from A direction is scattered by a single perfectly spherical particles at the P point. Now, the incident light is a monochromatic plane wave which the plane of vibration is linearly polarised parallel to the X-Z plane. The incident light is scattered by a particle having a radius of D_p and a refractive index of m, then spread as a spherical wave throughout a scattering medium. Let the wavelength of the incident light to be λ, the intensity of the scattered light in the direction of the scattering angle θ on the observation plane Y'-Z plane that makes an angle ϕ with the X-Z plane at a position B with a distance R from the particle at point P can be expressed as follows

$$I(\alpha, m, \theta, \phi, R) = I_0 \frac{\lambda^2}{4\pi^2 R^2} \left\{ i_1(\alpha, m, \theta) \sin^2 \phi + i_1(\alpha, m, \theta) \cos^2 \phi \right\} \quad . \tag{3.1}$$

Here, I_0 W/m^2 is the intensity[2] of incident light and α ($= 2\pi D_p/\lambda$) is the dimensionless particle size parameter. In the above equation, $\phi = \pi/2$ and zero correspond to the I_1 and

[2]Precisely speaking, W/m^2 is an irradiance, watts/steradian is an intensity, but common usage often finds intensity applied to W/m^2.

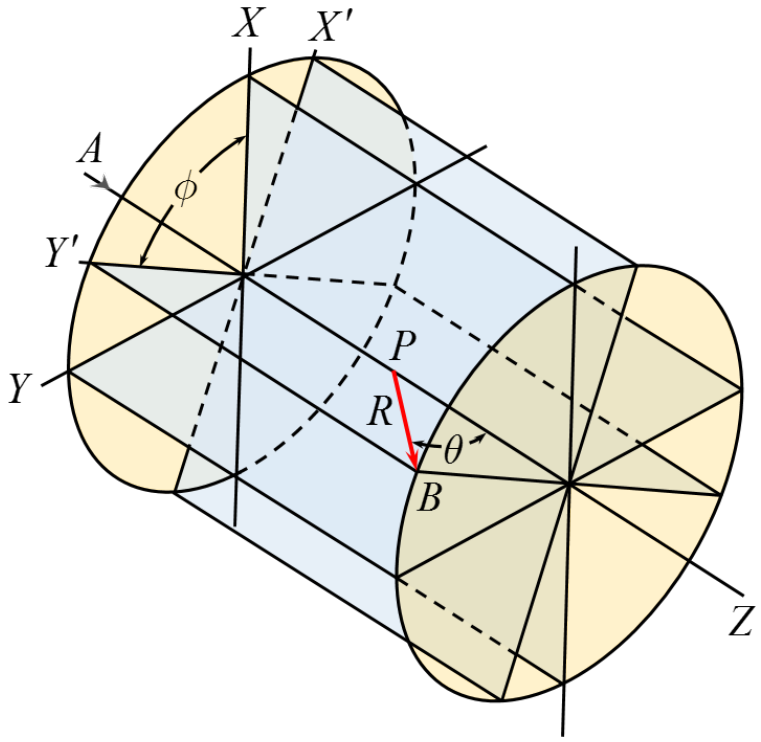

Figure 3.1: Angular relationship between the incident and scattered light in Mie theory light-scattering calculations.

I_2 which is when the observation plane is perpendicular and parallel to the polarisation plane of the incident light. I_1 and I_2 take a form of

$$\begin{aligned} I_1(\alpha, m, \theta, \phi, R) &= I_0 \frac{\lambda^2}{4\pi^2 R^2} i_1(\alpha, m, \theta) \quad , \\ I_2(\alpha, m, \theta, \phi, R) &= I_0 \frac{\lambda^2}{4\pi^2 R^2} i_2(\alpha, m, \theta) \quad . \end{aligned} \tag{3.2}$$

Where, i_1 and i_2 included in the above equation are the intensity of light vibrating perpendicular and parallel to the plane through the directions of propagation of the incident and scattered beam which can be given in the term of amplitude functions S_1 and S_2

$$\begin{aligned} i_1(\alpha, m, \theta) &= |S_1(\alpha, m, \theta)|^2 \quad , \\ i_2(\alpha, m, \theta) &= |S_2(\alpha, m, \theta)|^2 \quad . \end{aligned} \tag{3.3}$$

For a perfectly spherical particle, S_1 and S_2 can be analytically solved by means of Mie Theory [30]. For example, a detailed solution is presented by Van de Hulst [19] in his very famous book named *Light Scattering by Small Particles*. The solutions for S_1 and S_2 can be obtained by expanding the electric fields of the incident and scattered

waves, and the wave inside the particle in a series of spherical harmonics. Provided that the tangential components of the electric and magnetic fields are continuous across particle surface, the coefficients of these expansion functions can be derived, leading to the following series expressions for S_1 and S_2

$$\begin{aligned} S_1(\alpha, m, \theta) &= \sum_{n=1}^{\infty} \frac{2n+1}{n(n+1)} \left\{ a_n(\alpha, m)\, \pi_n(\cos\theta) + b_n(\alpha, m)\, \tau_n(\cos\theta) \right\} \quad , \\ S_2(\alpha, m, \theta) &= \sum_{n=1}^{\infty} \frac{2n+1}{n(n+1)} \left\{ b_n(\alpha, m)\, \pi_n(\cos\theta) + a_n(\alpha, m)\, \tau_n(\cos\theta) \right\} \quad . \end{aligned} \tag{3.4}$$

The size parameter-dependent coefficient functions a_n and b_n can be expressed in terms of refractive index $m$and dimensionless diameter parameter α as follows

$$\begin{aligned} a_n(\alpha, m) &= \frac{\psi_n(\alpha)\, \psi_n{}'(m\alpha) - m\psi_n(m\alpha)\, \psi_n{}'(\alpha)}{\zeta_n(\alpha)\, \psi_n{}'(m\alpha) - m\psi_n(m\alpha)\, \zeta_n{}'(\alpha)} \quad , \\ b_n(\alpha, m) &= \frac{m\psi_n(\alpha)\, \psi_n{}'(m\alpha) - \psi_n(m\alpha)\, \psi_n{}'(\alpha)}{m\zeta_n(\alpha)\, \psi_n{}'(m\alpha) - \psi_n(m\alpha)\, \zeta_n{}'(\alpha)} \quad . \end{aligned} \tag{3.5}$$

In this case unpolarised incident light, the azimuthal dependence completely cancels out, so that Equation (3.1) is simplified into

$$I(\alpha, m, \theta, \phi, R) = I_0 \frac{\lambda^2}{8\pi^2 R^2} \left\{ |S_1(\alpha, m, \theta)|^2 + |S_2(\alpha, m, \theta)|^2 \right\} \quad . \tag{3.6}$$

This is the principle used for many light-scattering techniques instruments such as aerosol photometer and DPC.

3.3 Response of an Aerosol Photometer

An aerosol photometer receives light scattered by a number of particles, simultaneously illuminated in an optical sensing volume. This measurement depends on the incident light, geometry of the photo-detecting optical system and the aerosol physical parameters. Given the Mie theory of particle-light scattering as described in section 3.2, the response of an aerosol photometer can be theoretically calculated. When particles have diameter D_p, refractive index m in an optical sensing volume V_s illuminated by an unpolarised

beam of a wavelength λ, the resulting light flux, collected by the collecting lens with a specific lens geometrical arrangement is given by

$$I_{c,\text{single}} = I_0 \frac{V_s \lambda^2}{8\pi^2 R^2} \int_0^\infty \int_0^\infty (i_1 + i_2) \omega F_N(D_p) \, \mathrm{d}\theta \mathrm{d}D_p \quad , \tag{3.7}$$

where $F_N(D_p)$ is the number of particles per unit volume with size parameter between D_p and $D_p + \mathrm{d}D_p$ as described in Equation (2.7). For the sake of ease, from here onwards, D_p will be used instead of α for describing the size parameter of a particle. The fraction of scattered light collected depends on collecting lens geometry is expressed by ω. In the presence of multiple particles inside the sensing volume, substituting $F_N(D_p)$ in Equation (3.7) may be rewritten in term of the probability density function of the particle size distribution

$$F_N(D_p) = C_N f(D_p) \quad , \tag{3.8}$$

where C_N is the number of particles per unit volume and $f(D_p)$ is the probability density function of a particle size distribution which can be represented by any probability density function such as log-normal distribution function. The resulting light flux collected by the collecting lens is given by

$$I_{c,multiple} \approx I_0 \frac{C_N V_s \lambda^2}{8\pi^2 R^2} \int_0^\infty \int_0^\infty (i_1 + i_2) \omega f(D_p) \, \mathrm{d}\theta \mathrm{d}D_p \quad . \tag{3.9}$$

Equation (3.9) demonstrates the problem of photometric measurements of particle concentration: if the aerosol photometer response varies, one cannot distinguish whether the number concentration C_N, the size distribution $f(D_p)$ or the optical properties m of the material have changed [3, 38]. Rearranging Equation (3.9) and using relations in Chapter 2 to express in term of mass concentration C_M we will get

$$I_{c,multiple} \approx K \frac{C_M}{\rho_p} \frac{1}{\int_0^\infty {D_p}^3 f(D_p) \, dD_p} \int_0^\infty \int_0^\infty (i_1 + i_2) \omega f(D_p) \, \mathrm{d}\theta \mathrm{d}D_p \quad . \tag{3.10}$$

In case of a homogeneous and monodisperse aerosol, Equation (3.10) can be simplified into

$$I_{c,multiple,mono} \approx K \frac{C_M}{\rho_p} \frac{1}{{D_p}^3} \int_0^\infty (i_1 + i_2) \, \omega \, \mathrm{d}\theta \quad . \tag{3.11}$$

The term homogeneous here implies the constancy of the particle density, refractive index and shape allowing the response to be functionally described by the geometric particle size alone. If the aerosol is polydisperse, this relationship has the form

$$I_{c,multiple,poly} \approx \frac{{D_p}^3}{\overline{{D_p}^3}} \int_0^\infty I_{c,multiple,mono} f\left(D_p\right)\ \mathrm{d}D_p \quad , \tag{3.12}$$

where K $(= 3I_0V_s/4\pi^3)$ is the constant on the aerosol photometer performance.

3.3.1 Geometrical Factor

The approximation symbol in the Equations (3.9)–(3.12) originates from the fact that the value of ω for each particle is slightly different due to different position inside an optical sensing volume. However, there is no problem as long as the size of the optical sensing volume is not particularly large. Even if it is somewhat large, an appropriate average value of ω can be selected to reduce the influence in the calculation value. The light intensity distribution function i_1 and i_2 can be calculated as described in previous section 3.2. On the other hand, the function ω determined by the geometric configuration of the aerosol photometer optical system is given by Gucker et al. [13] and Hodkinson et al. [18] as shown in equations below for the sideway scattering type (Figure 3.2a) and the forward scattering type (Figure 3.2b), respectively.

Sideway scattering type:

$$\begin{aligned} &\text{for } \psi - \gamma - \beta \le \theta \le \psi + \gamma + \beta; \\ &\quad \omega = \int_{\psi-\gamma}^{\psi+\gamma} 4 \sin\theta \sin\phi ACF\left(\beta,\theta,\phi\right) ACF\left(\gamma,\phi,\psi\right)\ \mathrm{d}\phi \quad . \\ &\text{for } \theta < \psi - \gamma - \beta,\ \theta > \psi + \gamma + \beta; \\ &\quad \omega = 0 \quad . \end{aligned} \tag{3.13}$$

Forward scattering type:

$$\begin{aligned} &\text{for } \eta - \beta \le \theta \le \gamma + \beta; \\ &\quad \omega = \int_{\eta}^{\gamma} 4\pi \sin\theta \sin\phi ACF\left(\beta,\theta,\phi\right)\ \mathrm{d}\phi \quad . \\ &\text{for } \theta < \eta - \beta,\ \theta > \gamma + \beta; \\ &\quad \omega = 0 \quad . \end{aligned} \tag{3.14}$$

where, γ is the semi-angle of the light incident, β is the semi-angle of the collection aperture, ψ is the angle between the axis of illumination and collection aperture for sideway scattering type and η is the semi-angle of the dark stop or light trap for the forward scattering type.

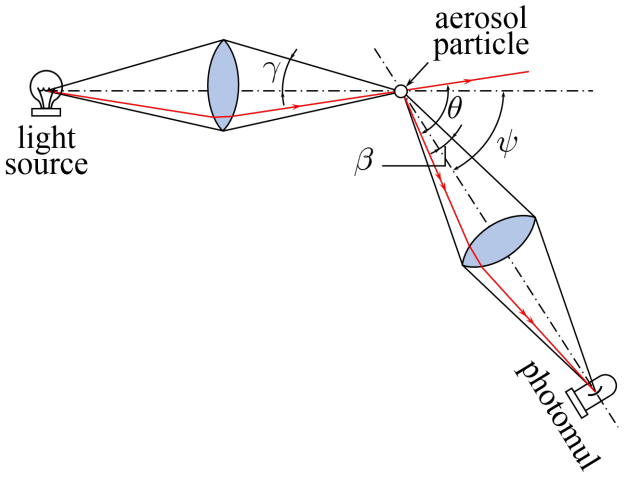

(a) Sideway scattering

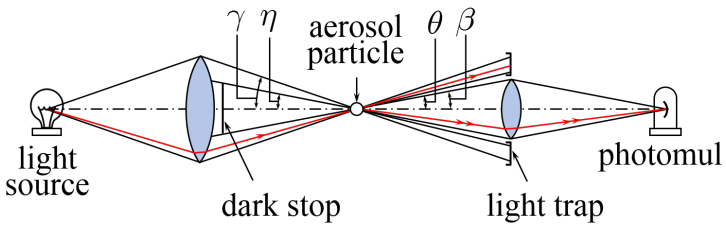

(b) Forward scattering

Figure 3.2: Schematic diagram of the typical optical systems of the aerosol photometer.

The $ACF(\beta, \theta, \phi)$ function is defined as

for $\theta < \beta - \phi$;

$$ACF\,(\beta, \theta, \phi) = \pi \quad .$$

for $\beta - \phi \leq \theta \leq \beta + \phi$;

$$ACF\,(\beta, \theta, \phi) = \cos^{-1} \frac{\cos\beta - \cos\theta\cos\phi}{\sin\theta\sin\phi} \quad . \tag{3.15}$$

for $\theta > \beta + \phi$;

$$ACF\,(\beta, \theta, \phi) = 0 \quad .$$

The details on other geometrical factors by different instrument optical arrangement are presented in Appendix A.

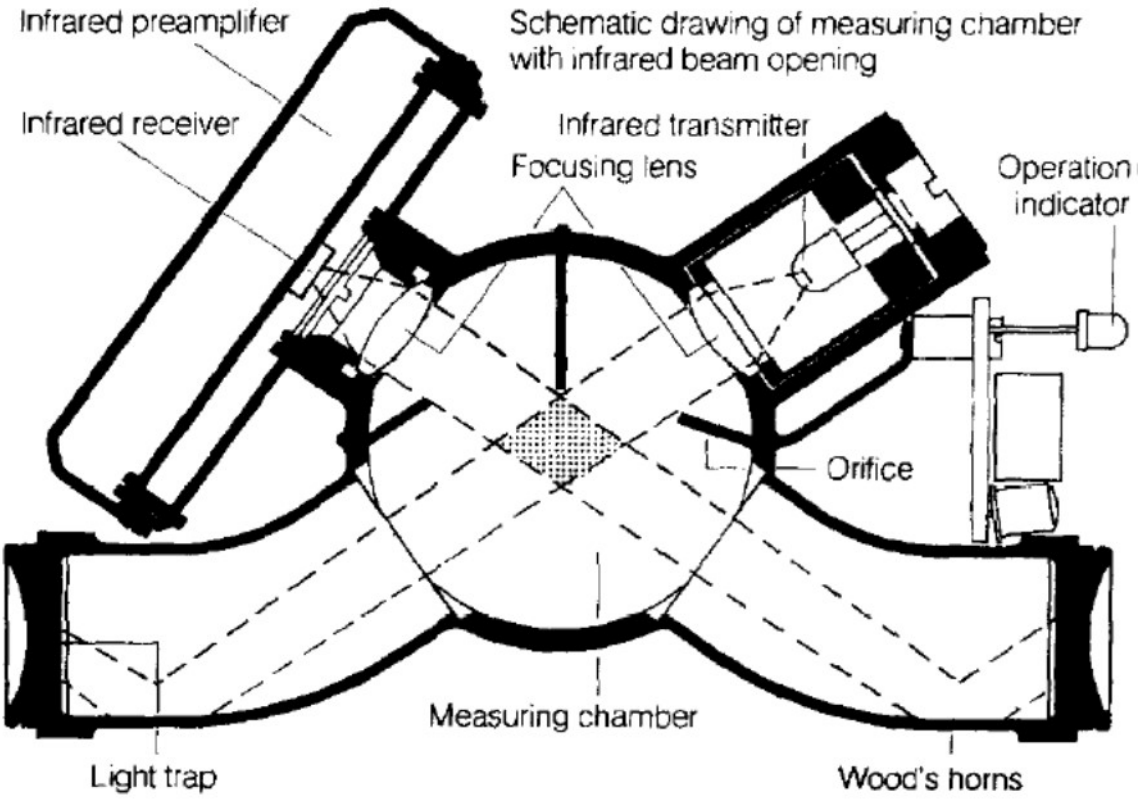

(a) HUND TM digital

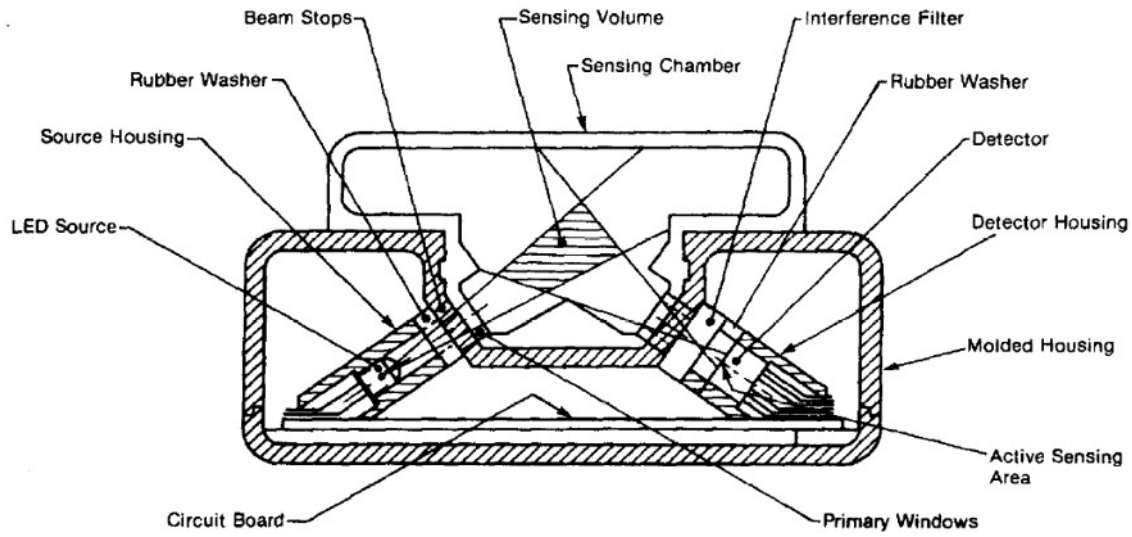

(b) MINIRAM PDM-3

Figure 3.3: Schematic of the aerosol photometer measuring chamber. **(a)** HUND TM digital µP. **(b)** MINIRAM PDM-3. Adapted with permission from [11], available at https://www.sciencedirect.com/science/article/pii/0021850295000496.

3.3.2 Reproduction of an Evaluation by the Aerosol Photometer method

By combining the Mie theory applied for an aerosol photometer as in Equation (3.12) and one single experimental measurement for an arbitrary aerosol, Gorner et al. [11] presented the theoretical way to evaluate the response characteristic of the HUND TM digital µP (H. Hund, GmbH, Wetzlar, F.R.G.) and MINIRAM PDM-3 (Mie Inc., Bedford, MA, U.S.A.) (see Figure 3.3). They introduced the calibration index k/CF which allows one to calculate the aerosol photometer response for any other aerosol with known physical parameters. The coefficient k is the ratio of transformation between scattered light intensity $I_{c,multiple}$ obtained by the calculation and the same intensity expressed in voltage output (mV) given by the aerosol photometer in the experiment. In other words, k is a value of amplification of the photodetector voltage signal. The value k remains as constant as long as the aerosol photometer calibration does not change. The conversation factor CF is given by the factory setting which is an analogic-numeric, or voltage-display correspondence of the aerosol photometer. The ratio of the calibration constant k and CF yields a calibration index k/CF of the aerosol photometer, relating the intensity of scattered light to the mass concentration in mg/m^3. Thus, the concentration measured by the photometric method corresponding to a polydisperse aerosol C_{PHO} is

$$C_{PHO} = \frac{k}{CF} I_{c,multiple,poly} \quad . \tag{3.16}$$

Table 3.1: Optical parameters of HUND TM digital µP.

Wavelength of illumination light beam, λ	950 nm
Angle of detection of scattered light, ϕ	70°
Semi-angle of light collection, β	10°

Using the same aerosol photometer specification as in Gorner et al. [11] (Table 3.1), the calculation of the aerosol photometer response $I_{c,multiple,mono}$ in mg/m^3 as a function of particle diameter was performed for PAO particles which is the same particle type that will be used for this study. The results are reported in Figure 3.4 versus particle

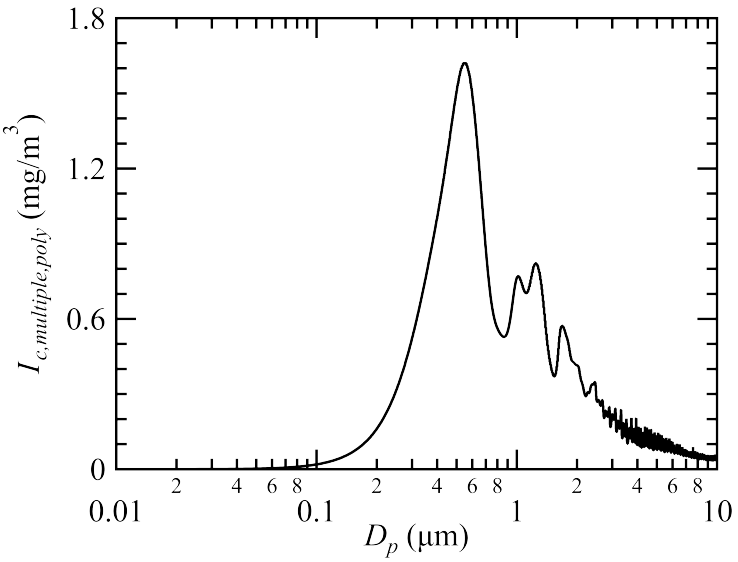

Figure 3.4: HUND TM digital µP aerosol photometer response function calculated as a function of the particle diameter for a polydisperse PAO particles.

diameter. The decline in response with an increasing particle size above 1 µm is common to all aerosol photometers [3, 4]. Complex interactions between the incident light and particle results in a wavy response curve. Finally, the leak rate evaluated by an aerosol photometer is calculated as below

$$L_{PHO} = \frac{C_{PHO,d}}{C_{PHO,u}} \quad . \tag{3.17}$$

3.4 Response of a Discrete Particle Counter

Discrete Particle Counter (DPC) counts and sizes aerosol particles by measuring the light that is scattered when an individual particle passes through a light beam. Figure 3.5 is a schematic diagram of a generic DPC data treatment process. Figure 3.5 illustrates the data processing required to convert from raw voltage pules data to a particle size distribution. A continuous stream of a single aerosol entered into detection chamber of a DPC via a narrow flow stream sandwiched by filtered sheath flows which then, these particles are illuminated by a light source[3] one at a time.

[3]white light has been used as a light source but current models use laser a light source

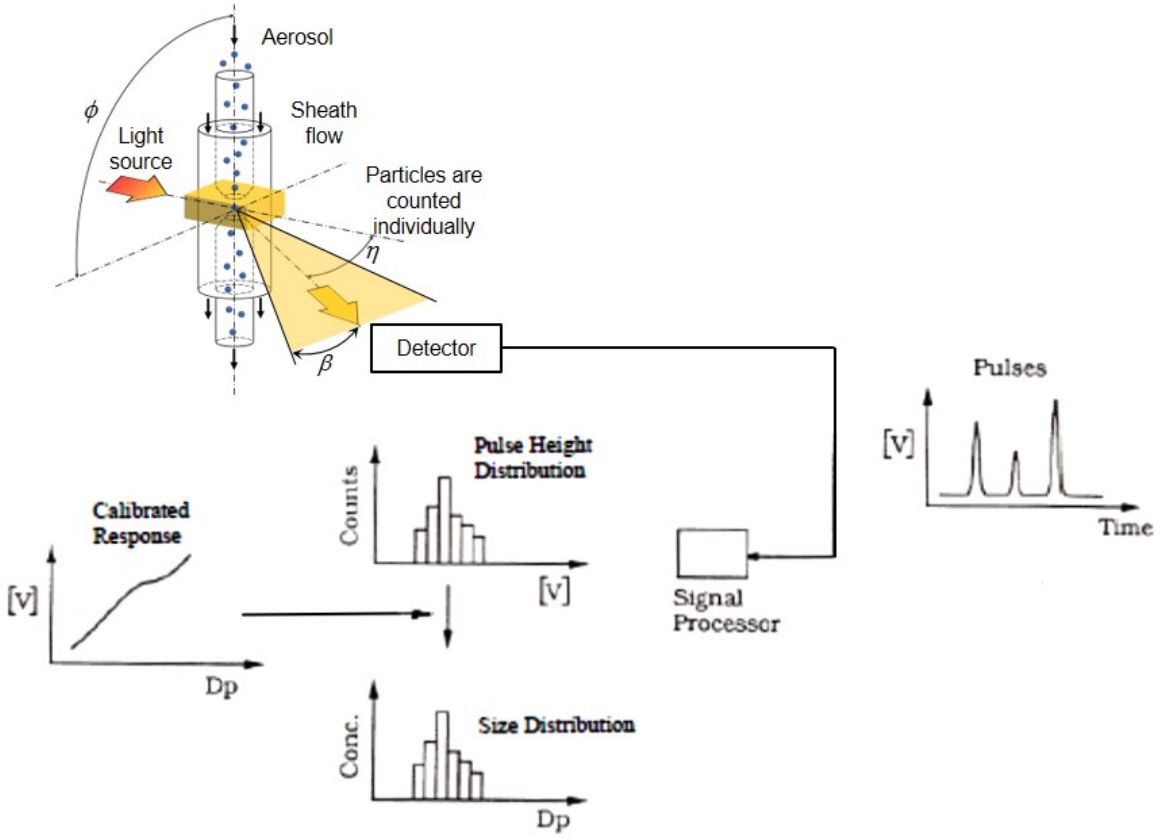

Figure 3.5: Discrete particle counter and data treatment process.

The scattered light by a single aerosol is collected by the photodetector position at a specific optical arrangement, thus, generates voltage pulse proportional to the total amount of scattered light. Then, via a signal processor, the pulse is amplified and grouped into several corresponding voltage bins (this is usually done by a built-in pulse height analyser (PHA)). Collection of these data formed a pulse height distribution data. A set of comparators (the threshold set to differentiate particle size according to different size intervals) then compare the pulse height distribution to the calibration data and finally converted them to a particle size distribution and reported as the particle number concentration per interval of particle diameter, which is called the channel.

The response of a DPC can be calculated using the same light scattering theory as explained in section 3.2. However due to complex post data processing, it is easier to use counting efficiency function of each channel that will be explained in the next subsection.

3.4.1 Counting Efficiency Function

An ideal DPC would have a counting efficiency function same as a step-function which represents 100% probability for larger particle size and 0% for smaller particle size than a specified particle size as illustrated by the dashed line in Figure 3.6a. This line will represent as boundaries for channels in a DPC. For this ideal DPC, a channel will produce a similar shape to a Dirac delta function as represented in (Figure 3.6b). In contrast, a real DPC will have a particular size resolution due to the effects such as non-uniform light intensity in the sensing area where the sample air passes through the illuminating flux, variations in the sensitivity of the surface of a photodetector and electrical noise. These factors will underestimate and overestimate the particle size reported by a DPC, thus producing not a step function counting efficiency but rather a curve with a slope.

The solid line in Figures 3.6a and 3.6b shows the counting efficiency function and the channel response (resulted by the subtraction of a two consecutive counting efficiency curves acting as the channel boundaries of a discrete size interval) of the PMS LAS-X particle counter by the Particle Measuring Systems used in this chapter. This model has been discussed and studied extensively in many research papers [37, 17]. PMS LAS-X is capable of particle sizing in the diameter range from 0.1 µm to 7.5 µm in which this size range is divided into 16 channels. The sigmoidal function according to the requirements of the ISO 21501-4: 2007 [22] and (JIS B 9921: 2010 [25]) standard are found to be the best fit for the counting efficiency function of the PMS LAS-X particle counter.

The counting efficiency of the DPC for any channel, $\eta_{i,eff}(D_p)$, can then be represented for any particle size as follows

$$\eta_{i,eff}\left(D_p\right) = A\left\{1 + erf\left(\frac{D_p - D_{bin}}{W\sqrt{2}}\right)\right\} \quad , \tag{3.18}$$

where, the function erf is the error function, W is a measure of the distribution width producing different resolution in the counting efficiency curve at a particular channel boundary size D_{bin}. The properties of $\eta_{i,eff}(D_p)$ is equal to >0 for $D_p \ll D_{bin}$, 0.5 for $D_p = D_{bin}$, and 1 for $D_p \gg D_{bin}$. Thus, D_{bin} becomes the radius representing the 50%

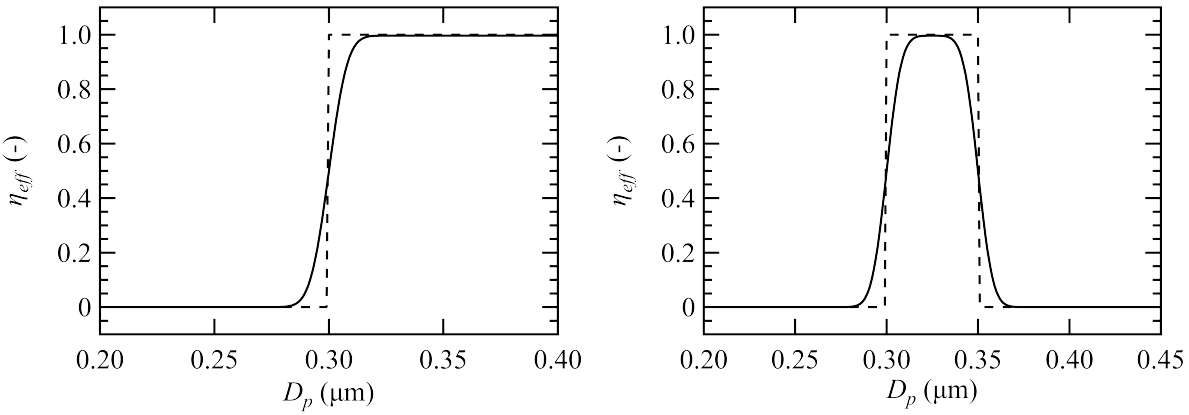

(a) Counting efficiency curves **(b)** Resulted channel measurement

Figure 3.6: Comparison between an ideal and a real DPC (PMS LAS-X particle counter). The dashed and solid lines represent an ideal particle counter and PMS LAS-X particle counter, respectively.

counting efficiency point for any one channel of the DPC. $\eta_{i,eff}(D_p)$ has the right limiting behaviour, and the rate at which $\eta_{i,eff}(D_p)$ approaches the lower and upper limits of 0 and 1, and the spread is determined by W.

3.4.2 Reproduction of an Evaluation by the DPC method

Assuming that a DPC with n number of channels counts a discrete set of measurement in each channel. The total number of particles detected by a DPC in a given sample with a number of particles per unit volume of C_N and particle size distribution function of $f(D_p)$

$$C_{DPC} = \sum_{i}^{n} \sum_{0}^{\infty} C_N \times \left| \eta_{i,eff}^{upper}(D_p) - \eta_{i,eff}^{lower}(D_p) \right| f(D_p), \quad i = 1, 2, ..., n \quad , \tag{3.19}$$

where, $\eta_{i,eff}^{upper}(D_p) - \eta_{i,eff}^{lower}(D_p)$ is the difference between the upper and lower counting efficiency boundary corresponding to the counting efficiency of the ith channel. By comparing the cumulative count between downstream and upstream challenge aerosol concentration, leak rate evaluated by DPC is as follows

$$L_{DPC} = \frac{C_{DPC,d}}{C_{DPC,u}} \quad . \tag{3.20}$$

3.5 Results and Discussion

Figure 3.8 shows the upstream and downstream particle concentration distribution of the H13 filter (standard penetration at MPPS: Most penetrating particle size is 0.05%) evaluated by the number concentration (Equation (2.16)) and DPC (Equation (3.20)). Similarly, Figure 3.7 shows the upstream and downstream particle concentration distribution evaluated by mass concentration (Equation (2.13)) and aerosol photometer (Equation (3.17)) methods. The leak rate for the number concentration and DPC methods in Figure 3.8 were calculated by comparing downstream concentration to upstream concentration cumulatively for particles larger than 0.3 µm shown by the area of the shaded regions. However, for the mass concentration and aerosol photometer methods, the integration across the whole particle range is considered in the leak rate calculation as illustrated by the shaded regions in Figure 3.7. These figures depict the case for a filter barely satisfies a standard performance (based on the EN 1822-1: 2009 [9] standard) with exactly no leak such as a pinhole or tear present of the filter media. If there are any leaks, the downstream concentration curve shown in the graph will indicate a larger value than presented in the figures.

As can be seen from the figures, all evaluation methods show a decreasing trend for larger particle size after peaking at certain particle size. In the case of filter upstream and downstream distribution, mass concentration and aerosol photometer evaluation methods peak at a larger particle size as compared to the number concentration and DPC evaluation methods. Furthermore, mass concentration and aerosol photometer methods have significantly lower the gradient for small and large particles with aerosol photometer having a higher value at the peak around particle size 0.5 µm and a steeper gradient for particle larger and smaller than peak particle size as compared to the mass concentration method. Aerosol photometer response decreases for particles smaller and larger than particle size around 0.5 µm which gives a less weighted value as compared to mass concentration evaluation method. Since the leak rate is the ratio between the

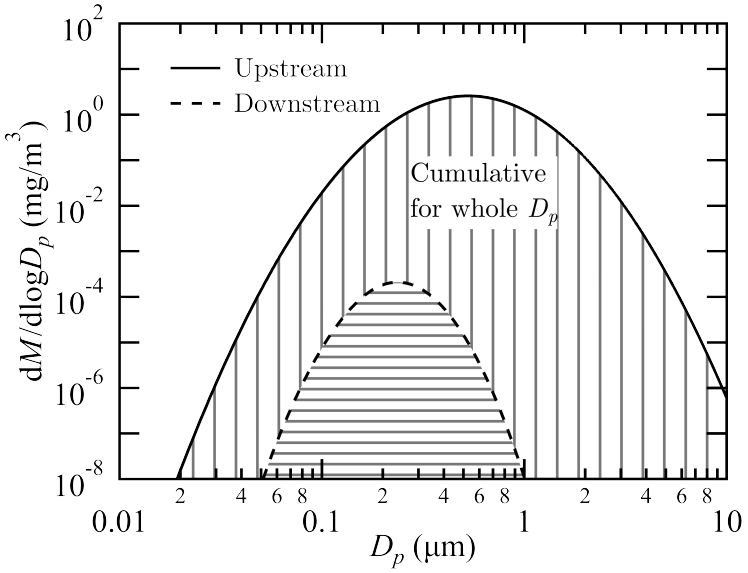

(a) Mass concentration

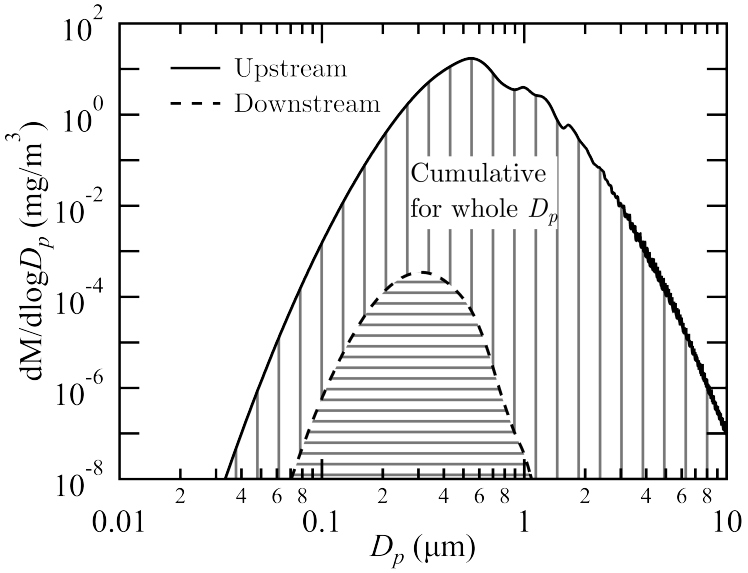

(b) HUND TM digital µP

Figure 3.7: Particle concentration distribution at the upstream and downstream side of an H13 filter (Standard penetration at MPPS: 0.05%) as a function of particle diameter evaluated by **(a)** mass concentration and **(b)** aerosol photometer (HUND TM digital µP). The leak rates for both methods were calculated by comparing the area of the shaded regions for the whole existing particle size range considered (0.01 µm to 10 µm) at the upstream and downstream of a filter.

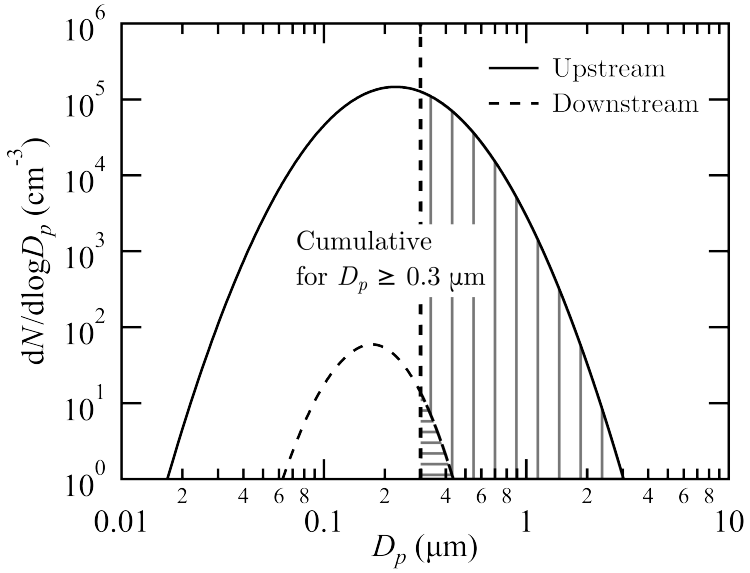

(a) Number concentration

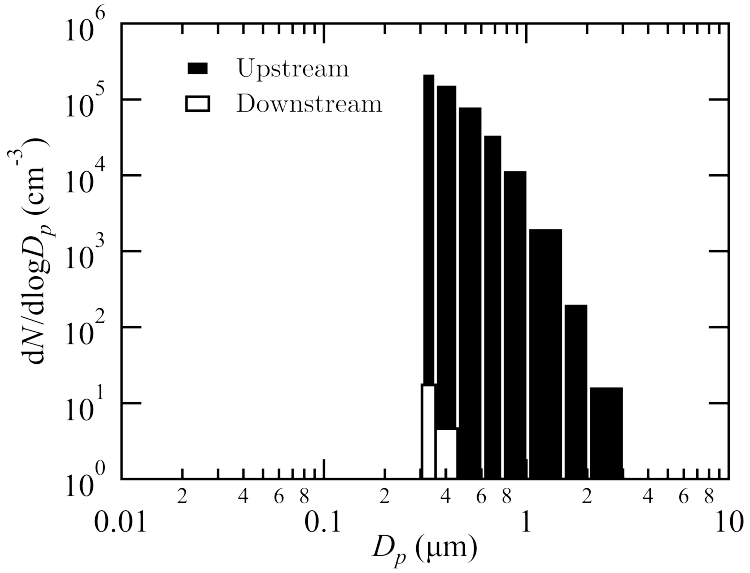

(b) PMS LAS-X

Figure 3.8: Particle concentration distribution at the upstream and downstream side of a H13 filter (Standard penetration at MPPS: 0.05%) as a function of particle diameter evaluated by **(a)** direct number concentration method and **(b)** number concentration measured by PMS LAS-X particle counter. The leak rates for both methods were calculated by comparing the area of the shaded regions for particle size ≥0.3 µm at the upstream and downstream of a filter.

area under the curves shown as two different hatched regions in each figure, the evaluation of the number concentration and DPC methods are expected to be more severe than the mass and aerosol photometer methods.

Table 3.2: Leakage rate of each filter evaluated by number concentration, DPC, mass concentration and aerosol photometer method. Green and red coloured cells represent leak rate value smaller and greater than 0.01% (1×10^{-4}), respectively.

Filter grade	Leakage rate			
	Number Conc.[a]	DPC	Mass Conc.[a]	Photometer
H13 (0.05% at MPPS)	2.86×10^{-5}	2.90×10^{-5}	2.03×10^{-5}	1.07×10^{-5}
H14 (0.005%)	2.86×10^{-6}	2.90×10^{-6}	2.03×10^{-6}	1.07×10^{-6}
U15 (0.0005%)	2.86×10^{-7}	2.90×10^{-7}	2.03×10^{-7}	1.07×10^{-7}
U16 (0.00005%)	2.86×10^{-8}	2.90×10^{-8}	2.03×10^{-8}	1.07×10^{-8}

[a] The same data as presented in Table 2.4 for cumulative leak evaluation at $Dp \leq 0.3$ µm.

Table 3.2 shows the leak rate for each filter from H13 to U16. As expected, number concentration and DPC methods produced larger values but within the same order as compared to mass concentration and aerosol photometer methods. DPC method has relatively the same value as the number concentration method. The difference between these two measurements is caused by the resolution of the counting efficiency curve of a particle counter as shown in Figure 3.6b. The aerosol photometer method has a leak rate value of approximately half of the mass concentration method. This is due to the different weighted value applied to particle correspond to the aerosol photometer response curve (Figure 3.4).

In the current ISO 14644-3: 2005 [21], an evaluation based on the detection of downstream particle concentration exceeding ten times the standard penetration of the test filter is currently used. This is based on the experimental result of Suzuki et al. [36] which became the basis of this standard. Suzuki et al. [36] found that pinhole leak could not be determined clearly unless a leak evaluation criterion about ten times of the standard penetration is being used. Therefore, based on the calculated leak rate, the leak criterion of 0.01% for H13 or higher performance filter perfectly matched this condition. However, in order to clearly assign the unification of leak evaluation criterion further investigation across allowable GSD, MMD and CMD range presented in ISO 14644-3: 2005 [21] were done.

Figure 3.9 illustrates the leak rate seen by the instruments for different polydisperse aerosols, all with GSD=1.7 for the H13 and H14 filters evaluated by Equations (3.17) and (3.20) for the aerosol photometer and DPC method, respectively. Both DPC and number concentration method measurements produced relatively flatter curve as compared to mass concentration and aerosol photometer methods. DPC and number concentration methods agree well with each other which is expected. Aerosol photometer leak rate curve resembles that of a mass concentration measurement method but detects maximum leak rate at a much smaller MMD. As explained before, both methods give more weight to the larger particles and see the aerosols as having a larger size than number concentration and DPC methods. However, since aerosol photometer utilises light scattering to observe particles, the particle size dependence weight is different from a normal mass concentration method due to the response function as illustrated in Figure 3.4.

A striking feature is that starting from a particular particle size, the DPC method seems to agree with aerosol photometer method for larger MMD and CMD. Aerosol photometer method produced leak rate of the same order to DPC method starting around MMD=0.2 µm (CMD=0.1 µm) and DPC method intersects with aerosol photometer method at CMD approximate to MPPS. The shaded region with green and yellow colour represents the allowable MMD (0.5 µm to 0.7 µm) and CMD range (0.1 µm to 0.5 µm) for aerosol photometer method and DPC methods as presented in ISO 14622-3: 2005 [21]. In the green shaded region, DPC and aerosol photometer methods have the same order in leak rate value but the difference increases as the MMD increases. In the case of H13 filter, leak rate within the allowable CMD range (0.1 µm to 0.5 µm) of a DPC method, the values of leak rate are very close to the leak evaluation rate criterion of 0.01% represented by the red dashed line which can be ambiguous if the same criterion shall be used for both aerosol photometer and DPC methods. This is not the case for H14 filter. All leak rate values are below than 0.01%.

Figures 3.10 and 3.11 summarise the results for log-normal aerosols concentration distribution having different GSDs in the range of 1.1, 1.3, 1.5 and 1.7 for H13 and H14

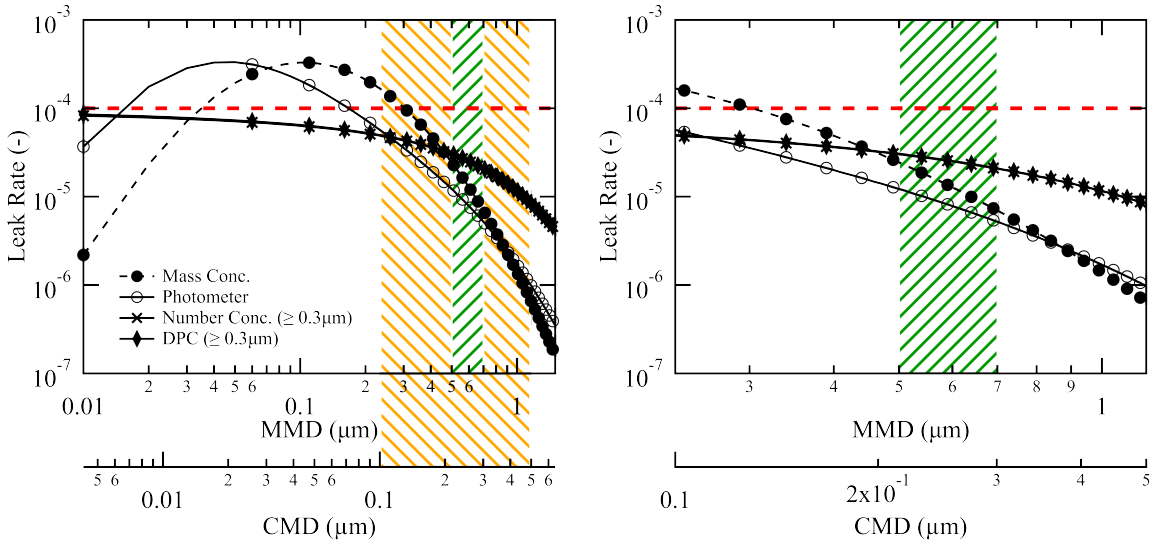

(a) H13

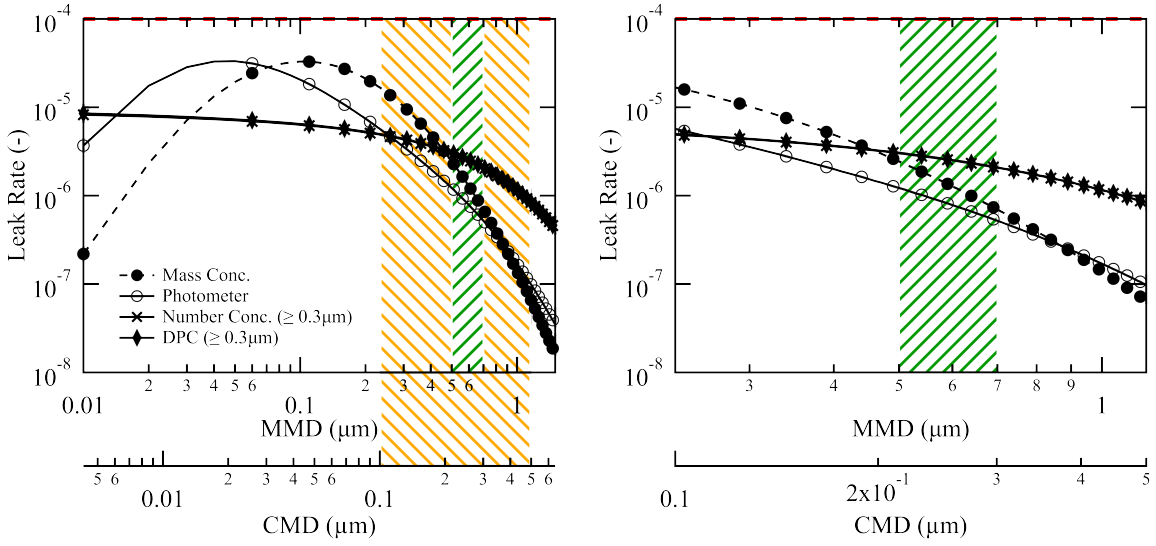

(b) H14

Figure 3.9: Leak rate calculated by the cumulative leak evaluation method for DPC method and aerosol photometer at GSD=1.7. The shaded areas represent the allowable MMD (0.5 to 0.7 µm) and CMD (0.1 to 0.5 µm) range for aerosol photometer and DPC in ISO 14644-3: 2005 [21], respectively. The left figure shows the result for MMD range (0.01 to 1.5 µm) used in the calculation. The right figure shows the zoomed-in result within the allowable CMD range. The red dashed line indicates the threshold criteria of 0.01% (1×10^{-4}).

filter, respectively. Results are plotted for both MMD and CMD within the allowable CMD (0.1 to 0.5 µm) range. As the aerosol comes closer to being monodisperse, the DPC and aerosol photometer methods leak rate agrees well regardless of the aerosol size. This convergence corresponds to the first limiting case for current calculation, regardless of any measurement methods but only concentration for corresponding particle size is calculated. For any given GSD, there is also an aerosol of a certain size that produces the same leak rate value. Such a family of curves exists having different leak rate. Although DPC and aerosol photometer methods differed in values, they correlated reasonably well within the allowable MMD and CMD range, which is unexpected since both yield a different unit of measurement. However, since we made a comparison based on the cumulative calculation across particle size range, the difference that was thought significant when the previously compared result between DPC leak rate value at a particular size to a single aerosol photometer leak rate value for the whole existing particle size range was significantly diminished.

The H13 filter leak rate result obtained by the DPC method for smaller GSD ($\leq$1.2) produced values larger than 0.01%. In contrast, all leak rate values by the DPC method for H14 filter had values under 0.01% even for small GSD. Practically, a low GSD $\leq$1.2 is usually not set for the upstream challenge aerosol due to the performance of the aerosol generator. However, this will create possibility of a misjudgement of leak during an inspection. For this reason, it is considered unreliable to apply for the same standard leak evaluation criteria of 0.01% as the aerosol photometer method to the filter with a performance of H13 or less for the DPC method. On the other hand, since the installed filter leak test is not done to evaluate the performance of the filter itself, leak evaluation criterion of 0.01% is considered applicable to the filters with H14 or higher performance (U15 and U16).

3.6 Conclusion

The responses of the aerosol photometer and DPC methods were considered to investigate theoretically the leak evaluation of air filters. The theoretical approach involves calculating

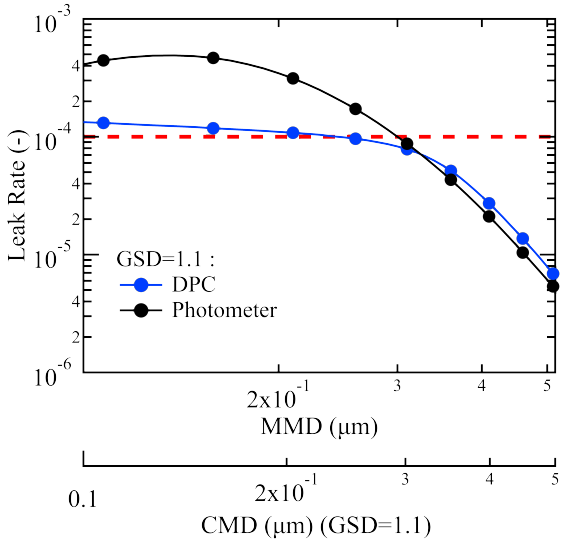

(a) GSD=1.1

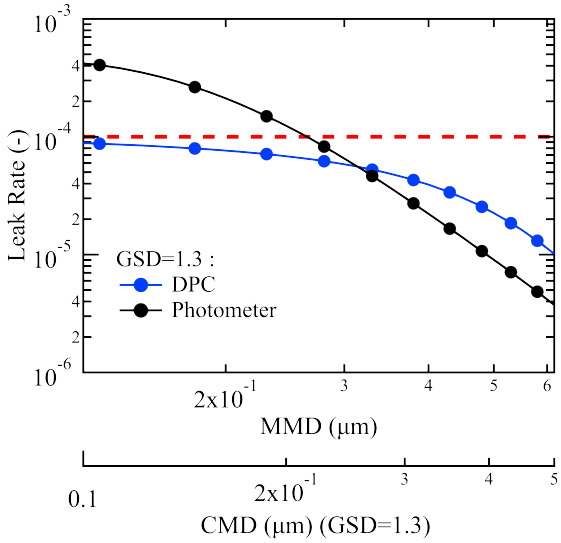

(b) GSD=1.3

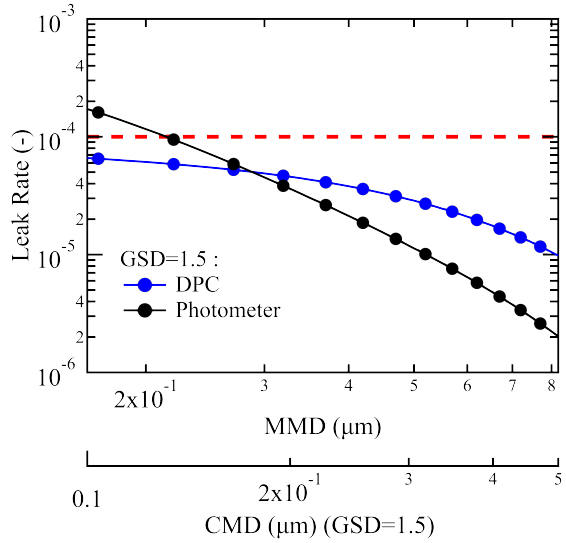

(c) GSD=1.5

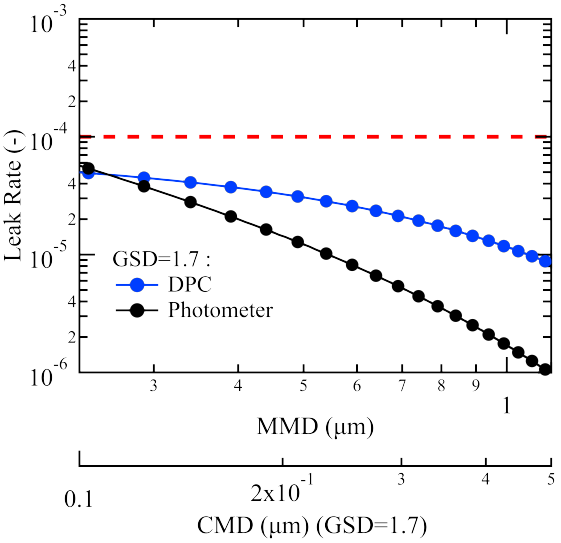

(d) GSD=1.7

Figure 3.10: Comparison of leak rates detected by the DPC and aerosol photometer for different upstream lognormal distribution of challenge aerosols (GSD=1.1, 1.3, 1.5 and 1.7) for H13 filter within the allowable range of CMD (0.1 to 0.5 µm). The red dashed line indicates the threshold criteria of 0.01% (1×10^{-4}).

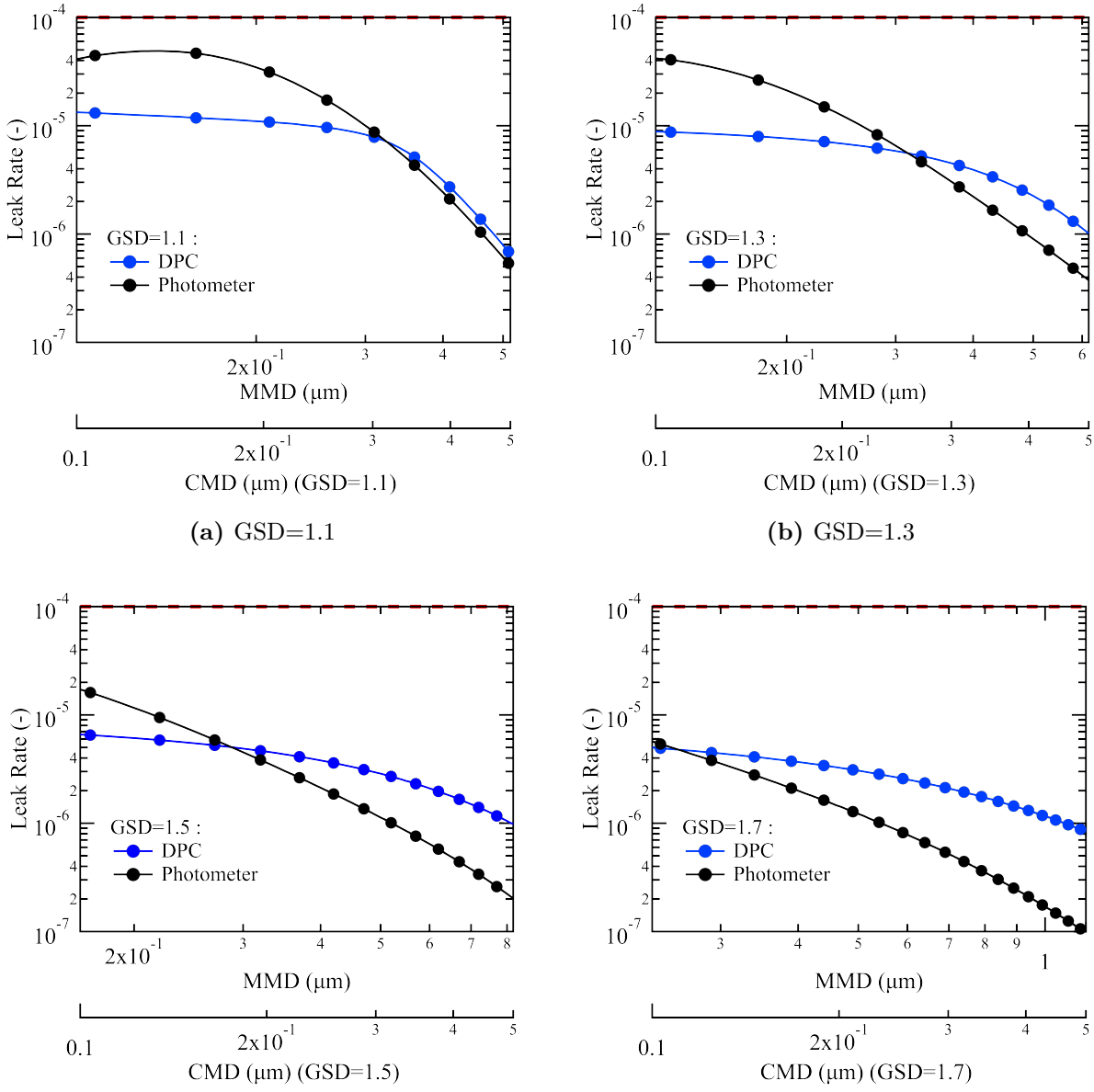

(a) GSD=1.1 **(b)** GSD=1.3

(c) GSD=1.5 **(d)** GSD=1.7

Figure 3.11: Comparison of leak rates detected by the DPC and aerosol photometer for different upstream lognormal distribution of challenge aerosols (GSD=1.1, 1.3, 1.5 and 1.7) for H14 filter within the allowable range of CMD (0.1 to 0.5 µm). The red dashed line indicates the threshold criteria of 0.01% (1×10^{-4}).

the filter leak rate in which an instrument measures by numerical integration of aerosol size distributions, filter penetration, aerosol photometer and DPC response functions. Based on the calculation, the DPC method produces a leak rate value that gives equal importance on each set of particle range regardless of its size. On the other hand, the aerosol photometer which emphasises more on the larger particles in a distribution, yields the value more closely associated with the particle mass concentration penetrating the filter. The differences between these two instruments are further dependent on the MMD or CMD of the challenge aerosol distribution. When test aerosols have a CMD greater than MPPS for the filter, the DPC method can be expected to have higher leak rate values than aerosol photometer method. In contrast, when aerosols have a CMD less than the MPPS, the aerosol photometer method shows higher leak rate values than the DPC method. The possibility of a unified criterion for a leak test of an installed filter system by considering the characteristics of DPC and aerosol photometer methods were studied through the trends and values of the calculated leak rate. As a result, it was found that for a filter having H14 or higher performance in European standard EN 1822-1: 2009 [9], the same leak evaluation standard 0.01% as the aerosol photometer method can be applied in the DPC method. On the other hand, it was found that it was not possible to apply the uniform criterion for filters with H13 or lower performance, therefore, it is necessary to establish different criteria.

Chapter 4

Evaluation by Different DPCs

Contents

4.1 Introduction

In Chapters 2 and 3 we discussed the fundamental differences between aerosol photometer and DPC method. In Chapter 2 we did a comparison between mass concentration and number concentration which is the principle measurement unit for aerosol photometer and DPC method, respectively. We found that in the current leak evaluation method for aerosol photometer (cumulative) and DPC (discrete) presented in ISO 14644-3: 2005 [21] differ tremendously in term of leak rate values calculated. It is not possible to use the same 0.01% threshold for DPC as used in the aerosol photometer method. Then, a cumulative leak evaluation method was proposed as an alternative method. Within the allowable range of GSD, MMD and CMD according to ISO 14644-3: 2005 [21], the cumulative leak evaluation method produced leak rate values lower leak rate than 0.01% and comparable to the aerosol photometer method.

Through the comparison between the real measurement value of the aerosol photometer and DPC method by considering the respective instrument responses, results with a similar trend were obtained. This shows that by using cumulative leak evaluation method instead of the discrete leak evaluation method currently presented in ISO 14644-3: 2005 [21] for DPC method give a possibility on unifying threshold criterion for both aerosol photometer method and DPC method. However, with that being said, based on the results from Chapters 2 and 3, the same threshold could not be used for all filter grades. For filter grade performance of equal to H14 and greater, the same threshold of 0.01% same as aerosol photometer can be used, while for filter grade equal to H13 and lower, a different threshold should be used.

The investigation done in the previous chapters in particular Chapter 3, only one type of DPC response (channel counting efficiency) was considered, the leak rate evaluated by DPC method for filter grade H13 came very close to the threshold criterion of 0.01%. Considering the risk of leaks to be misevaluated, we concluded the same conclusion as in Chapter 2. Furthermore, based on the studies done by Katagiri et al. [27] with 25 different

DPCs showed that with different optical configuration, light source type, amplification system and post-data processing treatment gives different counting efficiency function. This is due to different characteristics of scattered light produced, systemic error and noises occurred inside the DPC. In addition, they also found that even with the same DPC, the performance is different. This means that the age of a DPC also plays an important factor in the performance of the counting efficiency of a DPC.

Therefore, in order to establish a well-defined study, an elaborate study by considering other types of DPC responses need to be done. This will answer our remaining question, is the DPC reliable to produce constant leak rate value below 0.01% with presently used standard penetration rate function in this study. In this chapter, we will do calculations on various type of DPC responses based on measurement channel specification and counting efficiency performance.

4.2 Calibration Process and Source of Error of a DPC

In Chapter 3, the counting efficiency function was used to model the response of a DPC. The counting efficiency acts as the boundaries between channels. A response of a channel is obtained by the subtraction between two consecutive counting efficiency functions. The counting efficiency function used to model DPC in Chapter 3 was obtained from the experimental data of a monodisperse aerosol presented in the research paper. To our knowledge, data on the counting efficiency of a DPC is very limited[1]. Therefore, in order to model a counting efficiency of a DPC, we need to understand the fundamental principle of a DPC and some assumption and limitation need to be established.

Calibration of a DPC is done by passing a continuous stream of a monodisperse particle through DPC detection chamber (sensor). The particles are illuminated by the light source and scattering the light. This generates a series of electrical pulses (see Figure 4.1) with each pulse corresponds to a particular particle size, then, sorted to a distribution of pulse

[1]Most of counting efficiency reported are for condensation particle counter (CPC).

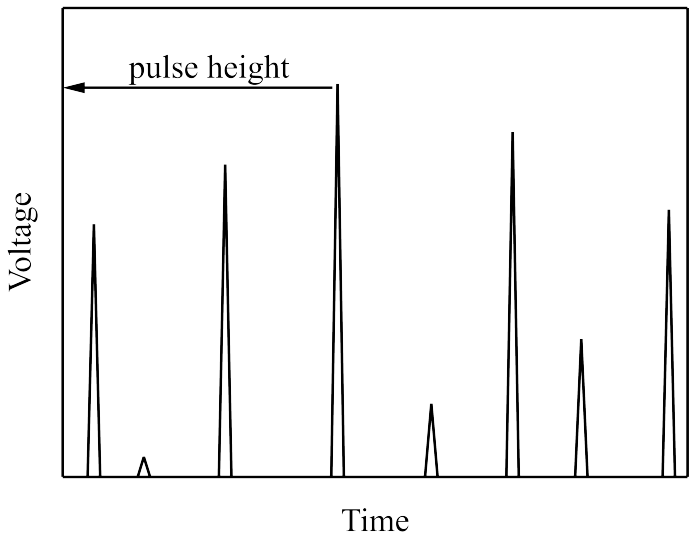

Figure 4.1: Series of electrical pulses generated by monodisperse aerosols

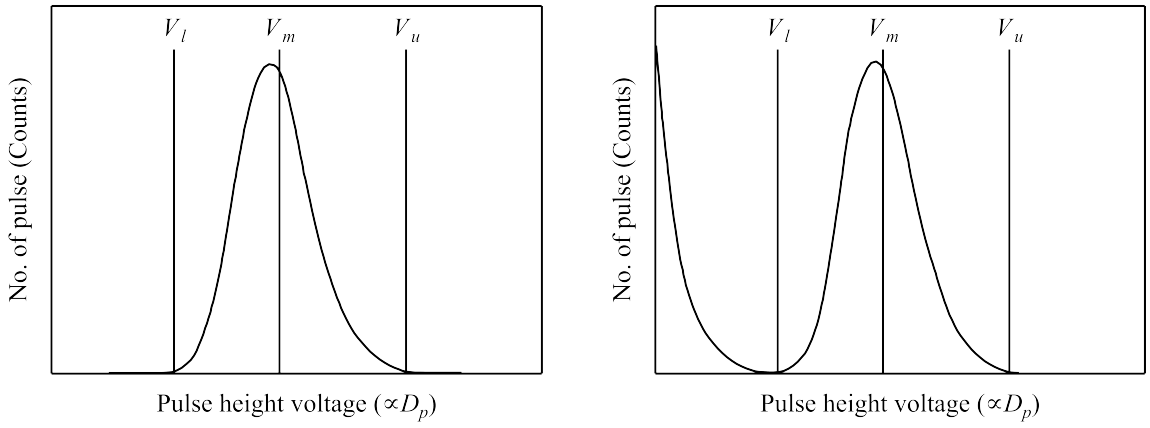

(a) Without noise **(b)** With noise

Figure 4.2: Pulse height distribution of a monodisperse aerosols.

heights. Figure 4.2 shows a typical pulse height distribution measured by a DPC for a sample of monodisperse aerosols for cases with and without noise. The median value of the distribution is treated as the appropriate channel calibration threshold for that particle size. Even though a sample consists of monodisperse aerosols being measured but resulting in a distribution with a spread, typically have a property similar to Gaussian distribution as in Figure 4.2. Although a theoretical light scattered (see section 3.1) by a single particle supposedly have a single-valued voltage, but due to the unavoidable spectra broadening effect creates what we called as resolution (as shown in Figure 4.3)

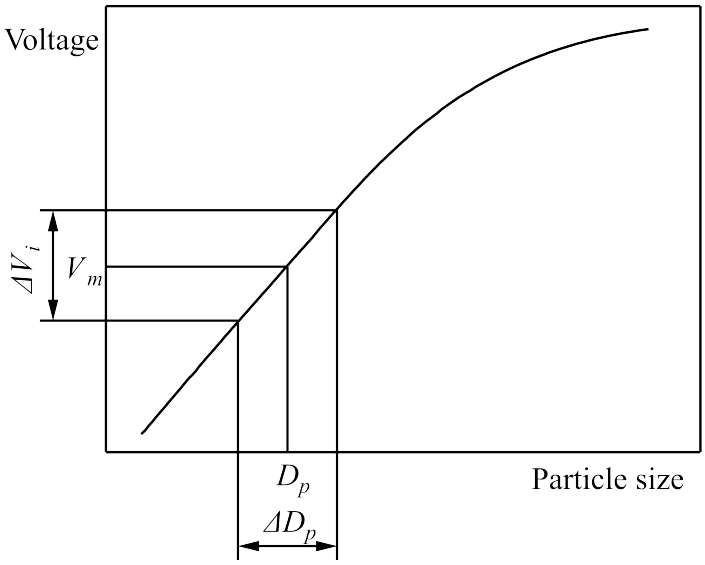

Figure 4.3: Resolution in light scattering response of a DPC.

in the DPC measurement. This spread is what is called spectra broadening effect of a DPC which truly depicts the response of a DPC.

4.2.1 Spectral Broadening Effect

The spectra broadening effect can be caused by several possible factors such as

(i) Photoelectron statistical broadening,

(ii) Different particle residence time in the illumination volume,

(iii) Non-uniformity in particle illumination,

(iv) variation in point-to-point photomultiplier tube (PMT) response.

The signal broadening can be further enhanced by other effects such as the varying orientation of aspherical particles with respect to the direction of the incident light and coincident count events. The latter becomes relevant for a very high particle concentration when the average inter-particle distances are not larger than the size of the sampling volume anymore. In such a case, the probability of erroneously interpreting the sum of several scattering signals from multiple particles as a single particle's signal increases.

In addition to an artificial deformation of the size distribution towards larger sizes, this entails an underestimation of total particle number concentration. These two effects can be minimised with proper calibration and aerosol generation.

Many studies have addressed the coincident error count by a DPC but only scarce studies focusing on the spectral broadening effect of a DPC. Pulse height distribution produced by a DPC exhibits the spectral broadening effect that typically in the form of Gaussian distribution. Van der Meulen et al. [29] and Deshler et al. [6] stated that the ideal counting efficiency function of a DPC is the product of the convolution of several Gaussian distributions. The first Gaussian distribution arises from generated sample aerosol which at each size measured, results from a narrow Gaussian distribution. The other Gaussian distributions arise from the PMTs used to obtain from the DPC measurement. The output of each PMT is a Gaussian pulse height distribution, which arises from the pulse broadening inherent to the PMTs used in the instrument.

The convolution of Gaussian distributions is also a Gaussian distribution with well-defined dependencies between the convolved distribution and the underlying distributions. Thus, it is reasonable to use a Gaussian function to represent since they resulted from the convolution of several Gaussian distributions. The measured counting efficiency of any DPC channel can be represented as the integral of a Gaussian distribution or cumulative distribution function, characterised by a distribution median and width as in Equation (3.18).

4.3 Requirements regarding the Counting Efficiency of a DPC

A brief explanation on ISO 21501-4: 2018 [22] was given in Chapter 3 as a basis to our DPC response modelling. This standard is a typical standard being used for instruments applied in contamination control monitoring in cleanrooms and the associated environment under the ISO 14644-1: 2015 [20] (JIS B 9920) standard. In accordance to this standard, the counting efficiency for a single particle measurement instrument should be within

30% to 70% which corresponds to 50%±20% for the minimum detectable particle size and within 90% to 110% corresponds to 100%±10% for particle size 1.5 to 2 times larger than the minimum detectable particle size. This does not mean that DPC will only count 50% of the minimum detectable particle size. In fact, all particles greater than 0.3 µm will be counted. Furthermore, if the next channel is smaller than 1.5 to 2 times the minimum detectable particle size, it does not means that the channel will have the counting efficiency at the channel lower particle size boundary. The fact is all channels in a properly calibrated DPC will, by definition have a counting efficiency of 50%±20% at the channel lower particle size boundary and a counting efficiency of 100%±10% at 1.5 to 2 times the channel lower particle size boundary. Figure 4.4 shows region where DPC counting efficiency bounded by the ISO 21501-4: 2018 [22] standard requirement.

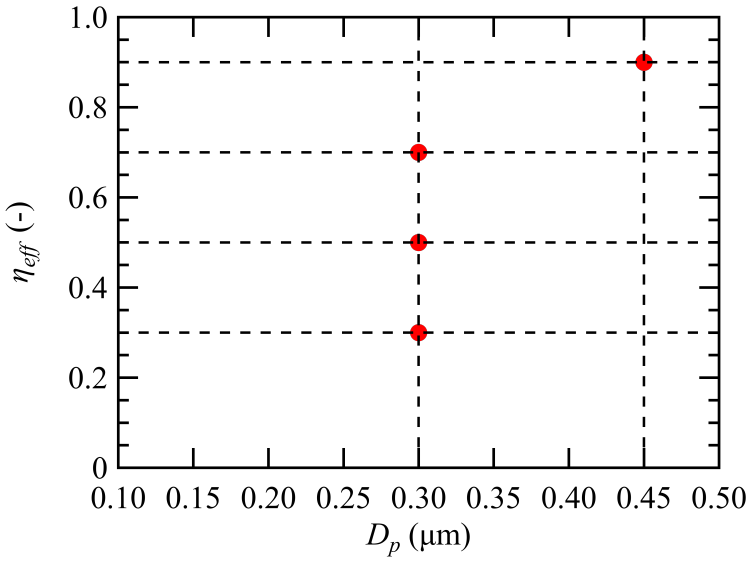

Figure 4.4: The limitations stated in ISO 21501-4: 2018 [22].

4.4 Modelling DPCs with different counting efficiency

As discussed in Chapter 3 (see section 3.4) a sigmoidal function as in Equation (3.18) proved to be the best fit for the counting efficiency function representing the upper

and lower boundaries for each channel in a DPC. Using a sigmoidal function and the limitation conditions provided by ISO 21501-4: 2018 [22], we tried to calculate the leak rate evaluated by a DPC using cumulative leak evaluation method proven to be suitable for threshold unification in order to determine whether a DPC is reliable to produce constant leak rate values below 0.01%.

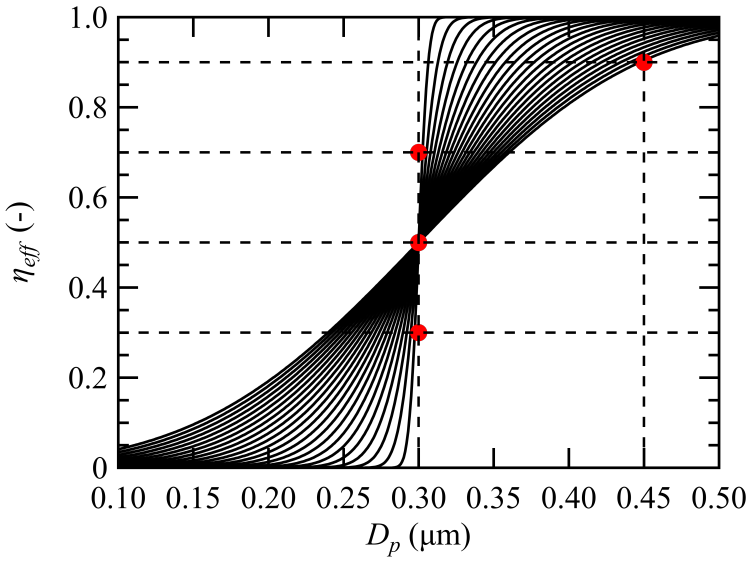

Figure 4.5: Different in resolution of the counting efficiency across 50% at 0.3 μm.

4.4.1 Difference in Resolution

In order to determine counting efficiency within this region, several parameters are needed to be assigned. Okui [32], in his paper on the counts difference between different DPCs, proposed two different parameters in order to differentiate the counting efficiency between different DPCs. The first one is the difference in resolution. The resolution of a DPC is represented by the gradient of the slope of the counting efficiency function. The slope gradient can be changed by adjusting the value of W in Equation (3.18). The difference in resolution by counting efficiency function is illustrated in Figure 4.5. A smaller value will give steeper counting efficiency function. In other words, a smaller value will give higher measurement resolution to the DPC. This is only limited for the

case of 50% counting efficiency at the minimum detectable particle size and the particle size at the lower boundary of each channel.

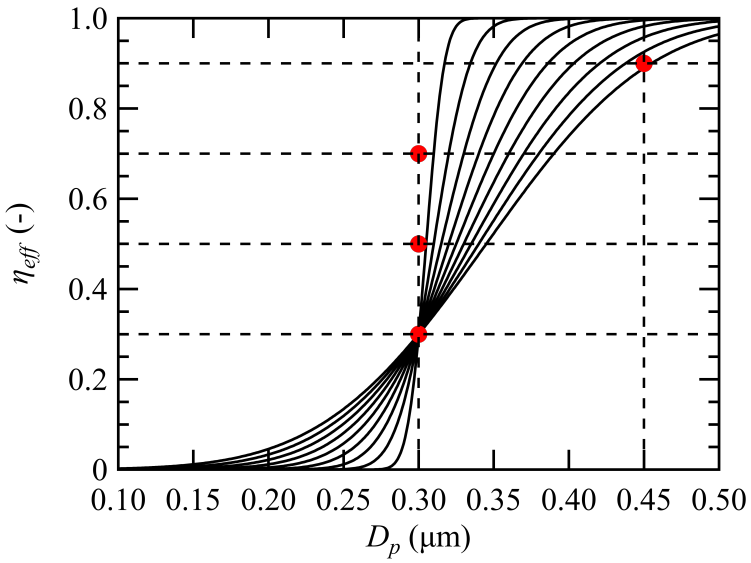

(a) Counting efficiency across 30% at 0.3 µm

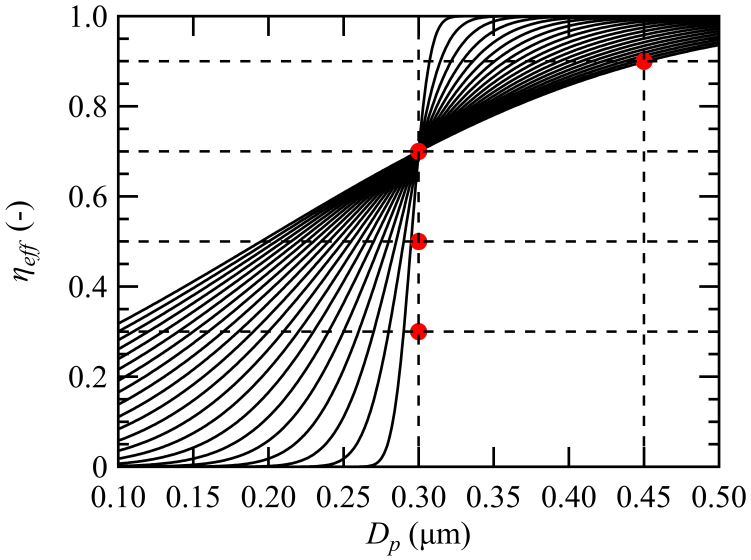

(b) Counting efficiency across 70% at 0.3 µm

Figure 4.6: Different in diameter of the counting efficiency across 30% and 70% at 0.3 µm.

4.4.2 Difference in Diameter Sensitivity

Next, is the difference in the diameter sensitivity. Diameter sensitivity is when the lower channel boundary have a counting efficiency that is not equal to 50%. However, this could not be done by only changing the spread of the function. This is because, Equation (3.18) is equal to >0 for $D_p \ll D_{bin}$, 0.5 for $D_p = D_{bin}$, and 1 for $D_p \gg D_{bin}$. Thus, D_{bin} becomes the radius representing the 50% counting efficiency point for any one channel of the DPC. Therefore we need to adjust both W and D_{bin} until we find the functions that agree with the limitations by the ISO 21501-4: 2018 [22] standard for counting efficiency 30% and 70% at the minimum detectable particle size. In Figure 4.6, counting efficiency functions with diameter sensitivities are illustrated. Based on the counting efficiency function of different resolutions and diameter sensitivities, the leak rate evaluated by the DPC method is calculated.

4.4.3 Channel Specifications

The other important thing needs to be considered is the channel specification of a DPC, DPC method is called discrete due to channel used as the principle measurement method. DPC counts particle at sets of different particle size interval. We surveyed some commercially available DPCs that are certified for the use of contamination monitoring of a cleanroom under ISO 14644-1: 2015 [20] and ISO 21501-4: 2018 [22] standard. Table 4.1 shows some of the DPC models with their respective channel specifications. Based on our survey, we found that ≥0.3 µm, ≥0.5 µm, ≥1.0 µm, ≥3.0 µm, ≥5.0 µm and ≥10.0 µm are the generally available channel specification in commercial DPC. In this chapter, this channel specification is chosen to be the principal channel specification in the calculations. Next, a parametric study for all filter grades of H13 to U16 were also taken with the different challenge aerosol concentrations at the upstream side through the allowable GSDs (up to 1.7) and CMDs (0.1 µm to 0.5 µm) for a DPC method in the ISO 14644-3: 2005 [21].

Table 4.1: Channel specification of DPCs

Brand	Model	Size Range
Met One [34]	3413/3423	≥0.3 µm, ≥0.5 µm, ≥1.0 µm, ≥3.0 µm, ≥5.0 µm, ≥10.0 µm
	3415/3425	≥0.5 µm, ≥1.0 µm, ≥2.0 µm, ≥3.0 µm, ≥5.0 µm, ≥10.0 µm or ≥25.0 µm
	3445	≥0.5 µm, ≥1.0 µm, ≥2.0 µm, ≥3.0 µm, ≥5.0 µm, ≥10.0 µm
	3411	≥0.1 µm, ≥0.2 µm, ≥0.3 µm, ≥0.5 µm, ≥1.0 µm, ≥5.0 µm
Rion [33]	KC-22A	≥0.1 µm, ≥0.15 µm, ≥0.2 µm, ≥0.3 µm, ≥0.5 µm
	KC-22B	≥0.08 µm, ≥0.1 µm, ≥0.2 µm, ≥0.3 µm, ≥0.5 µm
	KC-24	≥0.1 µm, ≥0.15 µm, ≥0.2 µm, ≥0.3 µm, ≥0.5 µm
	KC-31	≥0.3 µm, ≥0.5 µm, ≥1.0 µm, ≥2.0 µm, ≥5.0 µm, ≥10.0 µm
	KC-32	≥0.3 µm, ≥0.5 µm, ≥1.0 µm, ≥2.0 µm, ≥5.0 µm, ≥10.0 µm
	KC-01E	≥0.3 µm, ≥0.5 µm, ≥1.0 µm, ≥2.0 µm, ≥5.0 µm
	KC-03B	≥0.3 µm, ≥0.5 µm, ≥1.0 µm, ≥2.0 µm, ≥5.0 µm
PMS [28]	Lasair III 310B	≥0.3 µm, ≥0.5 µm, ≥1.0 µm, ≥3.0 µm ≥5.0 µm, ≥10.0 µm
	Lasair III 310C	≥0.3 µm, ≥0.5 µm, ≥1.0 µm, ≥5.0 µm ≥10.0 µm, ≥25.0 µm
	Lasair III 310L	≥0.3 µm, ≥0.5 µm, ≥1.0 µm, ≥5.0 µm, ≥10.0 µm, ≥25.0 µm
	Lasair III 5100	≥0.5 µm, ≥1.0 µm, ≥2.0 µm, ≥5.0 µm, ≥10.0 µm, ≥25.0 µm
Kanomax [35]	3905/3910	≥0.3 µm, ≥0.5 µm, ≥1.0 µm, ≥3.0 µm, ≥5.0 µm, ≥10.0 µm
TSI [1, 2]	AeroTrak 9110	≥0.1 µm, ≥0.15 µm, ≥0.2 µm, ≥0.25 µm, ≥0.3 µm, ≥0.5 µm, ≥1.0 µm, ≥5.0 µm
	AeroTrak 9310	≥0.3 µm, ≥0.5 µm, ≥1.0 µm, ≥3.0 µm, ≥5.0 µm, ≥10.0 µm
	AeroTrak 9350	≥0.3 µm, ≥0.5 µm, ≥1.0 µm, ≥3.0 µm, ≥5.0 µm, ≥10.0 µm

4.5 Results and Discussion

Based on the different resolutions and diameter sensitivities, the leak rate evaluated by the DPC method is calculated. Figure 4.7 shows a compilation of the leak rate values of the filter grades of H13 and H14 filter grades in which was calculated based on the cumulative leak evaluation method for different DPCs as described in equation tested with different GSDs of the challenge aerosol concentration distribution at the upstream side of the filter. Based on data plotted, some DPCs did not pass the test of producing the leak rate below 0.01% for filter grade H13. However, the maximum value of leak rate still in the order of 10^{-4} and below 0.1%. For all GSDs a divergence of the leak rate values at small CMDs were observed, while for larger CMDs the values converged into almost similar value for all different DPCs. Starting from the CDM at approximately 0.3 μm, leak rate values starts to go over 0.01% and diverge more towards smaller CMD.

It is important to emphasise that the purpose of this chapter is not to test the accuracy of a particular DPC specification, but instead, to confirm an important question whether can different DPCs produce a constant leak rate below 0.01% in order for the same

threshold criterion as in aerosol photometer to be used for DPC method. Based on our parametric study with different DPC counting efficiency functions, the results obtained from previous chapters still stand and true which is the same threshold criterion of 0.01% can be used for both aerosol photometer and DPC for filter grade H14 or higher but, different 0.01% could not be used for filter grade H13 and lower.

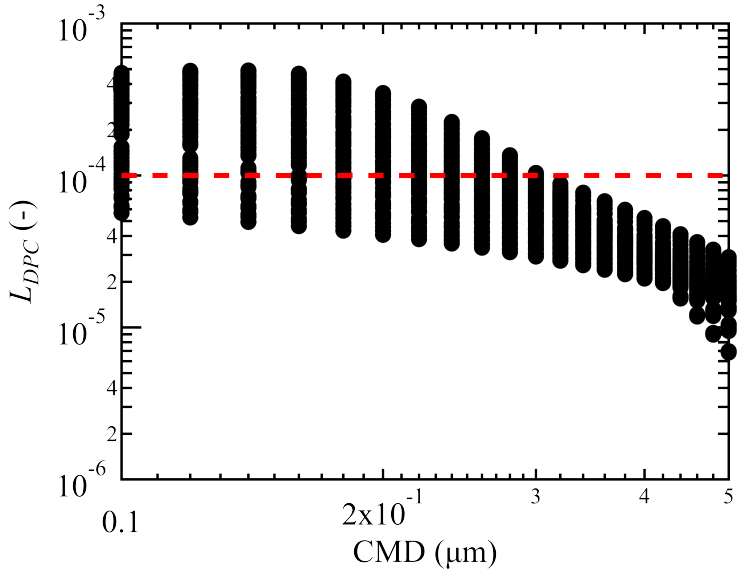

(a)

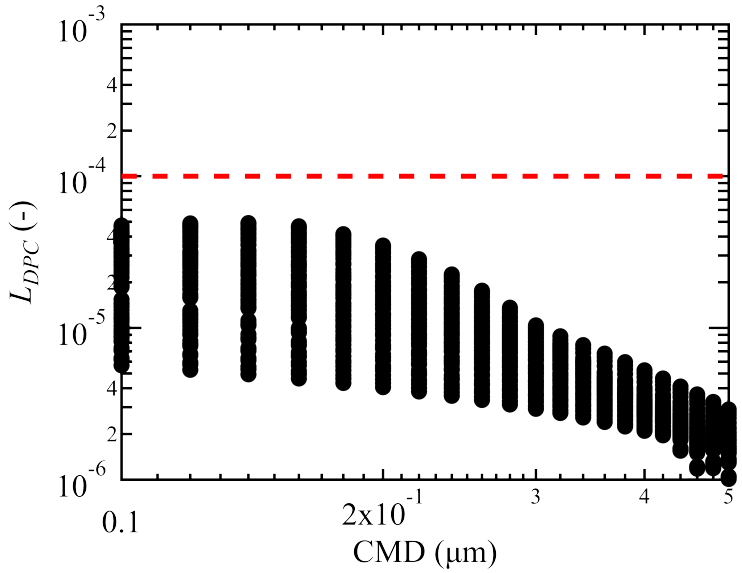

(b)

Figure 4.7: Leak rate for different DPCs with different GSDs and CMDs for upstream particle distribution.

4.6 Conclusion

In this chapter, we tested different DPC responses by changing the counting efficiencies in accordance to the limitations provided by the ISO 21501-4: 2018 [22]. We tested all filter grades but we only showed results for H13 since H13 presented a risk for misevaluation and misjudgement during filter leak test. This is based on the previously obtained result from Chapters 2 and 3 where H13 produced value below 0.01%, but since in Chapter 3, we only considered one type pf DPC response thus result alone does not represent all DPCs. In addition, a parametric study by changing the GSD and CMD of the upstream challenge aerosol distribution within the allowable ranges provided in ISO 14644-3: 2005 [21] were taken. Based on the result obtained some DPCs failed the test thus solidify the concluded remarks obtained in Chapters 2 and 3. The same threshold as for aerosol photometer can only be used for filter grade equal to H14 or higher, but for filter grade equal to H13 and below, a lower threshold should be used.

Chapter 5

Conclusion and Future Work

5.1 Conclusion

This dissertation is to study the possibility to unify the leak threshold criterion for both aerosol photometer and DPC method presented in ISO 14644-3: 2005 [21]. The idea is to use the leak threshold criterion of aerosol photometer method in DPC method. First, we did a comparison based on the difference in measuring unit and leak evaluation method. The measuring unit for both instruments provided different platform in the instruments' measurement. DPC always has more severe leak evaluation. However, we found that this matter can be improved if a different leak evaluation method is used. Instead of discrete leak evaluation method that is currently stated in ISO 14644-3: 2005, cumulative leak evaluation method provides more reliable leak rates for DPC method. The values are comparable with the aerosol photometer method. Thus, throughout this dissertation, the cumulative leak evaluation was tested for its validity towards the possibility for a unified threshold criterion.

This evaluation method was further was tested in the leak rate calculation with instrument responses considered. The only slight change was observed for DPC as compared to number concentration values. However, the leak rate evaluated by aerosol photometer has a relatively big change compared to the mass concentration measurement. This all because of the natural behaviour of the aerosol photometer response. Different weight is applied for each particle size. As a result, it was found that for a filter having H14 or higher performance in European standard EN 1822-1: 2009 [9], the same leak

evaluation standard 0.01% as the photometer method can be applied in the DPC method. On the other hand, similar to results obtained in chapter 2 it was found that it was not possible to apply the uniform criterion for filters with H13 or lower performance, therefore, it was necessary to establish criteria for each filter grade instead.

Next, different DPC responses by changing the counting efficiencies in accordance to the limitations provided by the ISO 21501-4. We tested all filter grades but we only showed results for H13 since H13 presented a risk for misevaluation and misjudgment during filter leak test. This is based on the previously obtained result from chapter 2 and 3 where H13 produced value below 0.01%, but since in chapter 3, we only considered one type of DPC response thus that result alone does not represents all DPCs. In addition, a parametric study by changing the GSD and CMD of the upstream challenge aerosol distribution within the allowable ranges provided in ISO 14644-3: 2005 [21] were taken. Based on the result obtained some DPCs failed the test, thus solidify the concluded remarks obtained in chapter 2 and 3. The same threshold as for aerosol photometer can only be used for filter grade equal to H14 or higher, but for filter grade equal to H13 and below, a lower threshold should be used.

The results presented in this dissertation were presented in the working group 3(WG3) consists of Technical Committee (TC) whose representing their respective standard organisations to discuss the revision of the ISO 14644-3: 2005 organised by International Standard Organization (ISO) named ISO/TC209. The Final Draft International Standard (FDIS) consisting the results and findings of this dissertation were proposed and through voting process by the principal members (P-members) carried out in July 2019, with 19 out of 20 votes with 95% acceptance rate (requirement: $\geq$66.66%) and 1 negative vote out of 23 votes in the member bodies meeting (requirement: $\leq$25%). Then, the FDIS was approved and ISO 14644-3: 2005 was also withdrawn and a new ISO 14644-3: 2019 was established. As a result, a leak detection threshold of 0.01% (same as used in aerosol photometer method) of the upstream challenge aerosol concentration for the H14 filter grade and higher, and a 0.1% threshold of the upstream challenge aerosol concentration for the H13 and lower were established in the new ISO 14644-3: 2019.

5.2 Future Work

Throughout this dissertation, a leak evaluation by the aerosol photometer and DPC method was theoretically investigated based on the requirements stated in ISO 14644-3: 2005. Therefore, all requirements applied in the calculation in this dissertation are based on the previous standard. Further detailed examination, including the experimental verification, is still necessary. Aside from that, there are still several things that are not covered in this dissertation but based on the findings from this dissertation opens up possibilities for improvement.

Although we managed to unify the leak threshold criteria between aerosol photometer and DPC, the basis of 0.01% as the leak threshold criteria remains unclear. To our knowledge, no explanation or background is given in any standard concerning the installed filter leak test. A study on the leak characteristic of an installed filter media needs to be done to determine the suitable leak threshold criteria. Regarding this matter, several questions might be considered, for example

(i) What is the smallest leak that can be detected?
(ii) What should be the criteria for a qualified claim of a leak?
(iii) Can a leak be detected without a filter scan?
(iv) What is the efficiency of leak for different particle sizes?

Next, till now, the scanning method is used as the test method in the installed leak test. It is a very time and cost consuming procedure. Study on alternative method in installed leak test is important, in particular for cleanroom that does not require a high level of cleanliness. We are already done a preliminary study on the idea of applying the overall filter leak test to the installed filter leak test. In this method, if a detectable in penetration is observed, considering that there are no other changes in test condition, this increase can be attributed to the existence of a leak. The overall filter leak test is a very quick way of separating the leaking filters from those that do not. Since the test period is relatively short, the filter will not be loaded as heavily as in the scanning test. The leaking filters can be scanned afterwards to pinpoint the location of the leak for repair if necessary.

Appendices

Appendix A

Geometrical Factor in Light-scattering Instruments

Contents

The calculation of the flux collected for various geometries have been discussed in many old literatures. Geometrical factor affects the total collection of scattered light by particles. The verification of the reported results on response function might be therefore difficult, especially when the formulation of geometrical factor is ambiguous. In this appendix, the explicit functional form of the geometrical factor for various geometries of the optical systems of commonly used light-scattering instruments is presented.

A.1 Definition of Geometrical Factor

Let the particle be illuminated by parallel rays making an angle ϕ with the axis of collection aperture, carrying unit energy flux, per unit transverse area. Let the intensity scattered by the particle in the direction θ be the $I(\theta)$ unit of flux per unit solid angle per unit transverse area of the particle. Then, the total flux F scattered through the angles θ and $\theta + \mathrm{d}\theta$, collected by the collection system for any geometry, may be written in a general form as

$$F = f(\theta, \phi) I(\theta)\ \mathrm{d}\theta \mathrm{d}\phi, \tag{A.1a}$$

or if $\phi = 0$

$$F = f(\theta, \phi) I(\theta)\ \mathrm{d}\theta, \tag{A.1b}$$

where, $F(\theta, \phi)$ may be defined as the geometrical factors for this geometry of illumination and collection system. Thus, $f(\theta, \phi)$ represents in a way the collection efficiency of the deferentially scattered flux through θ and $\theta + \mathrm{d}\theta$. This definition constitutes the basis for calculation of $f(\theta, \phi)$ for all the instrumental arrangements considered in this analysis.

A.2 Geometries of Illumination and Collection

In what follows the geometrical factor has been calculated and its plot discussed for various geometries in the order of their complexity. Such curves illustrating variations of geometrical factor have not yet been reported.

A.2.1 Instruments with Collimated Illumination along the Axis of Collection Aperture

In this type of instruments, laser light is normally employed for illumination in order to achieve a highly intense and collimated beam. Figure A.1 shows the geometry of illumination and collection for this arrangement. AB is the circular collection aperture which subtends an angle 2β at O, where the scattering particle is situated. OG represents

the direction of illumination beam. The light directed into the collection aperture is eliminated by a light trap of circular aperture which subtends an angle 2η at O. The whole light scattered through the angles η to β is collected.

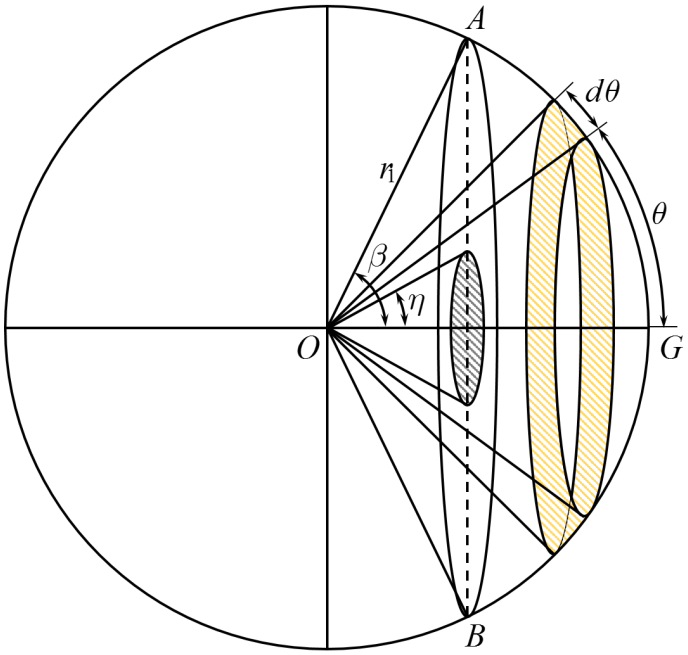

Figure A.1: A scheme of the instruments with collimated illumination along the axis of collection aperture, and OG is the direction of the illumination beam, η is the half-angle of the light trap, O is the illuminated particle.

The light scattered through angles θ to $\theta + \mathrm{d}\theta$ passes through a circular strip of radius $r_1 sin\theta$ and width $r_1 \mathrm{d}\theta$ to the surface of a sphere of radius r_1 centred at O. The area of this strip is $2\pi r_1^2 \sin\theta \mathrm{d}\theta$ which subtends at O solid angle

$$w_0 = 2\pi \sin\theta \ \mathrm{d}\theta. \tag{A.2}$$

Therefore, the flux F collected by the collection system is given by

$$F_1 = w_0(\theta) I(\theta) = 2\pi \sin\theta \ \mathrm{d}\theta I(\theta). \tag{A.3}$$

Comparing Equations (A.1) and (A.3), we can write

$$f_1(\theta, \phi) = 2\pi \sin\theta, \text{where } \eta < \theta < \beta, \text{ and } \phi = 0, \tag{A.4}$$

where, $f_1(\theta, \phi) = 2\pi \sin\theta$ is the geometrical factor for this simple geometry.

A.2.2 Instruments with Collimated Illumination Not Co-axial with Collection Aperture

In this type of instruments, the collimation direction makes the angle ϕ with the axis of collection aperture so that the collimated beam is not intercepted by the collection aperture. Figure A.2 shows the scheme of geometrical arrangement for such instruments. $KCBE$ represents the collection aperture of semi-angle β. The particle at O is illuminated by a pencil of rays travelling to the axis of collection aperture in the direction OB at an angle $\phi > \beta$. The locus of rays scattered through the angle θ is a cone of semi-angle θ about ON. CLE is the intersection of this cone with the spherical surface centred at O, and the collection aperture. All the scattered rays passing through CLE are collected. If the radius of the sphere is r_2, the angle $DAC = \cos^{-1}[\cos beta - \cos\theta - \cos\phi/\sin\theta\sin\phi]$, so that arc length $CLE = 2AC \times$ angle DAC. the increases of angle θ by $\mathrm{d}\theta$ widens this arc to a strip of the width $r_2\mathrm{d}\theta$ which subtends at O a solid angle

$$w_1(\theta,\phi) = 2\sin\theta\ \mathrm{d}\theta\cos^{-1}[\cos beta - \cos\theta - \cos\phi/\sin\theta\sin\phi]. \tag{A.5}$$

It is easily seen that if $\theta \leq \phi - \beta$ or $\theta \geq \phi + \beta$ no flux is collected. As required, $w_1 = 0$, when $\theta = \phi - \beta$ or $\theta = \phi - \beta$.

Equation (A.5) holds for the light scattered through an angle θ from all illuminating rays inclined at the angle ϕ to the axis of collection aperture. Thus, the total flux scattered into the collection system for this geometry can be written as

$$F_2 = w_1(\theta,\phi)I(\theta). \tag{A.6}$$

From Equation (A.1), it follows that for $\phi - \beta < \theta < \phi + \beta$

$$f_2(\theta,\phi) = 2\sin\theta\cos^{-1}[\cos beta - \cos\theta - \cos\phi/\sin\theta\sin\phi]. \tag{A.7}$$

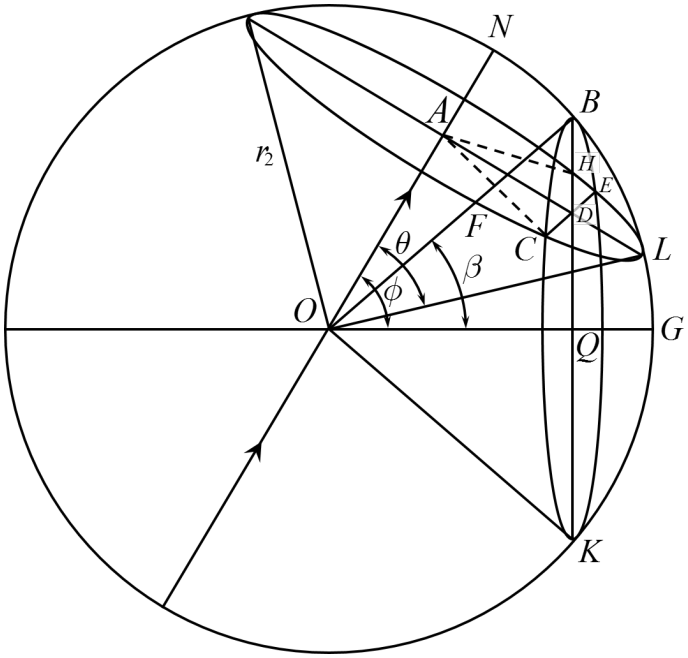

Figure A.2: A scheme of the instruments with collimated illumination not co-axial with collection aperture: ϕ is the angle between direction of collimation and axis of collection aperture.

A.2.3 Instruments with Convergent Illumination not Co-axial with Collection Aperture

In order to increase the level of illumination of this type of instruments, the illuminating rays should converge on the view volume. Here, the axis of collection aperture is inclined to the axis of illumination at an angle ψ such that no light from the illumination cone is intercepted by the collection aperture.

Let the illumination be provided by a lens of circular aperture $IXJW$ (Figure A.3) which subtends an angle 2γ at O where the light converged at the particle, and where the axis is inclined at an angle ψ to the axis OG will appear to originate from the circular are WYX, which is the intersection of the conical surface of semi-angle ϕ about collection axis, with the surface of the sphere. Thus, illuminating rays inclined to the collection axis OG at angles ϕ and $\phi + \mathrm{d}\phi$ originated from a band of the length WYX which subtends at O a solid angles

$$w_2(\theta, \psi) = 2 \sin\theta \; \mathrm{d}\theta \cos^{-1}\left(\frac{\cos\gamma - \cos\phi\cos\psi}{\sin\psi\sin\phi}\right). \tag{A.8}$$

Thus, for this geometry the scattered flux received from the particle will be

$$F_3 = w_1(\theta) w_2(\theta) I(\theta) \tag{A.9}$$

So that,

$$\begin{aligned} F_3(\theta, \phi) =& 4 \sin\theta \sin\phi \left[\cos^{-1} \frac{(\cos\beta - \cos\theta\cos\phi)}{\sin\theta\sin\phi} \right] \\ & \times \left[\cos^{-1} \frac{(\cos\gamma - \cos\theta\cos\psi)}{\sin\psi\sin\phi} \right], \end{aligned} \tag{A.10a}$$

$$\phi - \beta \leq \theta \leq \phi + \beta \quad \psi - \gamma \leq \phi\psi + \gamma. \tag{A.10b}$$

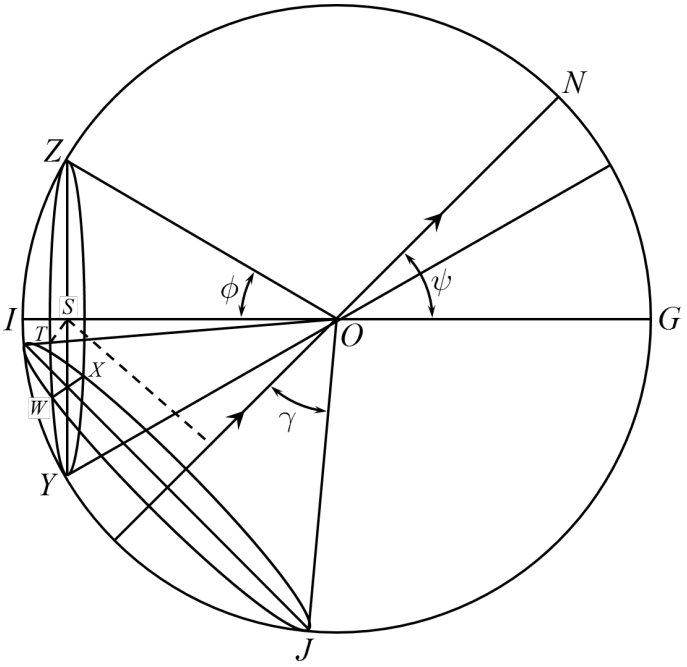

Figure A.3: A scheme of instruments with convergent illumination not co-axial with collection aperture: ψ is the angle between axis of illumination and collection aperture, γ is the half-angle of the illumination.

A.2.4 Instruments with Hollow-cone Illumination, Co-axial with Collection Aperture inside the Cone of Darkness

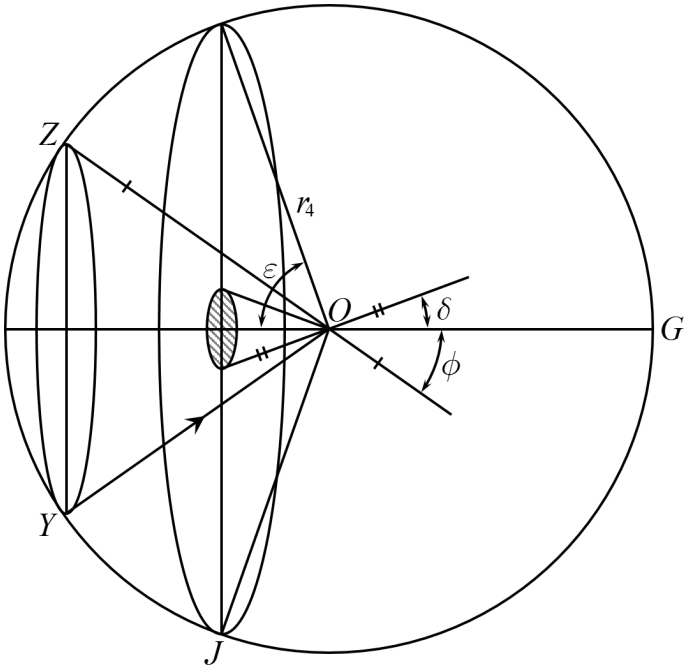

Figure A.4: A scheme of instruments with hollow cone illumination co-axial with collection aperture inside the cone of darkness: 2ϵ, 2β and 2δ are the angles subtended by the illumination lens, collection aperture and circular dark stop respectively at the particle.

As in the case of dark field microscopy, in this type of instruments illumination lens subtending angle 2ϵ (see Figure 7) at the particle is co-axial with the collection lens and has a circular dark stop which subtends at the particle an angle 2δ greater than 2β subtended by the collection lens. Now, the illuminating rays inclined at an angle ϕ to the common axis appear to originate from the entire circle YZ of the radius $r_4 \sin\phi$ made by the intersection of the cone with semi-angle ϕ about this axis and the sphere of radius r_4 centred at O. Illuminating rays, from ϕ to $\phi + \mathrm{d}\phi$, thus appeared to originate from a circular strip of width $r_4 \mathrm{d}\phi$. The solid angle subtended by this strip at O is given by

$$w_3 = 2\pi \sin\phi \ \mathrm{d}\phi. \tag{A.11}$$

Thus, the flux scattered through angles θ to $\theta + \mathrm{d}\theta$ from a circular strip of radius $r_4 \mathrm{d}phi$, collected by the collection aperture is given by

$$F_4 = w_1(\theta) w_3(\phi) = 2\pi \sin\phi I(\theta) \ \mathrm{d}\phi. \tag{A.12}$$

Thus

$$f_4(\theta,\phi) = 4\sin\phi\sin\theta\left[\cos^{-1}\frac{(\cos\beta-\cos\theta\cos\phi)}{\sin\theta\sin\phi}\right], \qquad \text{(A.13)}$$
$$\phi-\beta<\theta<\phi+\beta, \delta<\phi<\epsilon.$$

A.2.5 Instruments with Convergent Illumination, Co-axial with Collection Aperture having a Central Dark Stop

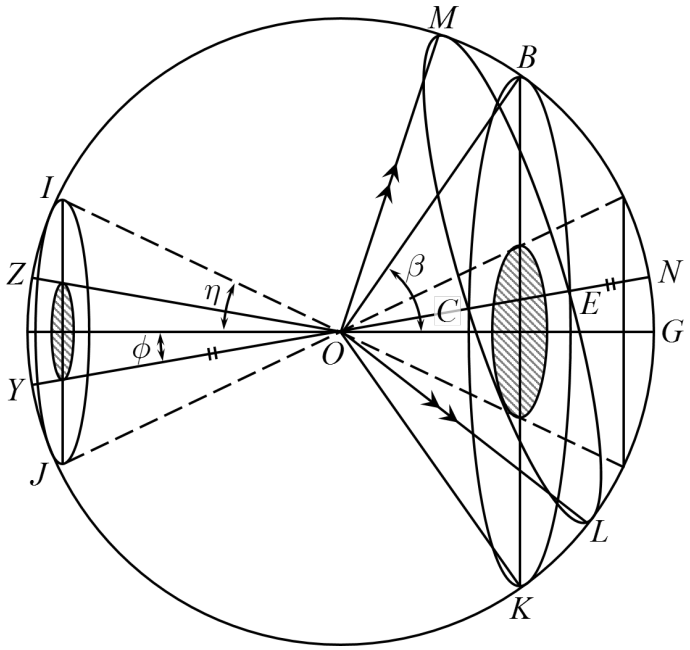

Figure A.5: A scheme of the instruments with convergent illumination co-axial with collection aperture having central dark stop: β, γ and η are the half angles subtended by collection aperture, illumination lens and light trap repectively at the particle.

A schematic representation of the geometry of this type of instruments is shown in Figure A.5. Here, BK represents the aperture of the collection lens which subtends an angle 2β at O. IJ is the intersection of a cone with semi-angle around the common axis OG, and sphere of arbitrary centred at O. The formulation of geometrical factor is slightly complicated in this case. This is because the collection of the flux scattered through angles θ and $\theta + \mathrm{d}\theta$ by illuminating rays inclined at an angle ϕ to the axis of collection is not always complete, as a part of the flux is lost in the light trap. A complete collection of scattered flux can be achieved only when $\eta + \phi < \theta < \beta - \phi$.

Under these conditions the total flux collected is

$$\begin{aligned} F_3 &= w_3(\phi) w_0 I(\theta) \\ &= 4\pi^2 \sin\theta \sin\phi I(\theta)\ \mathrm{d}\theta\mathrm{d}\phi \end{aligned} \tag{A.14}$$

In fact, flux is lost under the following circumstances:

(i) $\theta \leq \theta \leq \eta - \phi$: no flux is collected, as the whole scattered flux falls into the light trap.

(ii) $\eta - \phi \leq \theta \leq \eta + \phi$: only a part of the scattered light falls into the light trap, and the rest into the collection aperture.

(iii) $\beta - \phi \leq \theta \leq \theta$: part of flux falls outside the collection aperture and the rest falls into it.

(iv) $\beta + \phi \leq \theta \leq \pi$: the whole scattered flux falls outside the collection aperture.

Under condition (ii), the flux lost in the dark stop is calculated by putting $\eta = \beta$ in Equation (A.13)

$$F_4' = 4\pi \sin\theta \sin\phi\ \mathrm{d}\theta \cos^{-1}\left[\frac{(\cos\eta - \cos\theta\cos\phi)}{\sin\theta\sin\phi}\right]. \tag{A.15}$$

Similarly, based on the discussion in the previous section, the flux lost under the condition (iii) is given by

$$F_5' = 4\pi \sin\theta \sin\phi\ \mathrm{d}\theta\mathrm{d}\phi\left[\pi - \cos^{-1}\left\{\frac{(\cos\beta - \cos\theta\cos\phi)}{\sin\theta\sin\phi}\right\}\right]. \tag{A.16}$$

Thus, the total flux received by the collection aperture can be written as

$$F_5 = f_5(\theta,\phi) I(\theta)\ \mathrm{d}\theta\mathrm{d}\phi, \tag{A.17}$$

where

$$f_5(\theta,\phi) = A + B + C \tag{A.18a}$$

$$\begin{aligned} A &= 4\pi^2 \sin\theta\sin\phi, \quad (\eta - \phi \leq \theta \leq \beta + \phi), \\ B &= -4\pi \sin\theta\sin\phi \cos^{-1}\left(\frac{\cos\eta - \cos\theta\cos\phi}{\sin\theta\sin\phi}\right), \quad (\eta - \phi \leq \theta \leq \eta + \phi), \\ C &= -4\phi \sin\phi\sin\theta\left[\pi - \cos^{-1}\left(\frac{\cos\beta - \cos\theta\cos\phi}{\sin\theta\sin\phi}\right)\right], \quad (\beta - \phi \leq \theta \leq \beta + \phi). \end{aligned} \tag{A.18b}$$

References

[1] *AEROTRAK Portable Particle Counter*. URL: https://www.pmt.ie/fileadmin/Datasheets_UK/AeroTrak_Portable_9310-9510_5001207-Web-A4.pdf.

[2] *AEROTRAK Portable Particle Counter Model 9110*. URL: https://www.tsi.com/getmedia/a192db6f-d56d-4191-8e36-a4e26ff483f7/AeroTrak_Portable_9110-5001296-A4-web?ext=.pdf.

[3] Armbruster L., et al. "Photometric determination of respirable dust concentration without elutriation of coarse particles". *Particle & Particle Systems Characterization* 1.1-4 (1984), pp. 96–101.

[4] Armbruster, L. "A new generation of light-scattering instruments for respirable dust measurement". *The Annals of occupational hygiene* 31.2 (1987), pp. 181–193.

[5] Carbaugh, E. H. *Survey of HEPA filter experience*. Tech. rep. Pacific Northwest Lab., 1982.

[6] Deshler T., et al. "Retrieval of aerosol size distributions from in situ particle counter measurements: Instrument counting efficiency and comparisons with satellite measurements". *Journal of Geophysical Research: Atmospheres* 124.9 (2019), pp. 5058–5087.

[7] Dhaniyala, S. and Liu, B. "Investigations of particle penetration in fibrous filters: Part I. Experimental". *Journal of the IEST* 42.1 (1999), pp. 32–40.

[8] Dhaniyala, S. and Liu, B. "Investigations of particle penetration in fibrous filters: Part II. theoretical". *Journal of the IEST* 42.2 (1999), pp. 40–46.

[9] *EN 1822–1: High Efficiency Air Filters (EPA, HEPA and ULPA) – Part 1: Classification, Performance, Testing, Marking*. Standard. Brussels, Belgium: European Committee for Standardization, Oct. 2009.

[10] Gail, L. and Ripplinger, F. "Correlation of Alternative Aerosols and Test Methods for HEPA Filter Leak Testing". In: 1998, pp. 369–376.

[11] Görner P., et al. "Photometer measurement of polydisperse aerosols". *Journal of Aerosol Science* 26.8 (1995), pp. 1281–1302.

[12] Greiner, J. "HEPA Filter Leak Testing Using the Particle Counter Scan Method". *CleanRooms* 4.9 (1990), pp. 36–39.

[13] Gucker, F. T. and Tuma, J. "Influence of the collecting lens aperture on the light-scattering diagrams from single aerosol particles". *Journal of Colloid and Interface Science* 27.3 (1968), pp. 402–411.

[14] Hargreaves, J. and Thaveau, B. "French annex on comparative leak testing results". *ISO/TC209/WG3 N370* (2018).

[15] Hatch, Theodore and Choate, Sarah P. "Statistical description of the size properties of non uniform particulate substances". *Journal of the Franklin Institute* 207.3 (1929), pp. 369–387.

[16] Hinds, W. C. *Aerosol technology: properties, behavior, and measurement of airborne particles*. John Wiley & Sons, 1999.

[17] Hinds, W. C. and Kraske, G. "Performance of PMS model LAS-X optical particle counter". *Journal of aerosol science* 17.1 (1986), pp. 67–72.

[18] Hodkinson, J. R. and Greenfield, J. R. "Response calculations for light-scattering aerosol counters and photometers". *Applied optics* 4.11 (1965), pp. 1463–1474.

[19] Hulst, H. C. and Hulst, H. C. van de. *Light scattering by small particles*. Courier Corporation, 1981.

[20] *ISO 14644–3: Cleanrooms and associated controlled environments – Part 1: Classification of air cleanliness by particle concentration*. Standard. Geneva, CH: International Organization for Standardization, Dec. 2015.

[21] *ISO 14644–3: Cleanrooms and Associated Controlled Environments – Part 3: Test Methods*. Standard. Geneva, Switzerland: International Organization for Standardization, Dec. 2005.

[22] *ISO 21501–4: Determination of Particle Size Distribution Single Light Interactions Methods – Part 4: Light Scattering Airborne Particle Counter for Clean Spaces*. Standard. Geneva, Switzerland: International Organization for Standardization, May 2018.

[23] *ISO 29463–1: High-efficiency Filters and Filter Media for Removing Particles in Air – Part 1: Classification, Performance Testing and Marking*. Standard. Geneva, Switzerland: International Organization for Standardization, Oct. 2011.

[24] *JIS Z 8122: Contamination Control–Terminology*. (in Japanese). Standard. Tokyo, Japan: Japanese Industrial Standard, Mar. 2000.

[25] *JIS Z 8122: Light scattering airborne particle counter for clean spaces*. (in Japanese). Standard. Tokyo, Japan: Japanese Industrial Standard, Apr. 2010.

[26] Kase T., et al. "A Study on Testing of HEPA Filters". *Kuki Seijo to Kontamineshyon Kontororu Kenkyu Taikai Yokoshu* 9 (1990), pp. 221–224.

[27] Katagiri, T. and Ehara, K. "Comparative Test of Twenty Five Laser Particle Counters". In: *The 10th Kuki Seijo to Kontamineshyon Kontororu Kenkyu Taikai Yokoshu*. 1992.

[28] *Lasair III Airbourne Particle Counter*. (in Japanese). URL: https://www.pmeasuring.com/PMS/files/b5/b5077113-d171-4a86-9031-24d0d4c519e9.PDF.

[29] Meulen, A. van der, Van Elzakker, B. G., and Plomp, A. "Size resolution of laser optical particle counters". *Aerosol science and technology* 5.3 (1986), pp. 313–324.

[30] Mie, G. "Contribution to the optics of suspended media, specifically colloidal metal suspensions". *Ann. Phys* 25 (1908), pp. 377–445.

[31] Mohd Nor, M. A. B. and Suwa, Y. "Study on the Posibility of a Unified Criterion for a Leakage Test of an Installed Filter System". *Journal of Japan Air Cleaning Association* 56.6 (2019), pp. 29–34.

[32] Okui, K. "Counts Difference between Different Counters". *PDA Journal of GMP and Validation in Japan* 2.1 (2000), pp. 49–52.

[33] *Particle Counters General Catalog 2019-2020*. URL: https://www.rion.co.jp/english/product/particle/pdf/particle-E.pdf.

[34] *Particle Measurements General Catalog*. (in Japanese). URL: https://www.transtech.co.jp/wp/wp-content/uploads/2019/08/1particecounter_sougou.pdf.

[35] *Portable Particle Counter Model 3905/3910*. (in Japanese). URL: http://www.kanomax.co.jp/img_data/file_730_1568335591.pdf.

[36] Suzuki K., et al. "A Proposal of Simplified Procedure for In-situ Leakage Test of Installed Filter System". *Journal of Japan Air Cleaning Association* 49.6 (2012). (in Japanese), pp. 35–44.

[37] Szymanski, W. W. and Liu, B. Y. H. "On the sizing accuracy of laser optical particle counters". *Particle & particle systems characterization* 3.1 (1986), pp. 1–7.

[38] Thomas, A and Gebhart, J. "Correlations between gravimetry and light scattering photometry for atmospheric aerosols". *Atmospheric Environment* 28.5 (1994), pp. 935–938.

[39] *Vokes Air Hepatex CR: Setting the Quality Standards*. (in Japanese). URL: http://www.filterpak.fi/images/tuotetiedot/hepa%5C&ulpasuodattimet/Hepatex_CR_EN.pdf.

[40] Ward, S. "Photometer vs LSAPC APRIL 2018 SCW Rev1 Final". *ISO/TC209/WG3 N374* (2018).

[41] Whyte, William. *Cleanroom design*. Wiley Online Library, 1999.

[42] Zhou, B. and Shen, J. "Comparison Of HEPA/ULPA Filter Test Standards Between America And Europe". In: *Proceedings of Clima*. 2007.